Design and Synthesis of xCT Inhibitor Candidates

Jannike Sæle

Master Thesis in Chemistry

Universitetet i Bergen

Department of Chemistry

August 2022

Acknowledgements

First, I would like to thank my supervisor Hans-René Bjørsvik for letting me be a part of his research group and work in his laboratory. Thank you for always being supportive and contributing with great ideas whenever I got stuck with a synthesis.

I would also like to thank Eirin Alme, Sara Barranco Campos, Frida Lundevall and Francesco Angelucci for great help and answers whenever I had questions about any instrument or a synthesis. I am also very grateful for all the times you have helped me refill anhydrous solvents.

An extra thank you goes out to Frida who also helped me with the synthesis on continuous flow and changing the CO_2 bottle one to many times.

Lastly, I would like to thank my family, who have supported me from the start. Thank you for being a part of my journey and for hearing me out whenever it is needed.

Thank you,

Jannike Sæle

Abstract

Glioblastoma is the most common primary malignant brain tumor and has a survival rate of 14-15 months after diagnosis. The causes for glioblastoma are mostly unknown, however it has been discovered that the genetic abnormalities of the glioblastoma cells are larger than for the cells of other types of astrocytoma brain cancer. Most people that get the diagnosis is of older age, and the incidence rate is higher for men than for women. The symptom of glioblastoma varies, but the most common is worsening headaches, nausea, vomiting and seizures. The treatment depends on several factors, but the standard approach is surgery followed by radiation therapy and chemotherapy.

It has been discovered that a drug called sulfasalazine can inhibit the xCT antiporter, which is desirable because this slows down the synthesis of glutathione. Glutathione acts as an antioxidant for reactive oxygen species, which means that it removes the free radicals generated from oxidative stress as well as form irradiation during radiation therapy. With less glutathione in the cell, the radiation therapy becomes more effective, and this leads to increased cell deaths among the tumor cells.

A structure activity relationship (SAR) study has earlier been done on sulfasalazine, and 21 different analogues has been synthesized based on the result of this study. One of the analogues, DC21, showed great potential for inhibiting the xCT antiporter on four different cancer cell lines. The original synthesis pathway of DC21 consists of five steps with a low overall yield. A new synthesis pathway for DC21 have been developed in this project in addition to some new analogues that have been tried synthesized (Scheme 1).

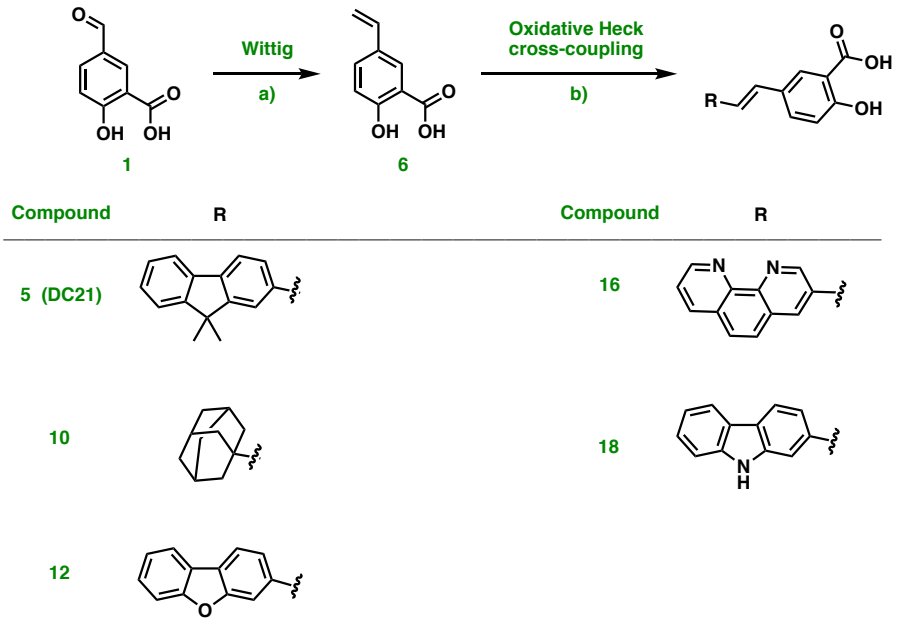

Reagents and reaction conditions: a) $CH_3P^{\oplus}(Ph)_3Br^{\ominus}$, t-BuOK, THF, 21°C, 18h (88%), b) Boronic acid (R-$B(OH)_2$), $Pd(OAc)_2$, $Cu(OAc)_2$, 2,3-di(pyridin-2-yl)pyrazine, DMF, 21°C, 18 h (~ 90%)

Scheme 1 The new synthesis of DC21 (compound **5**) and the other analogues.

Contents

1 INTRODUCTION

1.1 Glioblastoma

Glioblastoma (GBM) is the most common primary malignant brain tumor [1] and are classified as a grade 4 astrocytoma by the World Health Organization (WHO) [2]. The global incidence of GBM is less that 10 per 100 000 people. It is a crucial public health issue due to the poor prognosis with a survival rate of 14-15 months after diagnosis [3].

The reason why people get glioblastoma are largely unknown. However, it has been discovered that it often occurs in people with rare genetic conditions such as neurofibromatosis type 1, Turcot syndrome and Li Fraumeni syndrome. This is due to mutations in a specific gene. This is the same gene that causes many of the characteristic features of glioblastoma [4].

The genetic abnormalities of the GBM cells are larger than for the cells of other types of astrocytoma brain cancer. It is therefore believed that several different genetic mutations are involved. These mutations can be caused by inherited DNA defects, cumulative effects of exposure to chemicals and other carcinogens and high-dose exposure to ionizing radiation in addition to other reasons that has not been discovered yet [4].

Most people that get the diagnosis is of older age, with a median of 64 years [5]. The incidence rates by gender and age groups between the years 2006-2010 is shown in Figure 1.1. There is a peak in incidents at 75-84 years of age. It has also been reported higher incidence of GBM in men compared with women [1, 5].

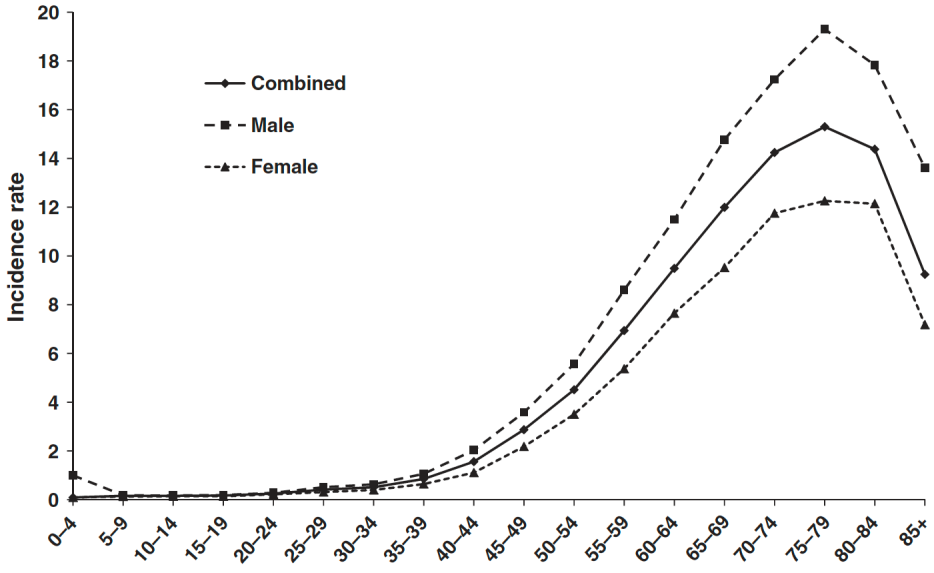

Figure 1.1 Incidence rates (per 100 000) by gender and age groups, 2006-2010 [1].

The symptoms of GBM varies from patient to patient, but the most common is worsening headaches, nausea, vomiting and seizures [6]. Other symptoms such as cognitive and personality changes as well as neurological deficits are less common, and are caused by compression and infiltration of normal, healthy brain tissue [7].

1.2 Treatment

The treatment of glioblastoma depends on several factors. Time of diagnosis, new growth or relapse and the age of the patient are some of them. The standard approach however is surgery followed by radiation therapy (RT) and chemotherapy [8]. Although GBM is an incurable disease [1], the treatment may slow down the progression of the cancer and reduce signs and symptoms [6].

Complete surgical removal of glioblastoma is often not possible. This is because these tumors grow into normal brain tissue, including areas that control speech, motor function, and the senses [9]. The goal is to remove as much of the tumor as possible with surgery, and then some additional treatments to target the remaining tumor cells [6].

Radiation therapy is usually recommended after surgery. Postoperative RT was standard treatment until 2005, but studies has shown that RT along with chemotherapy is more effective than RT alone [10]. The combined treatment consists of external beam irradiation five times a week for six weeks, as well as oral temozolomide (TMZ) daily [8].

Temozolomide is the only standard chemotherapy for patients with glioblastoma, but other agents can be tried if the patient does not respond to TMZ [11]. An overview of the other most used agents to treat GBM are shown in Table 1.1. What they all have in common are dreadful side effects.

Table 1.1 Side effects of commonly used chemotherapeutic agents.

Agent	Side Effects
Lomustine (CCNU)	Nausea, myelosuppression, pulmonary fibrosis
Temozolomide (TMZ)	Nausea, fatigue, headache, constipation, myelosuppression
Vincristine	Peripheral neuropathy, constipation
Bevacizumab	Bleeding gums, body pain, burning, tingling, numbness, chest pain, chills, convulsions, cough, cracks in the skin, difficult breathing, dilated neck veins
Procarbazine	Confusion, convulsions, tiredness, hallucinations, shortness of breath, thick bronchial secretions

1.3 Previous Work

The cystine-glutamate transporter, called x_c^- or xCT, is an antiporter system that imports cystine while exporting glutamate across the phospholipid membrane of the cell [12]. This is an essential precursor for glutathione (GSH) synthesis [13] which is shown in Figure 1.2 (a).

GSH works as an antioxidant for reactive oxygen species (ROS), which means that it removes the free radicals generated from oxidative stress as well as form irradiation during radio therapy [14]. This is illustrated in Figure 1.2 (b).

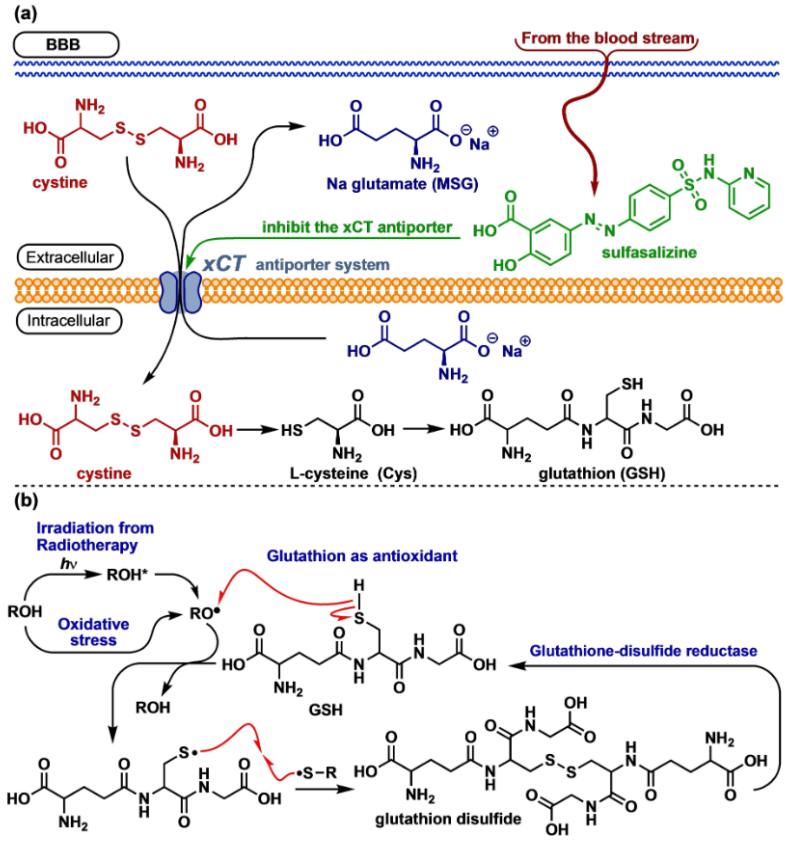

Figure 1.2 (a) Synthesis of glutathione, and sulfasalazine as xCT inhibitor. (b) Glutathione as antioxidant [14].

It has been reported earlier that sulfasalazine can inhibit the xCT antiporter [15]. Sulfasalazine is originally an anti-inflammatory drug used to treat ulcerative colitis, Crohn´s disease and rheumatoid arthritis [16]. The inhibition of the xCT antiporter is desirable because it slows down the synthesis of glutathione. With less GSH in the cell, the radiation therapy becomes more effective. This leads to increased cell deaths [17].

When sulfasalazine is taken orally, it metabolizes into an antibiotic (sulfapyridine) and an anti-inflammatory drug (mesalazine) [18], see Scheme 1.1. None of these metabolites possess xCT antiporter inhibitor activity. Sulfasalazine is also associated with side effects such as bone marrow suppression, liver damage, Stevens-Johnson syndrome and kidney injury [14]. However, these side effects have been linked to the sulfapyridine group [19].

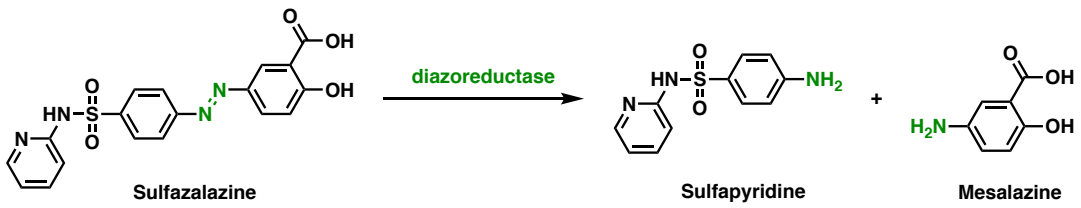

Scheme 1.1 Metabolization of sulfasalazine when taken orally.

Previously in the Bjørsvik research group, there has been done a structure-activity relationship assisted design of sulfasalazine. Based on this design, 21 different xCT inhibitor candidates have been synthesized and tested on four different cancer cell lines. A few of the candidates showed promising result, and the best so far is DC21 [14]. An overview of the candidates already made is shown in Figure 1.3, and the result of the testing is presented in Figure 1.4.

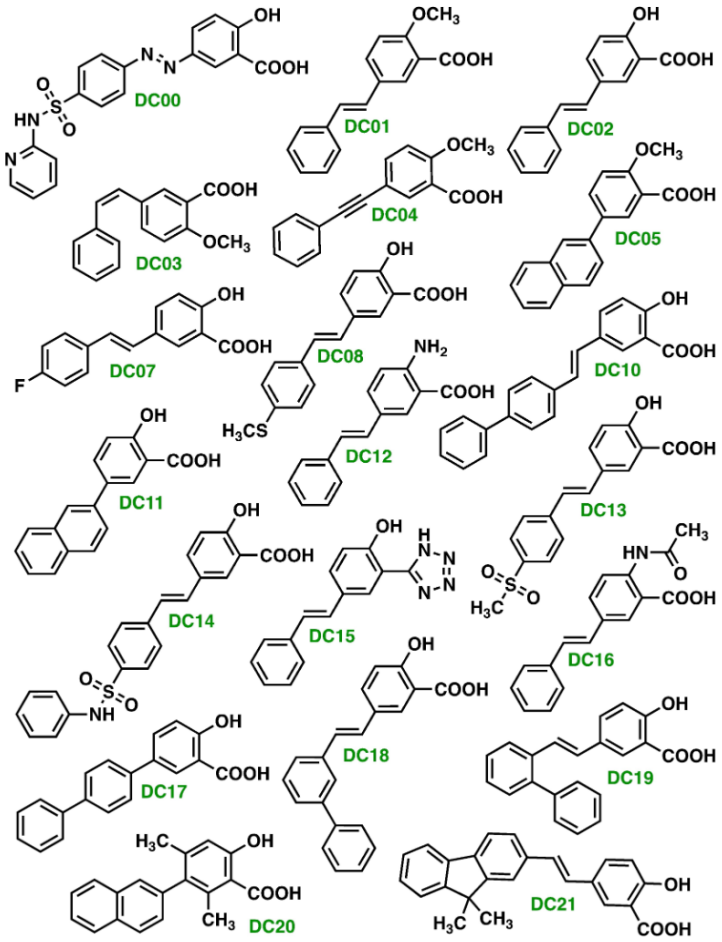

Figure 1.3 An overview of the previously made xCT inhibitor candidates [14].

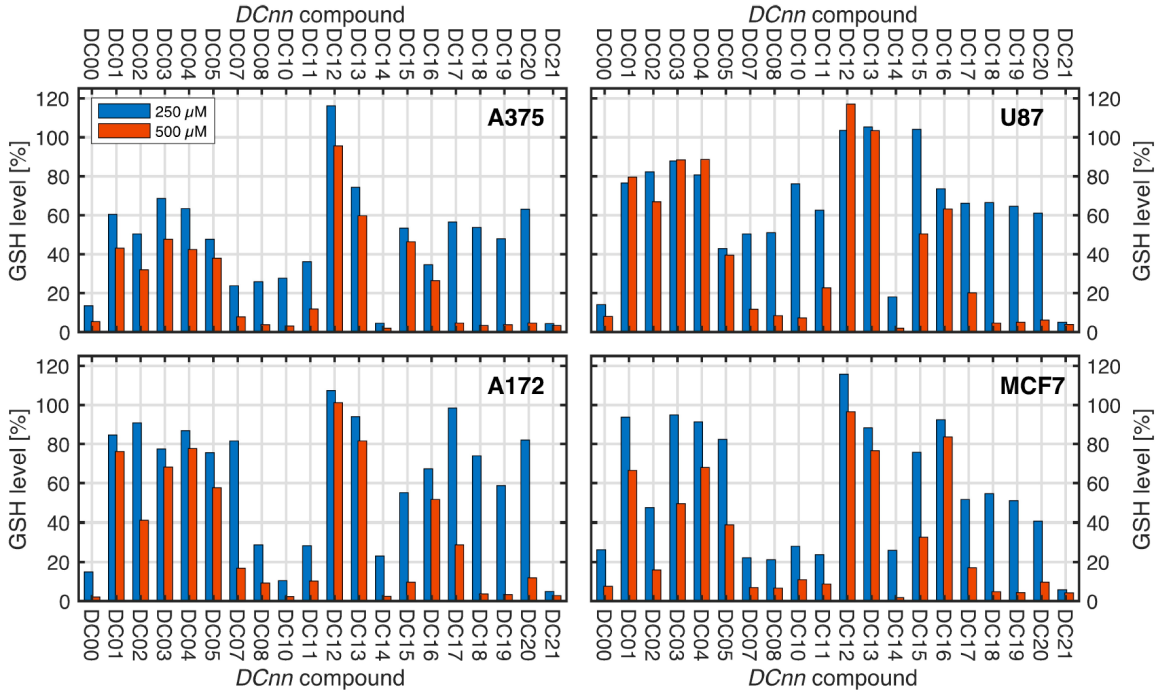

Figure 1.4 The xCT inhibitor candidates tested on four different cell lines with two different concentrations, 250 μM and 500 μM [14].

As seen in Figure 1.4, DC21 shows a low value of GSH in all the four cell lines for both concentrations of the drug. This makes DC21 an interesting compound for further testing, which means that a large scale of the compound needs to be synthesized. The original synthesis pathway for DC21 is presented in Scheme 1.2.

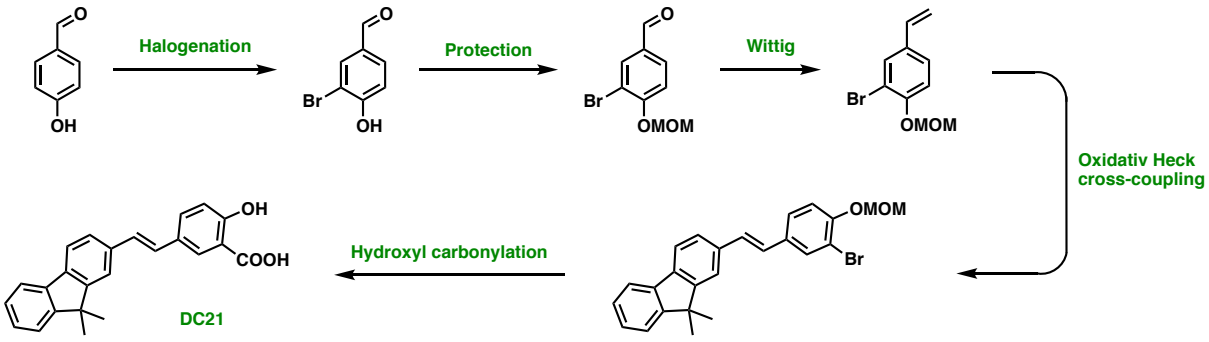

Scheme 1.2 Original synthesis pathway of DC21.

1.4 Aim of study

DC21 was originally a five-step synthesis as shown in Scheme 1.2. The aim of this project is to shorten this pathway to a two-step synthesis by changing the starting material. The synthesis will then consist of a Wittig reaction followed by an oxidative Heck cross coupling. This modification requires fewer chemicals and will also hopefully increase the overall yield of the synthesis. This makes the new reaction greener than the original synthesis, which is desirable for a large-scale synthesis.

As DC21 shows promising results on all the four cell lines [14], it will be sent further to animal testing. The synthesis of DC21 will then need to be upscaled. The aim is to do this on continuous flow chemistry as a part of this project.

Lastly, new xCT antiporter inhibitor candidates will be designed and synthesized.

2 THEORY AND METHODS

2.1 Nuclear Magnetic Resonance Spectroscopy

Nuclear magnetic resonance (NMR) spectroscopy is a highly useful and non-destructive technique in organic chemistry. It provides information about the number of magnetically distinct atoms in the type of nuclei being studied [20]. This is possible because the atomic nuclei have a property called spin, *I*. The value of *I* must in theory be nonzero for the nuclei to be detected on NMR. The most important nuclei for determination of organic structures are ^{1}H and ^{13}C, which both have spin of $\frac{1}{2}$ [21].

For any nucleus with a spin there are $(2I + 1)$ energy levels allowed. This means that for both ^{1}H and ^{13}C there are two possible energy levels, $(2 \times \frac{1}{2} + 1 = 2)$. If there is an applied magnetic field, B_0, the two energy levels move apart [21]. This is illustrated in Figure 2.1 where one energy level decreases, α, and the other increases, β. ΔE are the difference in energy between the two levels and are directly related to B_0. So as the magnetic field gets stronger, the energy difference gets greater.

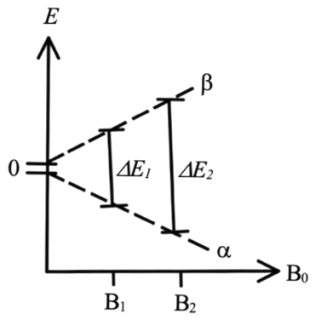

Figure 2.1 The two energy levels for $I = \frac{1}{2}$ with an applied magnetic field.

Absorption of energy can cause excitation of a nucleus from α to the β energy level. For absorption to occur, the system must be in resonance. This is when the applied frequency is tuned to the rotational frequency of the precessing nucleus. When the nucleus drops down to α energy level again, it gives up an amount of energy. This process is called relaxation. It is the emitted energy that produces an NMR signal [21]. An illustration of the basic element of the classical NMR spectrometer is shown in Figure 2.2.

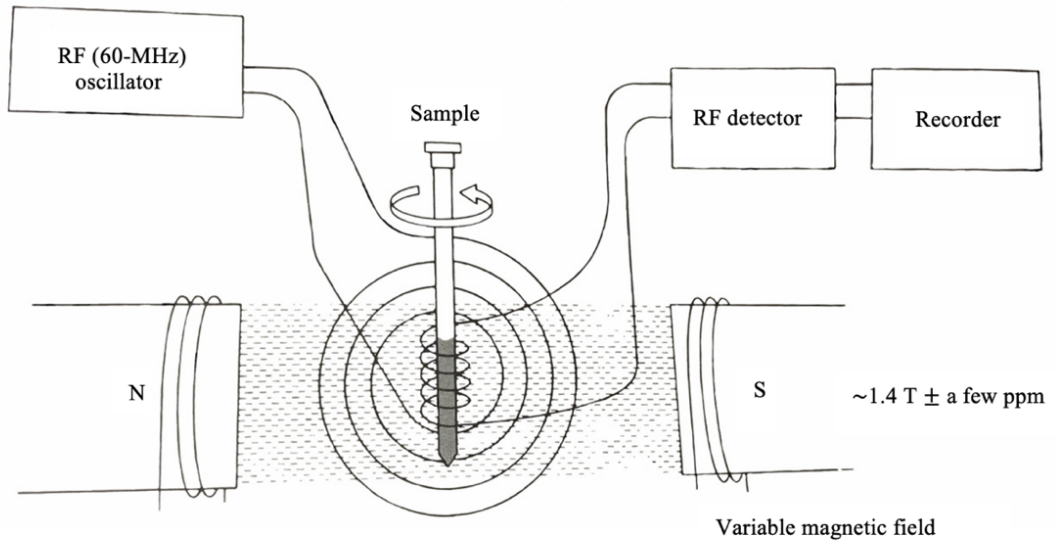

Figure 2.2 An illustration of the basic elements of the classical NMR spectrometer [20].

2.2 Mass Spectrometry

Mass spectrometry (MS) is a helpful but destructive method to find the mass of the compound being studied. It uses different techniques to ionize molecules to generate either cationic or anionic species. The mass spectrometer has five components that are shown in Figure 2.3.

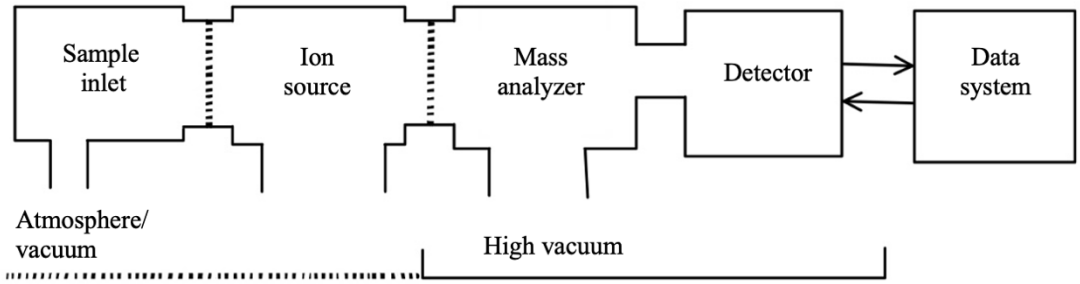

Figure 2.3 The five components of a mass spectrometer.

First, the sample is introduced to the ion source through the sample inlet. In the ion source, the sample molecules transform into gas phase ions. This can be done in many ways, such as electron ionization (EI), chemical ionization (CI), desorption ionization techniques and electrospray ionization (ESI) [20]. ESI is the most used method for liquid chromatography mass spectrometry (LC-MS), and that is the method used in this project.

Electrospray ionization uses electrical energy to transform the liquid sample into gas phase. This is done by spraying the sample molecules as charged droplets from a fine capillary containing high voltage into a heated chamber at nearly atmospheric pressure. In this chamber, the solvent evaporates, and the droplets break apart into smaller droplets until solvent-free sample ions are left in the gas phase [22]. This is illustrated in Figure 2.4.

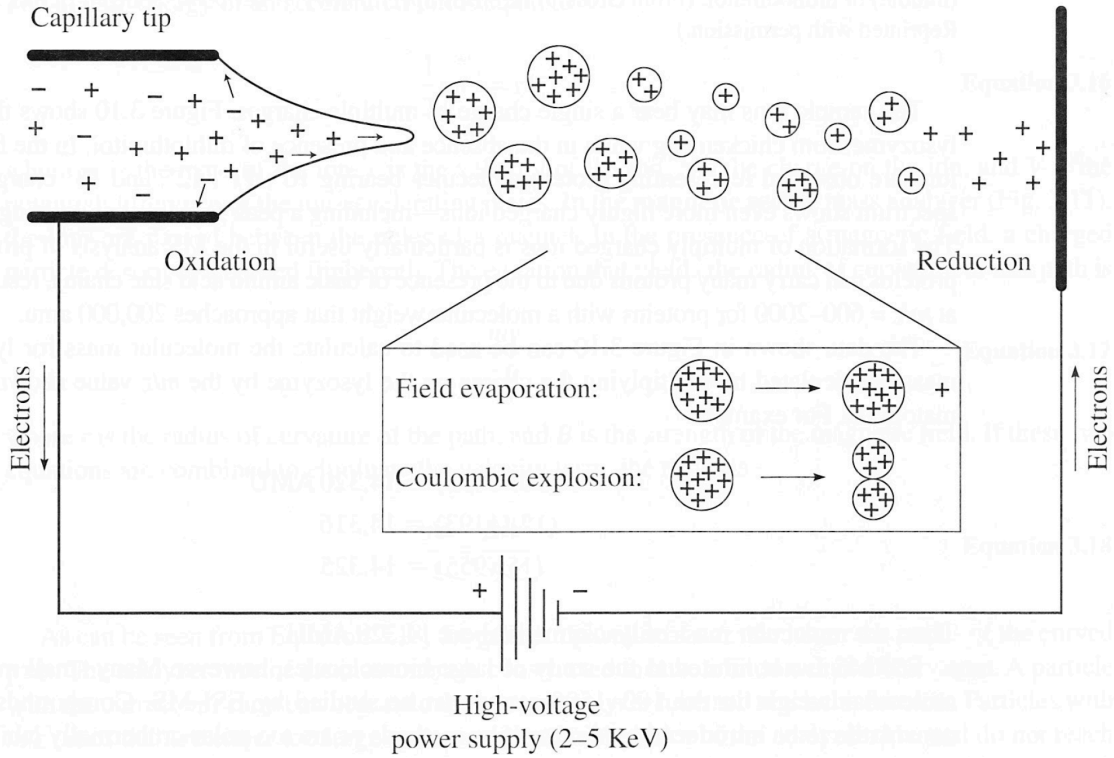

Figure 2.4 An illustration of electrospray ionization [20].

When the sample has been ionized, the ions is accelerated by an electric field into the mass analyzer. Here, the ions get separated according to their mass-to-charge ratio (m/z) [23]. There are several different mass analyzers. One of them is a triple quadrupole mass analyzer. It consists of four parallel metal rods which is kept at equal distance (see Figure 2.5).

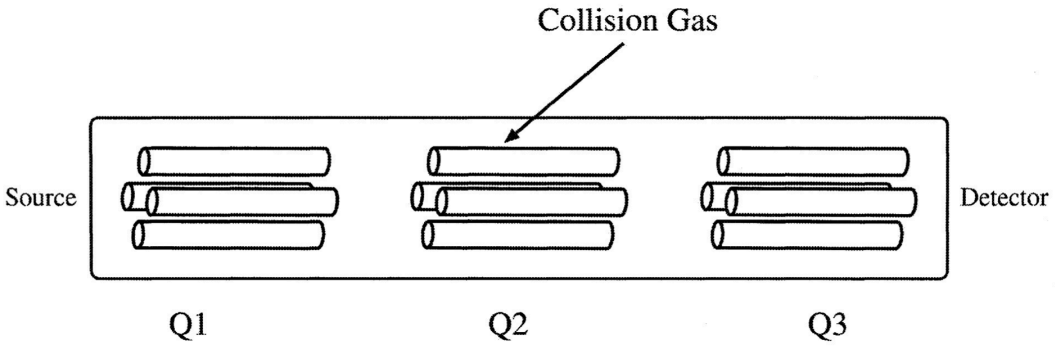

Figure 2.5 A triple quadrupole mass analyzer [22].

An oscillating electrostatic field is generated between the rods by a direct-current (DC) voltage and a radiofrequency (RF) that are applied to the rods. The ions with a desirable m/z ratio will be stable and travel through the mass analyzer without hitting the rods. The ions with an undesirable m/z ratio on the other hand will undergo unstable oscillation, where they hit the rods and get neutralized. These ions will then fail to reach the detector [22].

Lastly, the ions reach a detector that consists of a counter where a current is produced. This current is proportional to the number of ions that strikes the counter. The signal from the detector is sent to a data system which produces the mass spectrum [20].

2.3 High Performance Liquid Chromatography

High performance liquid chromatography (HPLC) is a destructive separation technique that is used to separate and quantify different components in a sample. The separated components pass through a detector (usually an UV spectrometer), which then registers a data peak for the compound. The area under the peak is proportional to the quantity of that compound [24].

Reverse-phase chromatography is the most used method, where the mobile phase is polar, and the stationary phase is non-polar. This means that the more polar compounds eluate first. An illustration of the different parts of an analytical HPLC instrument is shown in Figure 2.6. In this project, the HPLC-instrument was used to confirm that the product was pure.

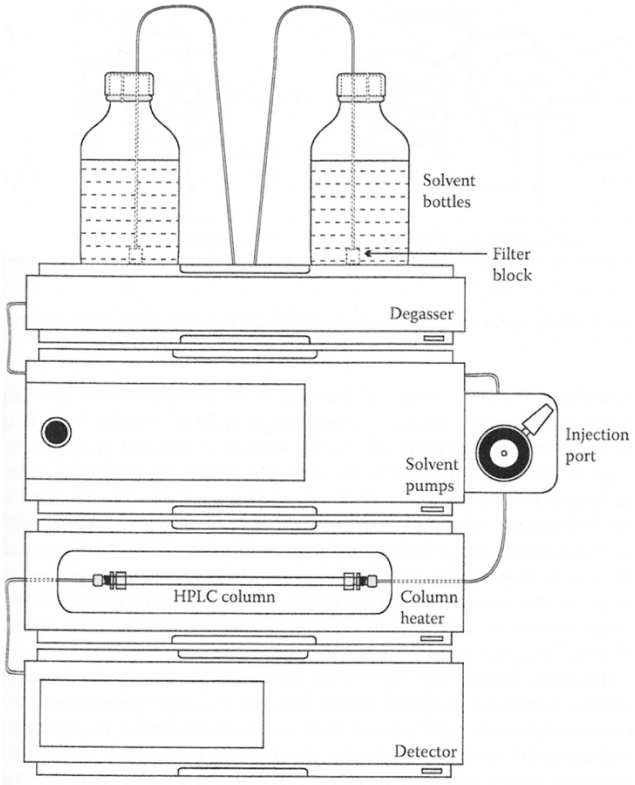

Figure 2.6 An analytical HPLC instrument [24].

2.4 Flow Chemistry

Continuous flow chemistry has been known since the late 1960s, however it has not been published as much before the early 1990s because of the lack of advanced fabrication technology to produce microreactors [25]. Today there are many different microreactors, but most of the suppliers provides microreactors for solution phase only [26].

When doing a reaction in flow, the flow rate must be calculated. This is done by following the Equation 2.1. Both residence time and reactor volume are variables that one chooses before doing the reaction.

$$Residence\ time = \frac{Reactor\ Volume}{Flow\ Rate} \qquad \textbf{Equation 2.1}$$

There are many advantages using flow chemistry, such as reduced reaction time, enhanced chemical selectivity and improved yields. These are a result of the efficient mixing of reagents and accurate control of reaction parameters. It is also safer because it handles all toxic and corrosive reagents and intermediates inside a closed system [27]. The basic components of a continuous flow system are presented in Figure 2.7. It is possible to add several pumps for reagent delivery if it is needed. A picture of the flow rigg in use is shown in Figure 2.8.

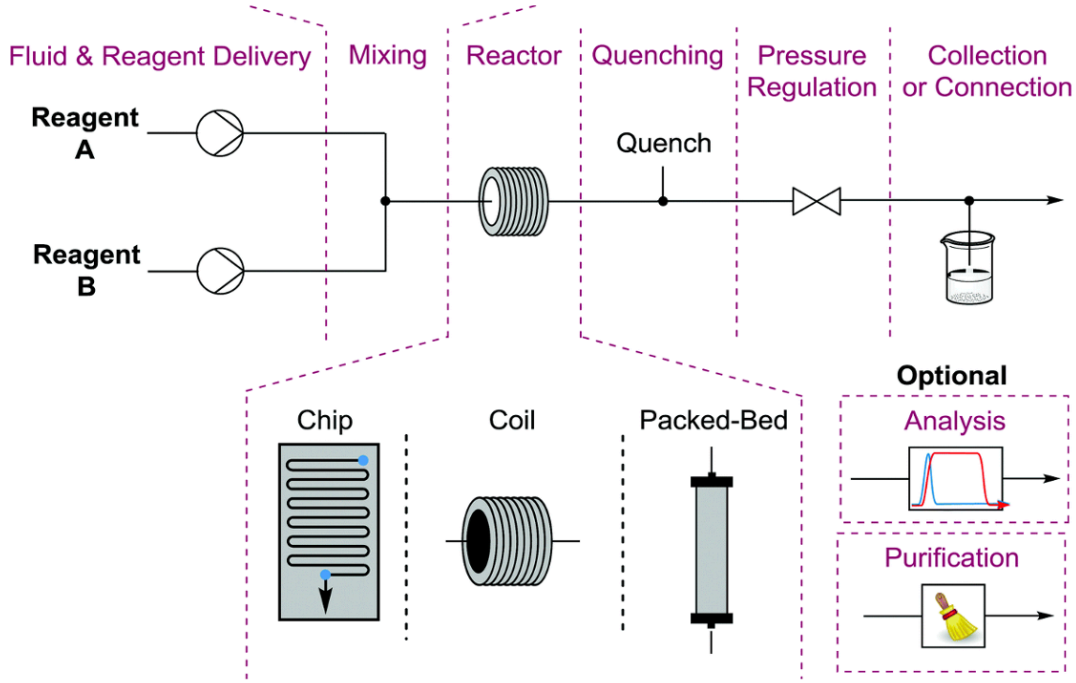

Figure 2.7 The basic components of a continuous flow system [28].

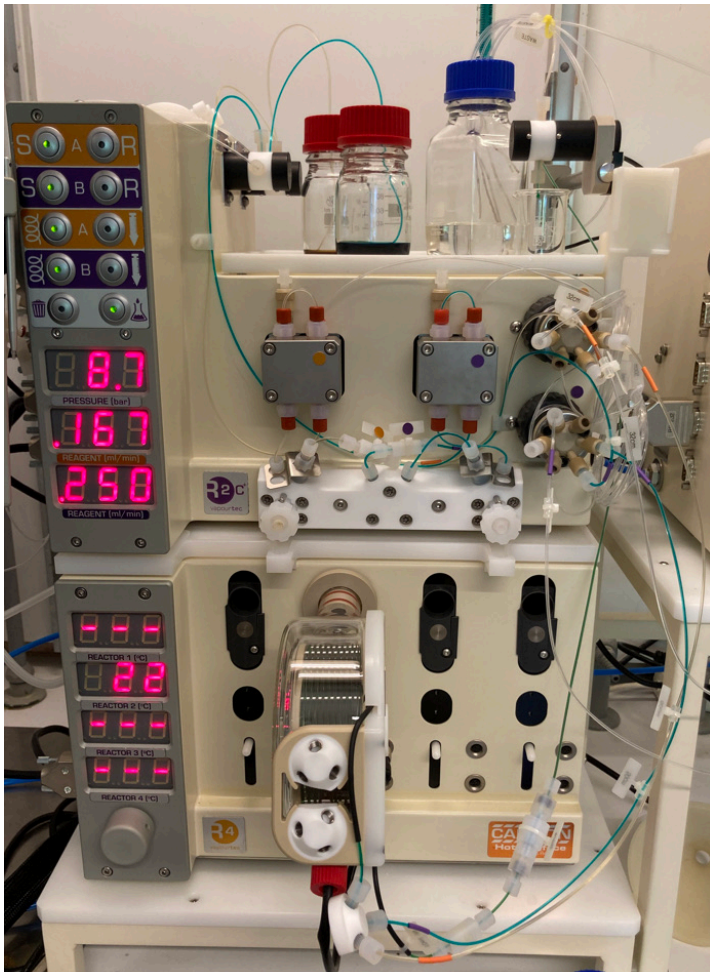

Figure 2.8 The flow machine running an oxidative Heck reaction.

2.5 Wittig Reaction

The Wittig reaction was discovered in 1953 by Georg Wittig [29], and it is a very useful method for making alkenes in organic chemistry. This is done by treating an alkyl phosphonium salt, usually a form of triphenyl phosphonium bromide or iodide, with a strong base such as NaH or n-BuLi. This forms an ylide which then reacts with an aldehyde or ketone to make an alkene [30]. A general Wittig reaction is shown in Scheme 2.1 and the mechanism is shown in Scheme 2.2.

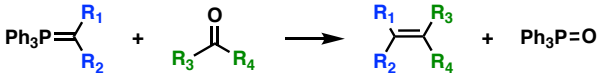

Scheme 2.1 A general Wittig reaction.

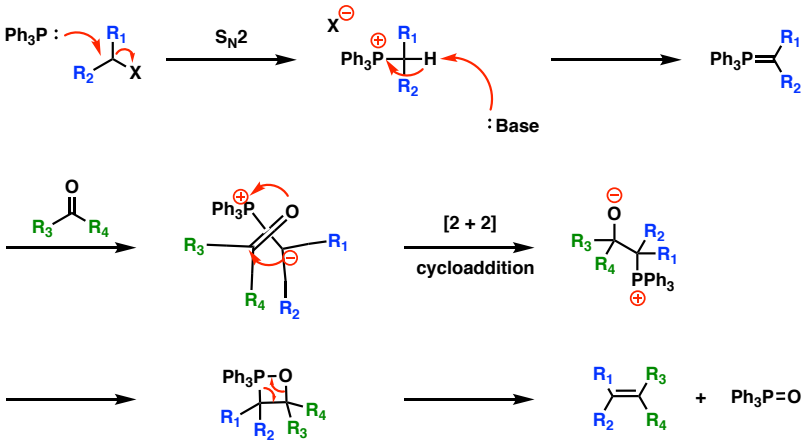

Scheme 2.2 A general mechanism for the Wittig reaction.

With this method, the chemist has full control over the position of the double bond and some control over its geometry [31]. One of the reactions done by Wittig himself is shown in Scheme 2.3 [32].

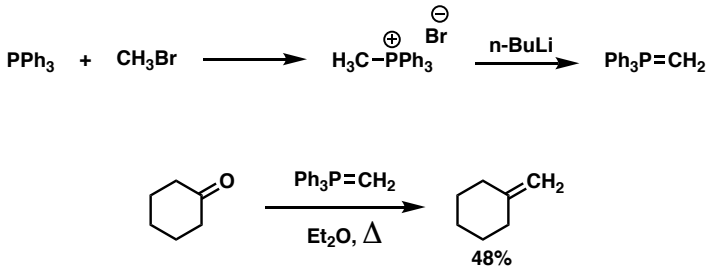

Scheme 2.3 One of the reactions done by Wittig, published in 1954.

2.6 Oxidative Heck Cross-Coupling

The oxidative Heck cross-coupling is a Pd(II) catalyzed reaction which involves a terminal olefin and an aromatic boronic acid. There also need to be an oxidant present to re-oxidize Pd(0) to Pd(II) at the end of the catalytic cycle [33]. A general oxidative Heck reaction is shown in Scheme 2.4, and a proposed general mechanism is shown in Scheme 2.5

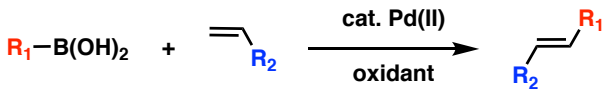

Scheme 2.4 A general oxidative Heck reaction.

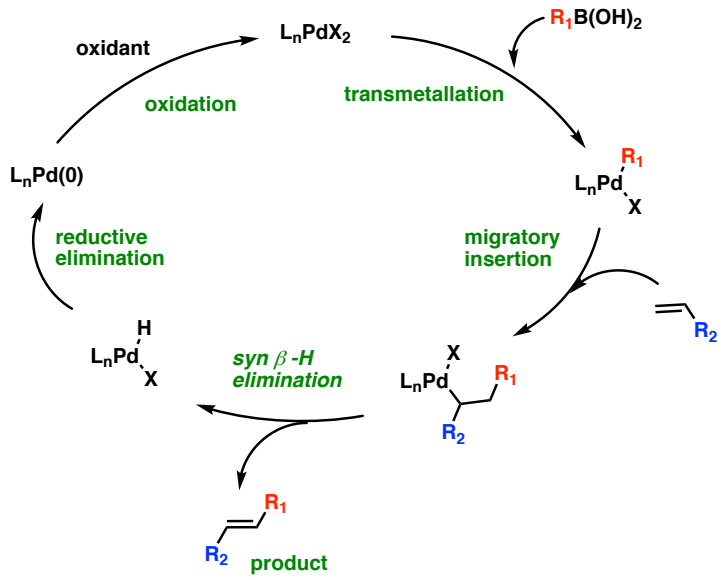

Scheme 2.5 A proposed mechanism for the oxidative Heck cross-coupling reaction.

This reaction is known to be efficient, mild, tolerant of air and moisture and have good functional group tolerance. Another benefit is that both N-based and P-based ligands can be used [33]. The ligand is not required in the reaction, but it has been proven that the ligand promotes the release of the coupling product and the recovery of the active catalyst among other things [34].

3 PROCESS DEVELOPMENT

3.1 Retrosynthesis

A retrosynthetic pathway was made to find a starting material (SM) for the new synthesis of target molecule (TM) **5** (Scheme 3.1). First a C-C disconnection was done with the oxidative Heck reaction in mind. Molecule **6** are very expensive and difficult to purchase, so this was not an option as SM. Further, a C=C disconnection was tried. This gave the Wittig reaction as an alternative, and molecule **1** as SM. **1** is an inexpensive compound with a lot of suppliers. It was therefore decided to use **1** as the starting material for the new synthesis of TM **5**.

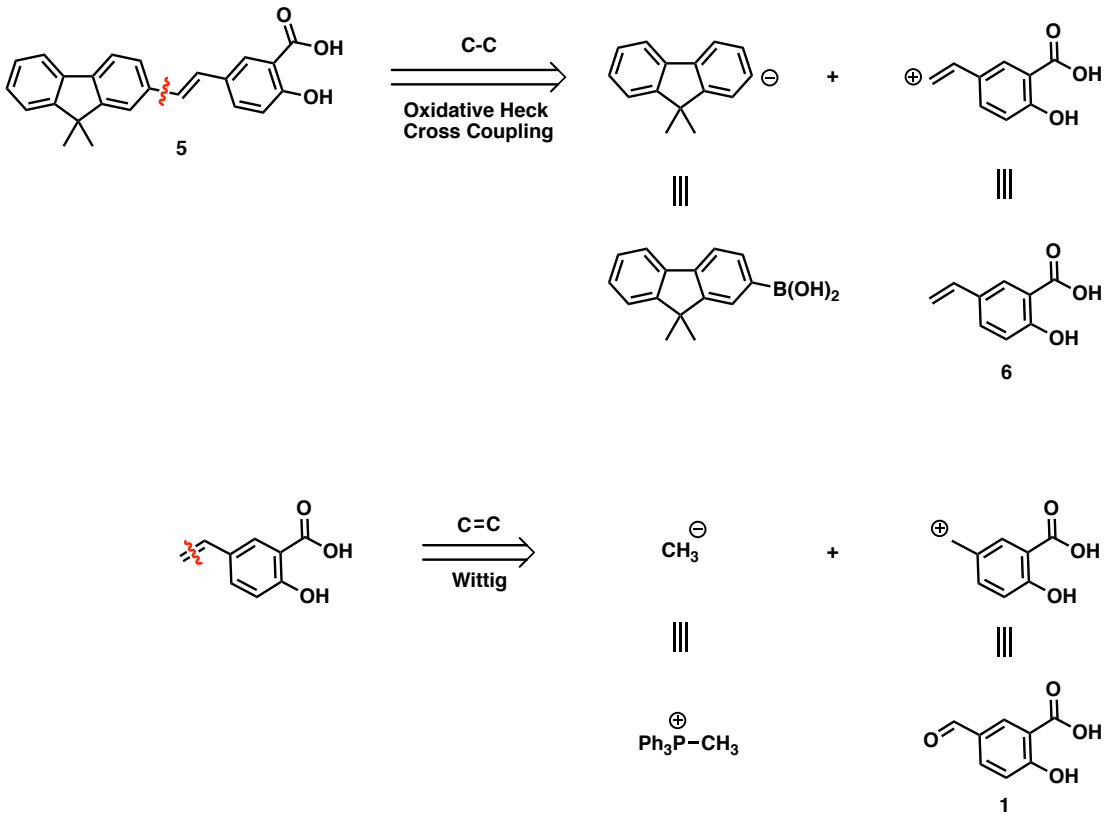

Scheme 3.1 Retrosynthesis of TM **5** to find a new starting material.

3.2 Synthetic strategy

It was established during the retrosynthetic analysis that **1** is the new SM. The oxidative Heck cross-coupling on molecule **6** have earlier been tried in the Bjørsvik research group. It was not a successful reaction, so it was decided to protect the SM with acetone. The new synthesis for **5** is shown in Scheme 3.2.

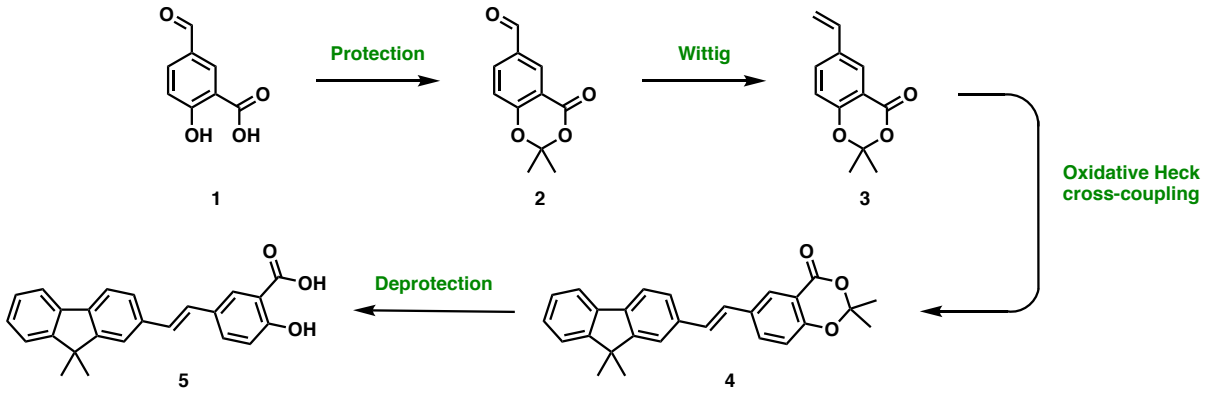

Scheme 3.2 New synthesis with protection group.

After some time, when the new synthesis with protection group was finalized, the oxidative Heck without protection was tried again. This time it was successful, and the original plan for a two-step synthesis for TM **5** as shown in Scheme 3.3 was accomplished.

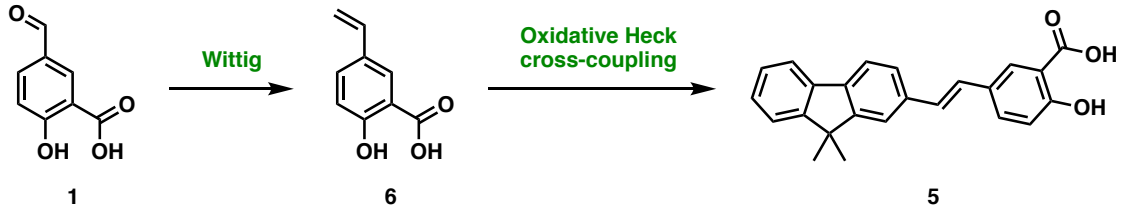

Scheme 3.3 Finalized two-step synthesis of TM **5**.

It was also desirable to create a synthesis which is greener than the original synthesis. Since the new pathway already is set out to have fewer steps, it means less reactants, less workup and purification and less solvents.

3.3 Green chemistry

When it comes to green chemistry, it is desirable to make all the reactions as green as possible. In this project, the focus was on making the new synthesis of TM **5** greener than the originally synthesis. Scheme 3.4 shows the original synthesis with reaction conditions and yields.

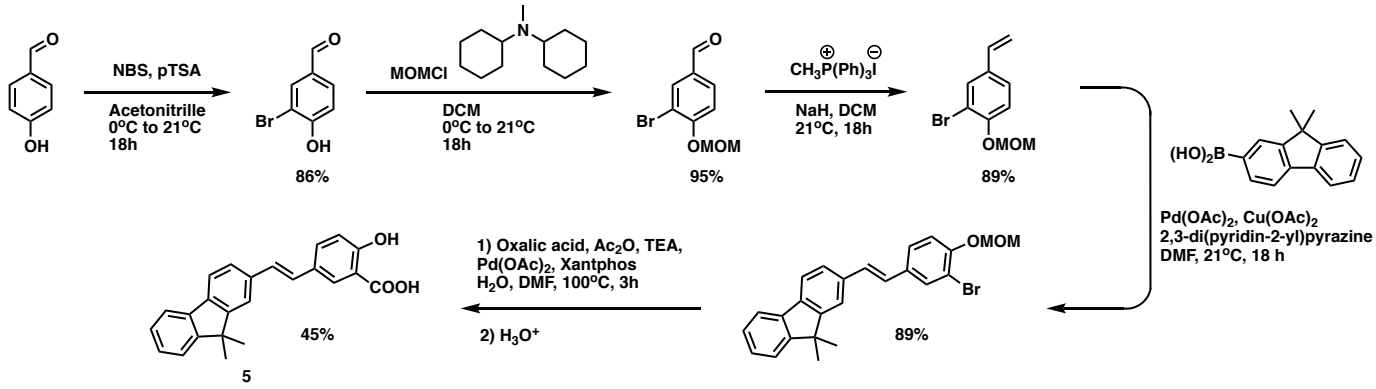

Scheme 3.4 Original synthesis of TM **5** with reaction conditions and yields.

As seen in Scheme 3.4, there is a lot of steps and a lot of reagents. Some of these are very expensive and not environmentally friendly. Each step has good yield, except the last one. However, the total yield of the synthesis is only 29%.

The first synthesis pathway made in this project was with the protection of the starting material. This synthesis with conditions and yields is shown in Scheme 3.5.

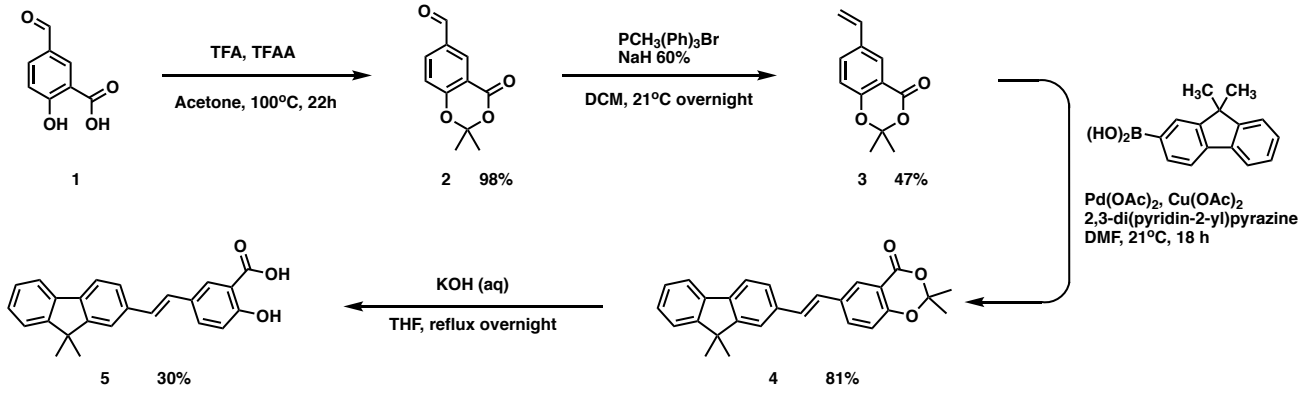

Scheme 3.5 Synthesis pathway for TM **5** with protection of the starting material.

This synthesis has four steps and requires fewer chemicals than the original synthesis. However, the overall yield is only 11%, so this was not a successful way of synthesizing compound **5**.

The other pathway was without the protection group and are presented in Scheme 3.6 with reaction conditions and yields.

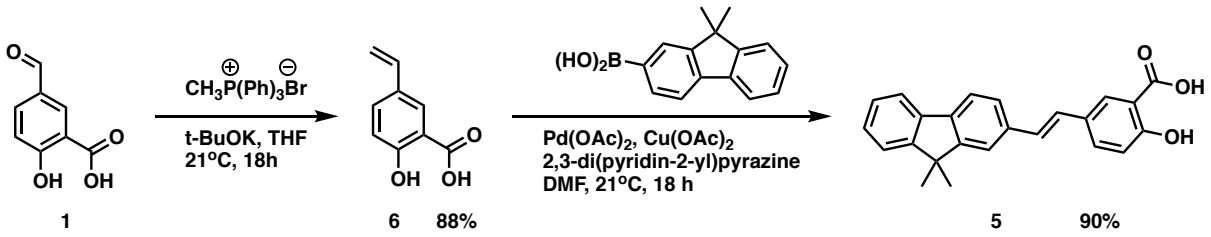

Scheme 3.6 New two-step synthesis of TM **5** with reaction conditions and yields.

This synthesis has only two steps, which means fewer reagents and solvents. Some of these are not environmentally friendly either, such as $Cu(OAc)_2$. Copper acetate is used as oxidant because this is reported in the literature to be the best oxidant [35], but other oxidants such as O_2 can also be used. The question is then if it is better with a green oxidant or higher yield. The reaction with O_2 as oxidant can also be optimized later if needed. The total yield of the synthesis is 79%, which is an extreme improvement from both the original synthesis and the first alternative shown in Scheme 3.5.

3.4 Design of new analogues

It is desirable that the drug can be taken orally to make it easier and more convenient for the patient who needs it. It was discovered that compound **5** may have a bit high log P value, log P = 5.93, for being able to be taken orally.

Orally absorbed drugs tend to follow Lipinski´s rule of five. The rules are [36]:

- A molecular weight less than 500
- No more than 5 hydrogen bond donor (HBD) groups
- No more than 10 hydrogen bond acceptor (HBA) groups
- A calculated log P value less than +5

Figure 4.10 shows the hydrogen bond donors and hydrogen bond acceptors of compound **5**. The groups marked with green can act as both HBD and HBA, and the pink one as HBA. This means that it in total is three hydrogen bond acceptors and two hydrogen bond donors, which is fine according to the rule. The molecular weight (MW) for the compound is also lower than 500 which the rule says. The only problem according to this rule is therefore the log P value. However, Lipinski himself said that if a compound did not break more than one of his rules, the compound was likely to be orally active [36].

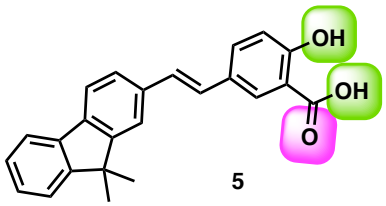

5

MW = 356.42, log P = 5.93

Figure 3.1 HBD, HBA, molecular weight and log P for compound **5**.

It was decided to synthesize the new analogues with a lower log P value to see if those were better alternatives for oral activity. Three of the analogues tried synthesized in this project is shown in Figure 3.2.

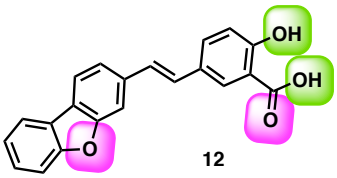

12

MW = 330.34, log P = 4.57

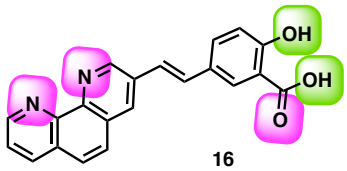

16

MW = 342.35, log P = 3.56

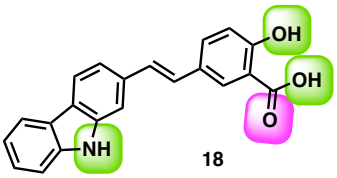

18

MW = 329.36, log P = 4.50

Figure 3.2 Three of the new analogues tried synthesized in this project.

4 RESULT AND DISCUSSION

4.1 Synthesis towards DC21, (*E*)-5-(2-(9,9-dimethyl-9*H*-fluoren-2-yl)vinyl)-2-hydroxybenzoic acid **5**, with protection of the starting material

4.1.1 Synthesis of 2,2-dimethyl-4-oxo-4*H*-benzo[*d*][1,3]dioxine-6-carbaldehyde **2** in both batch and continuous flow

The starting material **1** was protected with acetone to prevent conflicts with the hydroxy- and carboxylic acid groups during the Wittig and oxidative Heck reactions. This was done by solving 5-formyl-2-hydroxybenzoic acid **1** in trifluoracetic acid (TFA) at 0°C before adding trifluoroacetic anhydride (TFAA) and acetone dropwise. The mixture was then heated to 100°C and stirred for 24h. It was later discovered that the cooling of the reaction mixture was not necessary, so after this, the first step of the reaction was done at 21°C before heating.

This protection has been reported in the literature with a yield of 40% [37]. With some modifications of the reaction conditions such as higher reaction temperature and longer reaction time, the isolated yield in this project is 98%. The batch synthesis of **2** is shown in Scheme 4.1.

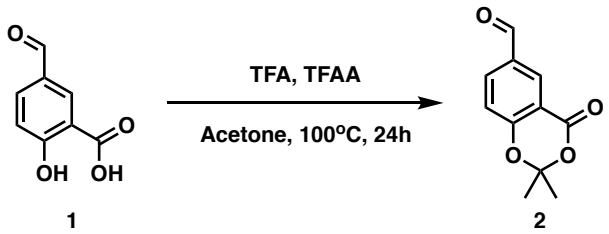

Scheme 4.1 Synthesis of 2,2-dimethyl-4-oxo-4*H*-benzo[*d*][1,3]dioxine-6-carbaldehyde **2**.

This synthesis was also tried in continuous flow chemistry. The flow diagram is shown in Figure 4.1. In reservoir one (R1) is a mixture of the SM **1**, TFA and TFAA. This is mixed with acetone from reservoir two (R2) at the y-mixer and warmed to 100°C in the reactor coil.

The flow rates for pump one (P1) and pump two (P2) was calculated from Equation 2.1, where the residence time was set to be 60 min for both. The reactor volume was 17 mL for R1 and 3mL for R2. The minimum flow rate that can be used for this reactor is 0.05 mL/min. To avoid air bubbles in the reactor, the flow rate for P2 was turned up to 0.06 mL/min instead of 0.05 mL/min that was the flow rate that should be used from the equation.

$$P1: \quad Flow\ rate = \frac{17\ mL}{60\ min} = 0.283\ mL/min$$

$$P2: \quad Flow\ rate = \frac{3.0\ mL}{60\ min} = 0.050\ mL/min$$

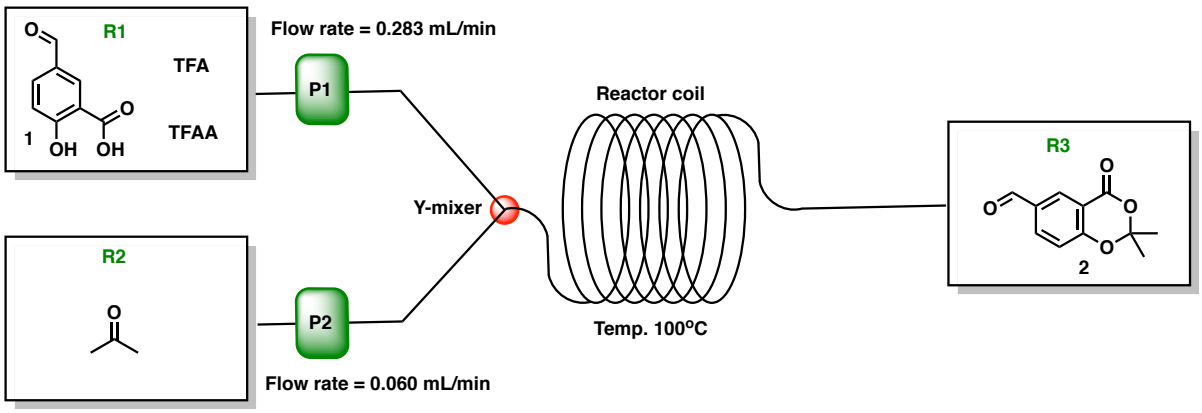

Figure 4.1 Flow diagram for the synthesis of **2**.

This synthesis was tried a few times, and the highest isolated yield was 65%. This is not as high as the yield from batch, but still higher that what is reported in the literature. Since the batch reaction got higher yield from longer reaction time and higher temperature, it indicates that with a lower flow rate for P1 the yield for the flow synthesis may increase. This was not tried because of the two-step synthesis towards TM **5** was discovered and used instead.

The ^{1}H NMR spectrum of compound **2** confirms the structure for both the batch and the flow synthesis. There is one new signal in the upfield alkane region at 1.78 ppm that integrates to six hydrogens as expected for the protection group. In addition to this, there is three signals in the aromatic region that corresponds to the aromatic hydrogens, and one most downfield at 9.96 ppm that corresponds to the aldehyde, see Figure 4.2. The structure was also confirmed with ^{13}C NMR spectroscopy [Appendix].

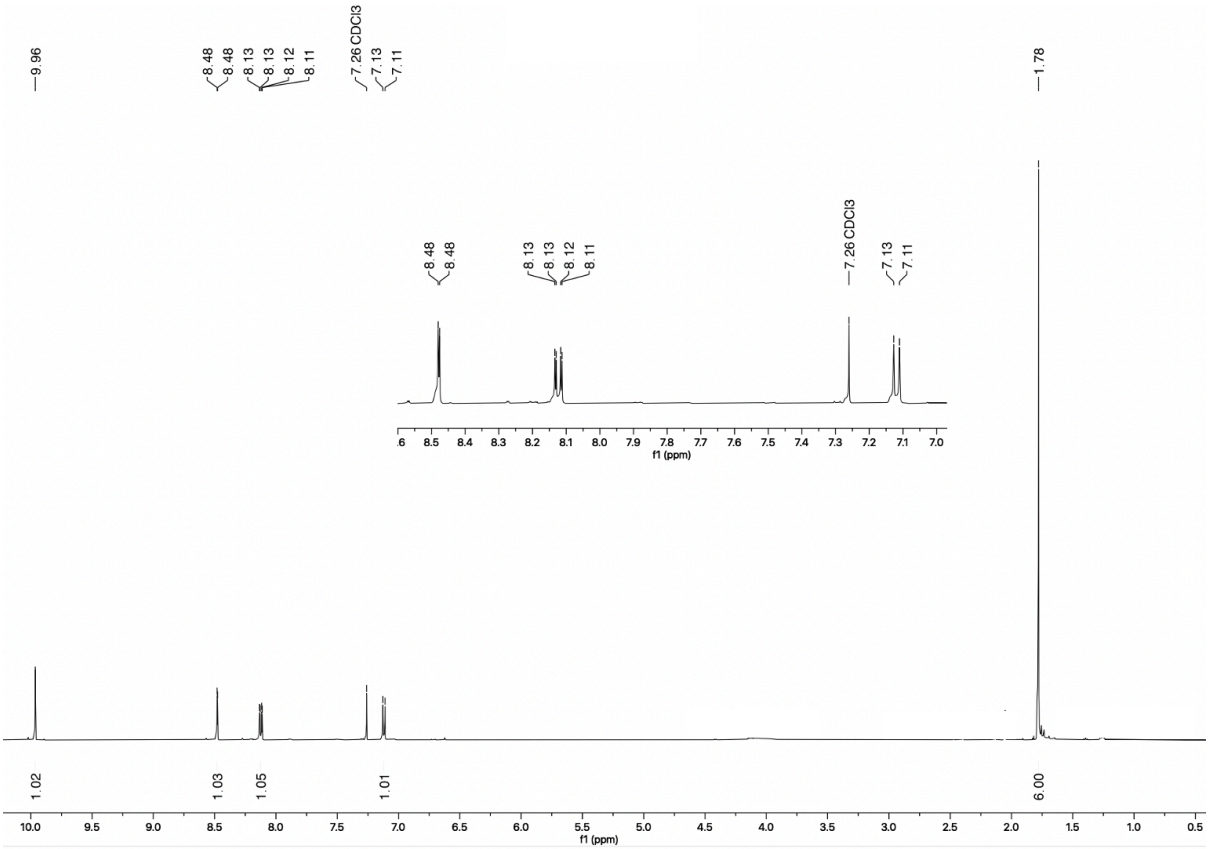

Figure 4.2 ^{1}H NMR spectrum of compound **2**.

4.1.2 Optimization of the Wittig reaction for the synthesis of 2,2-dimethyl-6-vinyl-4*H*-benzo[*d*][1,3]dioxin-4-one **3**

Compound **3** was made in two different ways. The first method was a Wittig reaction on compound **2** using a variety of different reaction conditions, that are shown in Table 4.1, to try to increase the yield. The first method for synthesizing **3** is presented in Scheme 4.2. This was done by solving methyltriphenylphosphonium bromide in dichloromethane (DCM) at 0°C before adding NaH. This was stirred for 30 min before compound **2** was added. The reaction was then left for stirring at 21°C for 16 h.

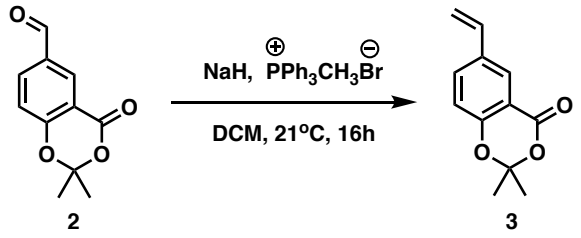

Scheme 4.2 First method for synthesizing 2,2-dimethyl-6-vinyl-4*H*-benzo[*d*][1,3]dioxin-4-one **3**.

In addition to the different reaction conditions shown in Table 4.1, the equivalents (equiv.) of the base and both anhydrous and regular solvent was tried in various combinations. None of these combinations showed much of a difference. The change of the phosphonium salt from methyltriphenylphosphonium bromide (MTPBr) to methyltriphenylphosphonium iodide (MTPI) was not successful for increasing the yield either.

Table 4.1 Different reaction conditions in the synthesis of **3** to try to increase the yield.

Entry	Base	Solvent	Reaction time	MTPBr/ MTPI	Yield (%)
1	NaH	DCM	16 h	MTPBr	48
2	NaOH (aq)	DCM	30 min.	MTPBr	21
3	tBuOK	THF	18 h	MTPBr	26
4	nBuLi	THF	1 h	MTPBr	-
5	NaH	DCM	16 h	MTPI	45

A second method for synthesizing **3** was tried to see if the yield increased. The Wittig reaction was done on SM **1** and gave compound **6** in high yield. Then the protection was done on compound **6**. The second method for synthesizing **3** is shown in Scheme 4.3.

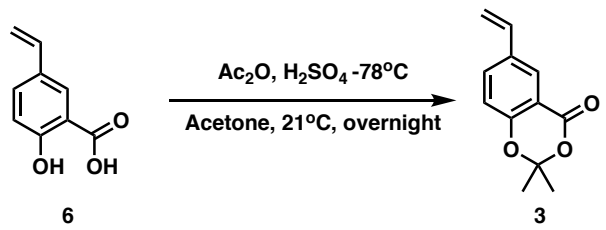

Scheme 4.3 Second method for synthesizing 2,2-dimethyl-6-vinyl-4*H*-benzo[*d*][1,3]dioxin-4-one **3**.

The reaction conditions for the protection of SM **1** (Scheme 4.1) were first tried on compound **6**. This gave no result, so a different method was carried out (Scheme 4.3). This was done by solving compound **6** in acetic anhydride and acetone before cooling the mixture to -78°C in a dry ice/acetone bath. The sulphuric acid was added slowly before the mixture was allowed to warm to 21°C and was left for stirring overnight. This method gave compound **3** in low yield (24 %). The overall yield is therefore higher for the synthetic rout where the protection is done first, followed by the Wittig reaction.

Compound **3** from both these reactions were confirmed with ^{1}H NMR spectroscopy (Figure 4.3). The signal for the aldehyde at 9.96 ppm is gone, and there are signals at 6.67 ppm, 5.72 ppm and 5.27 ppm which corresponds to the new alkene. These signals have high coupling constants, 17.6 and 10.9 Hz, which is characteristic for alkenes. The signals at 7.98 ppm, 7.60 ppm and 6.93 ppm are for the aromatic hydrogens as expected. The protection group is also present at 1.73 ppm. The structure of compound **3** was also confirmed with ^{13}C NMR spectroscopy [Appendix].

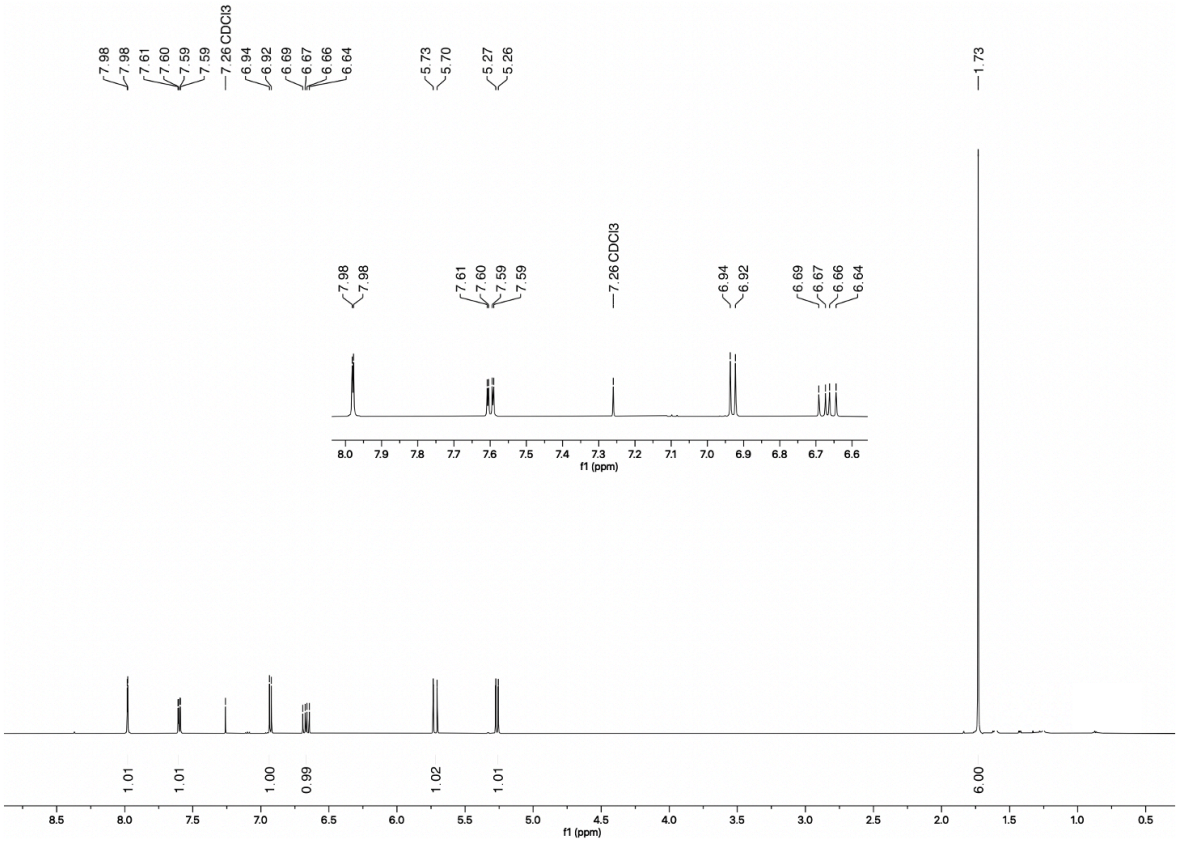

Figure 4.3 ^{1}H NMR spectrum of compound **3**.

As mentioned above, the change of the phosphonium salt from methyltriphenylphosphonium bromide to methyltriphenylphosphonium iodide was done as an attempt to increase the yield for the Wittig reaction. This reaction was done by solving triphenylphosphine in tetrahydrofuran (THF) before adding iodomethane slowly. The mixture was flushed with nitrogen and stirred at reflux for 18h. The reaction is shown in Scheme 4.4.

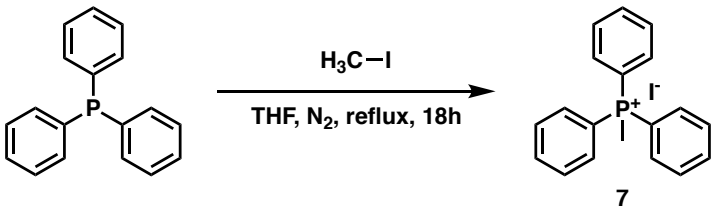

Scheme 4.4 Synthesis of methyltriphenylphosphonium iodide **7**.

It was not expected a major difference from the methyltriphenylphosphonium bromide since the halogen plays no part in the further Wittig reaction, but it was decided to try anyways since the literature reported higher yield when MTPI was used [14]. As seen in Table 4.1, there is no remarkable difference, it gives in fact a slightly lower yield in the synthesis of compound **3**.

The structure of compound **7** was confirmed using ^{1}H NMR spectroscopy [Appendix].

4.1.3 Synthesis of (*E*)-6-(2-(9,9-dimethyl-9*H*-fluoren-2-yl)vinyl)-2,2-dimethyl-4*H*-benzo[*d*][1,3]dioxin-4-one **4**

The oxidative Heck cross-coupling came with some difficulties. It was not reported in the literature [14] that it was important to add the oxidant after the other reagents. The first time this reaction was done (Scheme 4.5) the oxidant was added along with the other reagents like the literature reported. Since no product was observed, other oxidants such as MnO_2 and O_2 balloon was tried. This gave no successful result either.

After doing some additional research, it was decided to try to add all the reagents except the oxidant ($Cu(OAc)_2$), and solve them in dimethylformamide (DMF). $Cu(OAc)_2$ was then added, and the reaction mixture was left for stirring for 18h. Compound **4** was then collected in high yield (81%). The oxidant $Cu(OAc)_2$ was removed by extraction with a solution of ethylenediaminetetraacetic acid (EDTA) in water before further purifications.

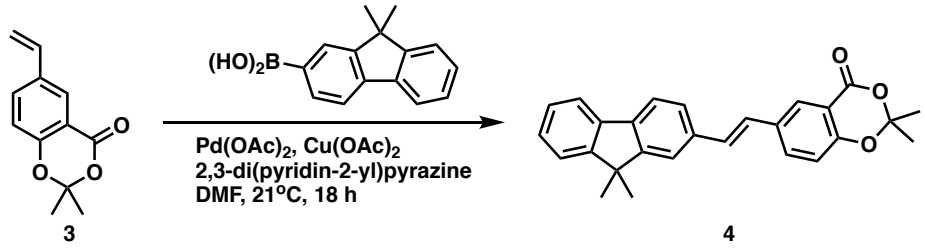

Scheme 4.5 Synthesis of (*E*)-6-(2-(9,9-dimethyl-9*H*-fluoren-2-yl)vinyl)-2,2-dimethyl-4*H*-benzo[*d*][1,3]dioxin-4-one **4**.

The structure of compound **4** was confirmed with ^{1}H NMR spectroscopy, see Figure 4.4. There are two signals in the upfield alkane region at 1.54 ppm and 1.77 ppm which both integrates to 6H. These signals belong to the protection group (1.77 ppm) and the two -CH_3 groups from the boronic acid (1.54 ppm). There is also a lot of signals in the downfield aromatic region (8.15 ppm – 6.97 ppm) which is expected for this compound. The signals at 7.19 ppm and 7.12 ppm have both a coupling constant of 16.3 Hz which is characteristic for a trans alkene [38]. There is a total of 24 hydrogens in this specter which is the same number of hydrogens in compound **4**. There are signals that belongs to hexane in the most upfield region of the specter at 1.26 ppm and 0.88 ppm. Hexane was used as eluent (hexane/ethyl acetate 9:1) for flash column chromatography. The structure was also confirmed with ^{13}C NMR spectroscopy [Appendix].

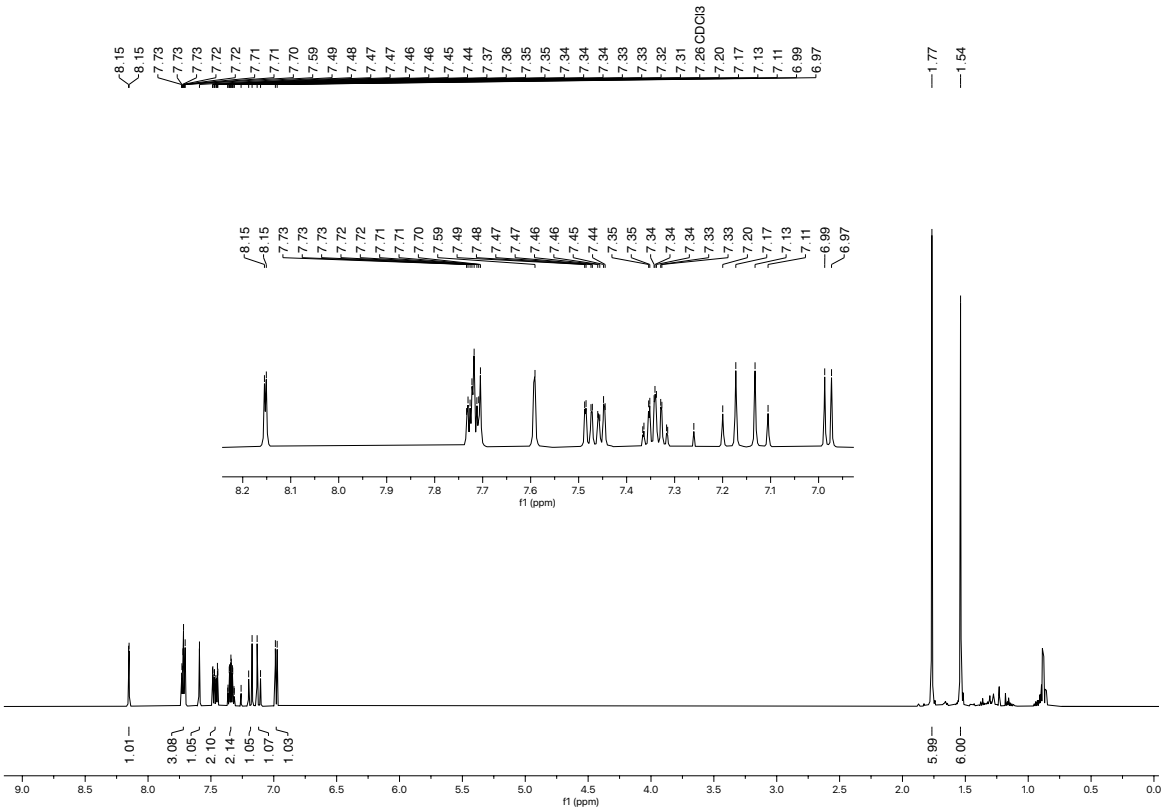

Figure 4.4 ^{1}H NMR spectrum of compound **4**.

4.1.4 Deprotection to get DC21, (*E*)-5-(2-(9,9-dimethyl-9*H*-fluoren-2-yl)vinyl)-2-hydroxybenzoic acid **5**

The synthesis of compound **5** is shown in Scheme 4.6. Compound **4** was solved in THF before KOH solved in water was added. The reaction mixture was heated to reflux and stirred overnight. The crude product was a yellow oil in high yield (95%). The NMR- and LC-MS spectrum of compound **5** showed a pure product, but the HPLC chromatogram did not. There were two signals overlapping. When the crude was dissolved in chloroform, there was a white powder that precipitated. This was collected by vacuum filtration, and a new HPLC analysis was done. This time it was only one signal, but the yield had decreased to 40%.

Another method for synthesizing compound **5** was done (Scheme 4.8). This reaction is discussed below along with the continuous flow synthesis.

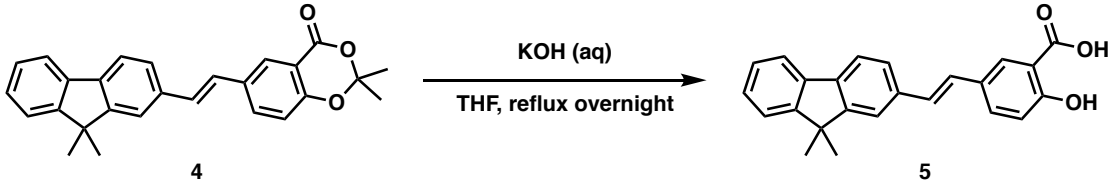

4 **5**

Scheme 4.6 Synthesis of (*E*)-5-(2-(9,9-dimethyl-9*H*-fluoren-2-yl)vinyl)-2-hydroxybenzoic acid **5**.

The structure of compound **5** was confirmed with ^{1}H NMR spectroscopy, Figure 4.5. The spectrum is similar to the one for compound **4**, but the protection group at 1.77 ppm is gone. There is a lot of signals in the aromatic region, 8.04 ppm – 7.00 ppm, that corresponds to the structure. The two hydrogens for the hydroxy and carboxyl groups are not visible in this spectrum. The total amount of hydrogens visible is therefore 18, which matches the number of 20 hydrogens (including hydroxy and carboxyl group) in compound **5**. The structure was also confirmed with ^{13}C NMR spectroscopy, the mass was confirmed with LC-MS and the purity was analyzed with HPLC [Appendix].

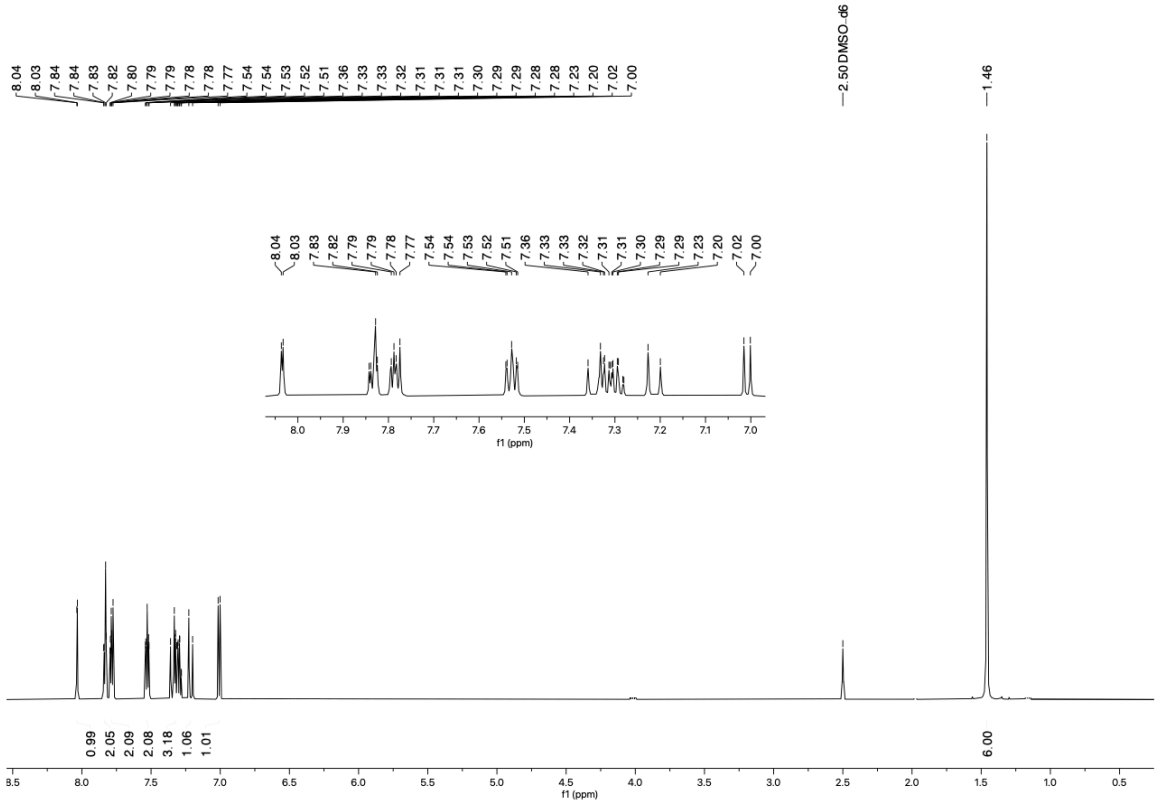

Figure 4.5 ^{1}H NMR spectrum of compound **5**.

4.2 Two-step synthesis towards DC21, (*E*)-5-(2-(9,9-dimethyl-9*H*-fluoren-2-yl)vinyl)-2-hydroxybenzoic acid **5** in both batch and flow

After the four-step synthesis of compound **5** was completed, it was decided to try to synthesize the compound without protection. This did not give a successful result when it was done earlier, but since the overall yield of the four-step synthesis was very low, it was decided that it was worth a try. This time it was successful, and the new two-step synthesis towards compound **5** is presented below.

4.2.1 Synthesis of 2-hydroxy-5-vinylbenzoic acid **6**

The Wittig reaction was tried direct on the unprotected starting material **1**. At 0°C, methyltriphenylphosphonium bromide was added to a round bottom flask along with THF. Potassium tert-butoxide was slowly added and the suspension was left for stirring for 30 min before being warmed to 21°C. SM **1** was added, and the mixture was left for stirring for 16h.

Following the reaction conditions presented in Scheme 4.7, compound **6** were isolated in a yield of 90%. This is far better than any of the other Wittig reactions done in this project.

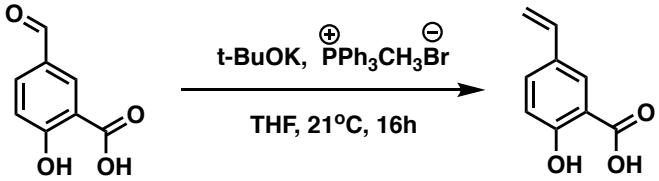

Scheme 4.7 Synthesis of 2-hydroxy-5-vinylbenzoic acid **6**.

To be able to do this step on continuous flow chemistry, some changes had to be done from the conditions in Scheme 4.7. This is because the mixture is not in solution at any time during the reaction course which is required by the microreactor.

The main problem is that MTPBr/MTPI is not soluble in THF, and the base t-BuOK are very sensitive to a variety of solvents [39]. However, it was decided to try some different solvent systems to see if the reagents would go into solution. Some of the different solvent system tried is shown in Table 4.2.

Table 4.2 Some of the solvent system that were tried to get the reaction in solution.

Entry	Solvent	Co-solvent	Solubility
1	t-BuOH	-	Not soluble
2	t-BuOH	MeOH	Not soluble
3	THF	DCM	Not soluble
4	t-BuOH	DCM	Not soluble

Since none of the solvent combinations worked, it was decided to change the base. NaH was not an alternative as base as it is insoluble in most organic solvents [40]. Another base that could be used is NaOH. The reaction was first tested in batch, where 0.2 M NaOH was used as base, and DCM as solvent. This gave no product, so other experiments were carried out with the conditions presented in Table 4.3.

Table 4.3 Some of the reagents tried to synthesize compound **6** in solution phase.

Entry	Base	Solvent	Result
1	0.2 M NaOH	DCM, H_2O	No product observed
2	1.0 M NaOH	DCM, DMF, H_2O	No product observed
3	0.5 M $NaOCH_3$	MeOH	No product observed

There has not been found a successful reaction where compound **6** is synthesized, and the reaction mixture is in solution phase. This means that it is not possible to synthesize this compound on continuous flow right now. There must be done some more research on which reaction conditions that can provide the product and do it in solution. Another possibility is to purchase a microreactor that can be used with slurries.

The structure of compound **6** was confirmed with ^{1}H NMR spectroscopy, Figure 4.6. There are three signals in the aromatic region, most downfield in the spectrum, at 7.82 ppm, 7.69 ppm and 6.95 ppm which corresponds to the aromatic hydrogens. The signals at 6.70 ppm, 5.70 ppm and 5.16 ppm correspond to the alkene. These has also higher coupling constant than the aromatic signals as expected for alkenes. There is also no signal for aldehyde, which confirms that compound **6** has been synthesized. The structure was also confirmed by ^{13}C NMR spectroscopy, and the mass of the compound was confirmed using LC-MS spectrometry [Appendix].

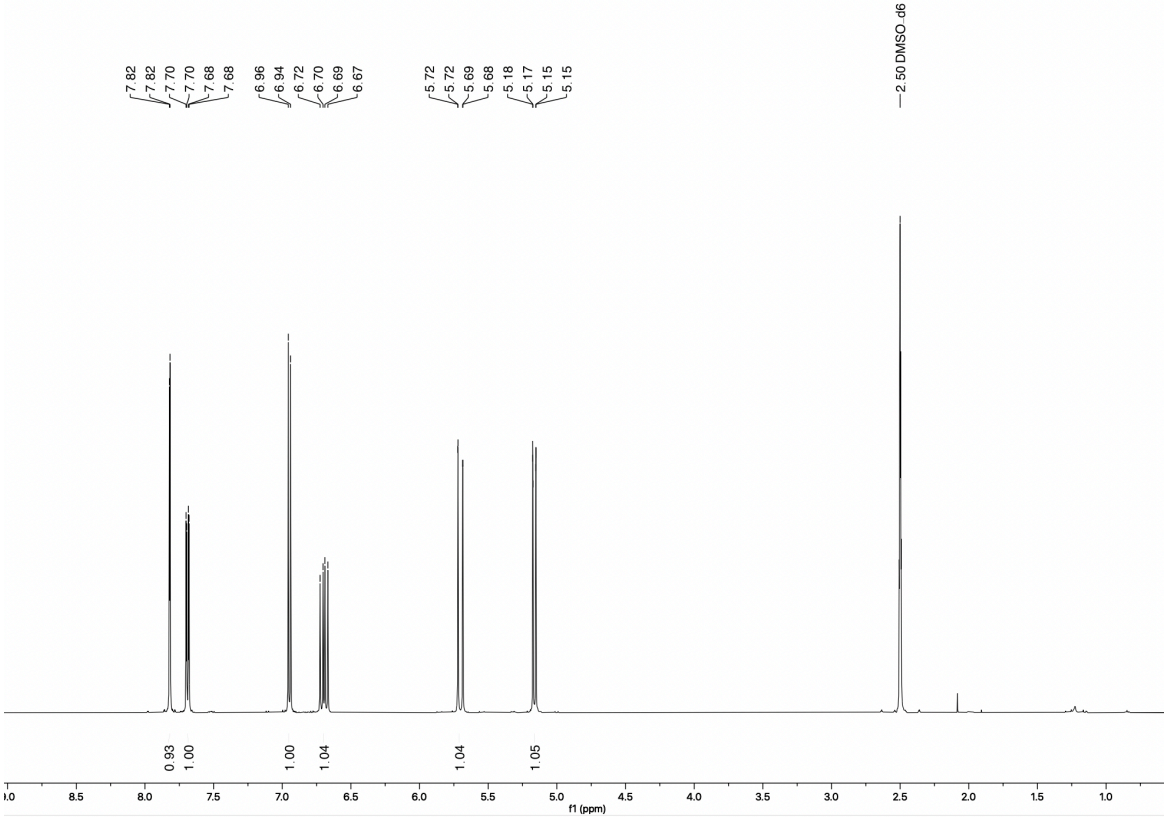

Figure 4.6 ^{1}H NMR spectrum of compound **6**.

4.2.2 A different way of synthesizing DC21, (*E*)-5-(2-(9,9-dimethyl-9*H*-fluoren-2-yl)vinyl)-2-hydroxybenzoic acid **5**

Another method for synthesizing compound **5** is shown in Scheme 4.8. It was decided to try to do the oxidative Heck reaction direct on the unprotected Wittig product **6**. As mentioned earlier, this reaction has been tried before, but was not successful. This time the reaction worked, maybe because of the order of which the reagents were added to the reaction mixture. The reaction was carried out as described for compound **4**, where all the other reagents except the oxidant were solved in DMF before adding $Cu(OAc)_2$. The reaction was stirred at 21°C for 18h. Compound **5** was collected in high yield (90%) as expected for the oxidative Heck cross-coupling.

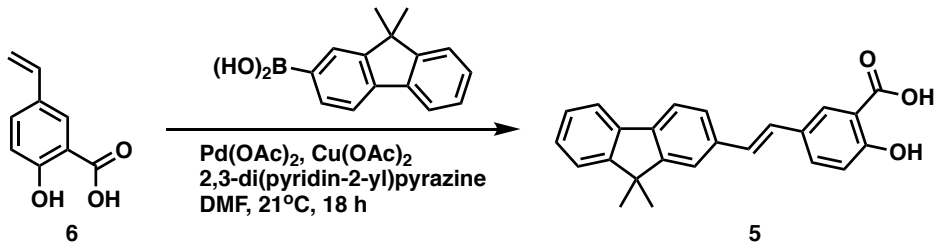

Scheme 4.8 A second method for synthesizing compound **5**.

Compound **5** were also synthesized using continuous flow chemistry to see if it was possible to synthesize the compound with a shorter reaction time. The flow diagram is shown in Figure 4.7. In reservoir one is a mixture of compound **5**, the boronic acid, the ligand and the catalyst. This is mixed with the oxidant from R2 at the y-mixer and transferred through the reactor coil at 22°C.

The flow rate for P1 and P2 was calculated from Equation 2.1, where the residence time was set to be 60 min for both. The reactor volume was 10 mL for reservoir one and 15 mL for reservoir two. This gives a flow rate equal to 0.167 mL/min for P1 and 0.250 mL/min for P2.

$$P1: \quad Flow\ rate = \frac{10\ mL}{60\ min} = 0.167\ mL/min$$

$$P2: \quad Flow\ rate = \frac{15\ mL}{60\ min} = 0.250\ mL/min$$

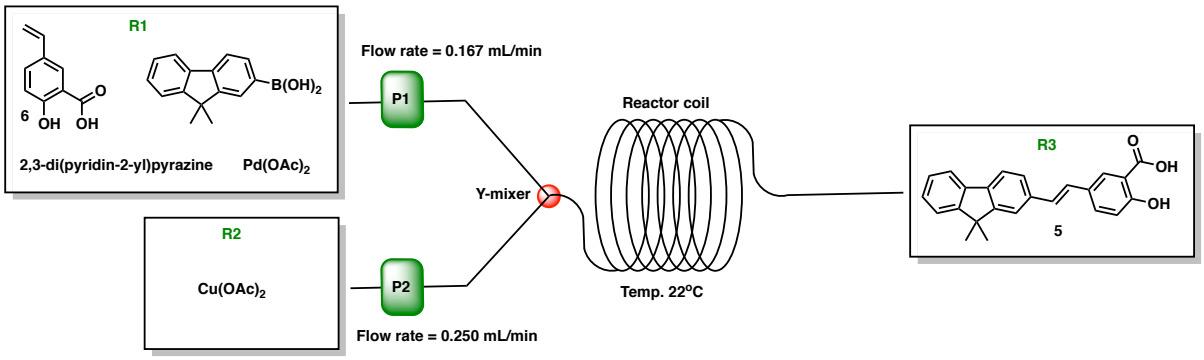

Figure 4.7 Flow diagram for the synthesis of **5.**

The yield for this reaction was only 34%. This may be because of the flow rate. Another explanation could be that a third reservoir and pump is needed, so that the catalysator is introduced alone as well.

The structure was confirmed by the same methods as described above in section 4.1.4, and the ^{1}H NMR spectrum is shown in Figure 4.5.

4.3 Synthesis towards (*E*)-5-(2-(adamantan-1-yl)vinyl)-2-hydroxybenzoic acid **10**

4.3.1 Optimization of the n-butyl lithium reaction for the synthesis of adamantan-1-ylboronic acid **8**

One of the new analogues that was tried synthesized for this project is compound **10**. To make this analogue, a new boronic acid (**8**) is required. This compound is challenging and expensive to purchase with few suppliers, so it was synthesized from 1-bromoadamantane.

This was done by solving 1-bromoadamantane in anhydrous THF and cooling the mixture to -78°C before adding n-butyl lithium slowly. The mixture was left for stirring for 30 min before trimethyl borate was added. The reaction mixture was stirred for another 30 min before being warmed to 21°C and treated with acidic water, see Scheme 4.9.

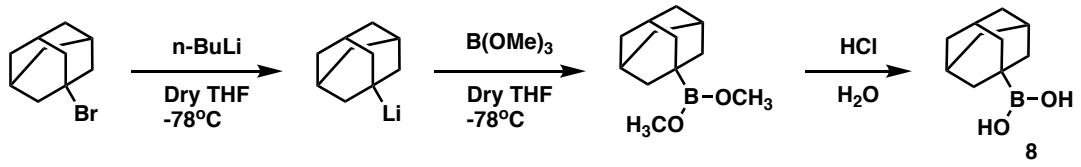

Scheme 4.9 Synthesis of adamantan-1-ylboronic acid **8**.

Several experiments with different reaction conditions were carried out in order to optimize the reaction and get the highest yield possible. The equivalents of n-butyllithium and trimethyl borate as well as the reaction time (RT) before the next step are the parameters that has been varied in these experiments. Some of these are presented in Table 4.4.

Table 4.4 An overview of some of the experiments carried out to try to optimize the reaction.

Entry	Equiv. of n-BuLi	RT n-BuLi	Equiv. of $B(OMe)_3$	RT $B(OMe)_3$	Yield (%)
1	1.2	1h	1.5	1.5h	12
2	2	40 min	3	30 min	27
3	1.2	30 min	1.5	30 min	48
4	2	30 min	3	1h	35

As seen in Table 4.4, entry three gave the best result. Another thing worth mentioning is that when the reaction is done, the crude is dissolved in hexane were the starting material dissolves, but compound **8** does not. Compound **8** is then isolated with vacuum filtration. If this is done to early, before the crude is completely dry, most of the product dissolves along with the SM. In this case, the solvent is removed, and the crude is again left to dry, and the process is repeated.

The structure of compound **8** is confirmed by ^{1}H- and ^{11}B NMR spectroscopy (Figure 4.8 and Figure 4.9). The proton spectrum shown signals in the upfield region at 1.34 ppm – 1.18 ppm, 0.84 ppm and 0.57 ppm that corresponds to adamantane. There is also a signal at 7.32 ppm that is for the RB-$(OH)_2$ group. The boron NMR spectrum has one signal at 32.34 ppm that can be an RB-$(OH)_2$ or an RB-$(OR^1)_2$ signal. Since there is no signal for methyl in the proton specter, only one for hydroxy in addition to those for adamantane, the signal in the boron specter belongs to RB-$(OH)_2$.

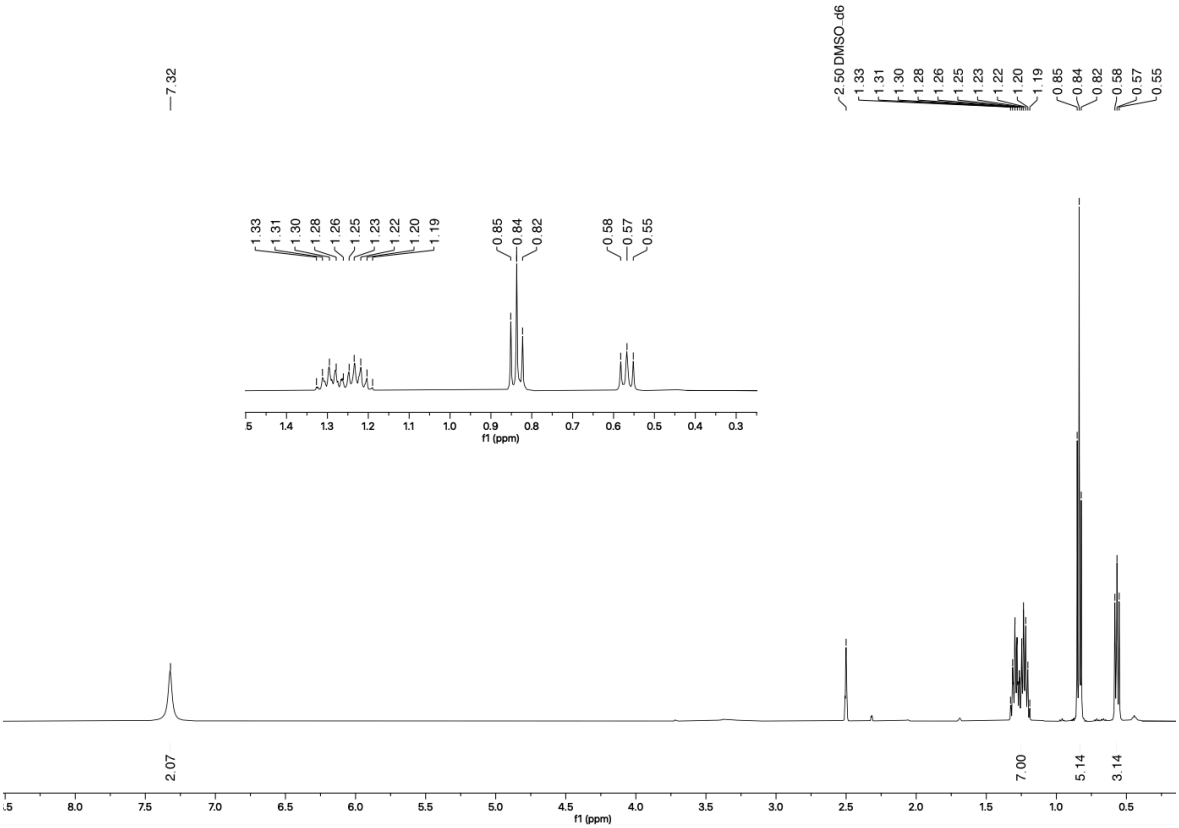

Figure 4.8 ^{1}H NMR spectrum of compound **8**.

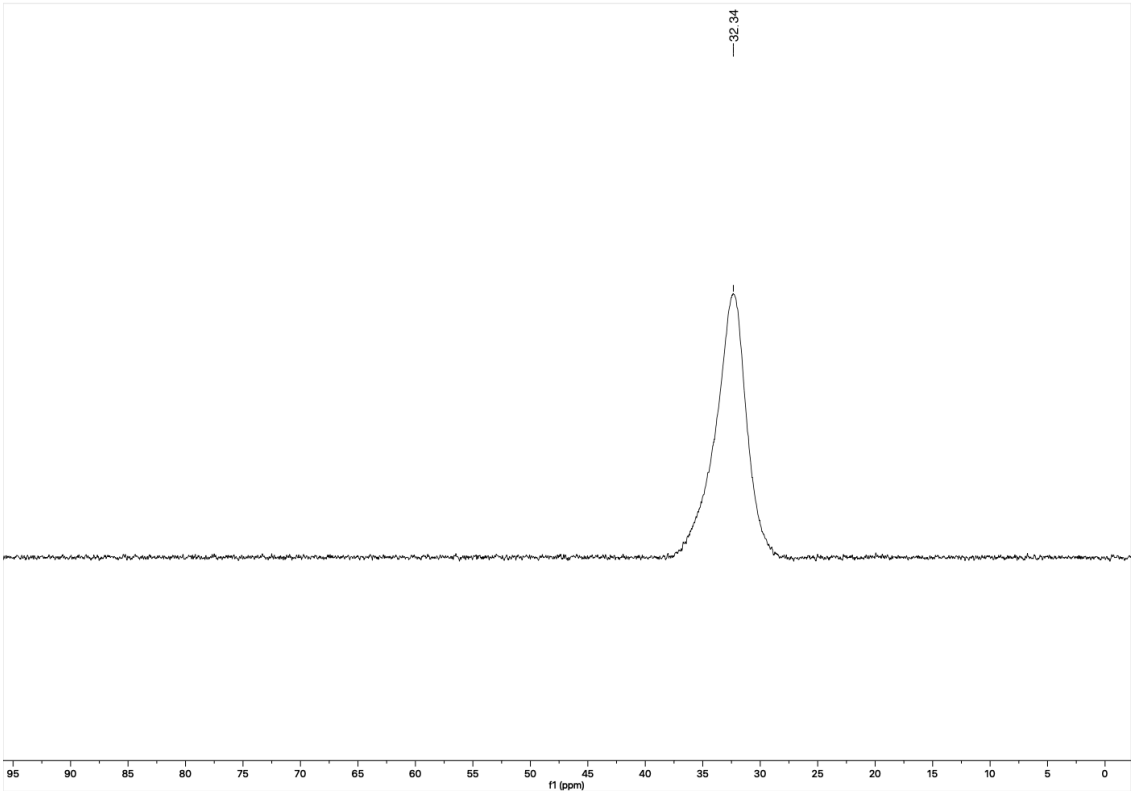

Figure 4.9 ^{11}B NMR spectrum of compound **8**.

4.3.2 Synthesis of (*E*)-6-(2-(adamantan-1-yl)vinyl)-2,2-dimethyl-4*H*-benzo[*d*][1,3]dioxin-4-one **9**

Several different syntheses were tried out in order to make compound **9**. One of these are shown in Scheme 4.10. As seen in the scheme, the reaction conditions are the same as for all the other oxidative Heck reactions, and it was carried out in the same way. The only exception is the reaction time. The course of the reaction was monitored by thin-layer chromatography (TLC) using hexane/ethyl acetate 9:1 as eluent. After 18h there was no sign of the product, only the starting material. The reaction was left stirring for five days where samples was taken out after each day. The product was nowhere to be found in any of the samples.

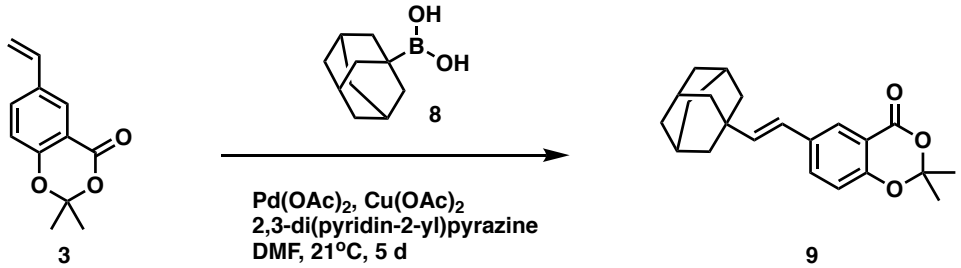

Scheme 4.10 One of the syntheses tried out in order to make compound **9**.

An ^{1}H NMR spectrum of the crude was taken to be sure that the product was not formed. As shown in Figure 4.10, compound **3** and the boronic acid did not form a bond. There are three signals for the alkene at 6.66 ppm, 5.71 ppm and 5.26 ppm, but there should only be two if the compounds were connected. The signal for RB-$(OH)_2$ are present at 5.13 ppm, which should not be there either if the two did form a bond. There are also signals at 7.98 ppm, 2.95 ppm and 2.87 ppm that belongs to the solvent, DMF.

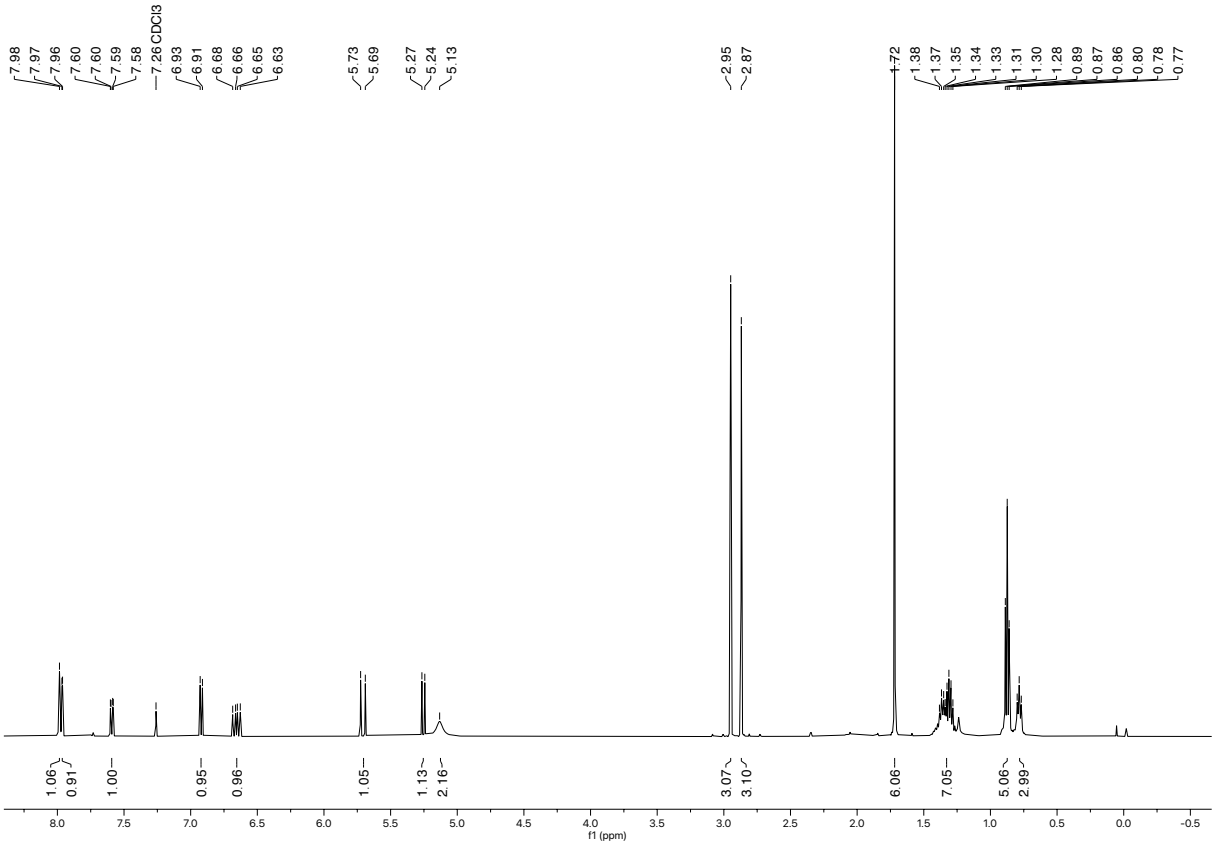

Figure 4.10 ^{1}H NMR spectrum of the crude of compound **9**.

Some other reactions were tried as well. Scheme 4.11 shows a different oxidative Heck reaction, with another oxidant and ligand, and different reaction temperature and reaction time. The reaction was carried out in similar way as the other oxidative Heck reactions. Compound **9** was not observed in this reaction either.

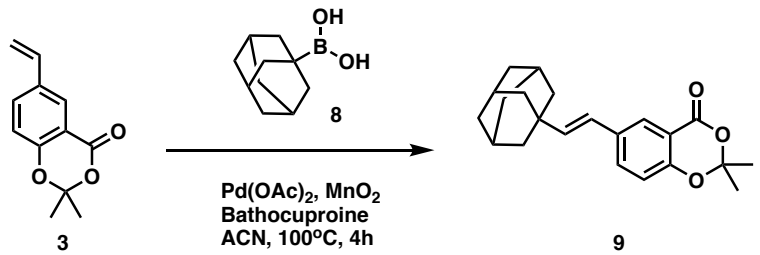

Scheme 4.11 An oxidative Heck reaction with different reaction conditions.

There was tried a regular Heck reaction as well as shown in Scheme 4.12. Compound **3**, 1-bromoadamantane and $Pd(OAc)_2$ were solved in DMF before K_2CO_3 was added. The mixture was heated to 60°C and stirred for four days. The reaction was again monitored by TLC using hexane/ethyl acetate 9:1 as eluent. The reaction time was originally 16h, but there was so sign of compound **9** after this time, so the mixture was left for stirring for four days. Samples was again taken out each day, but there was no product to be found in any of these samples either.

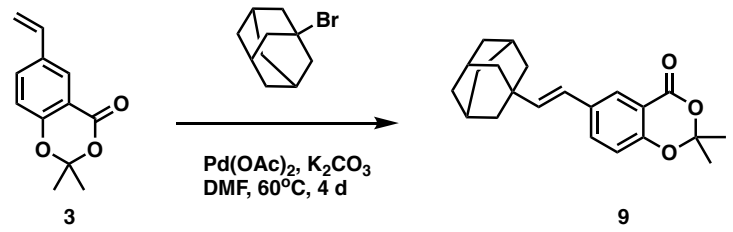

Scheme 4.12 A Heck reaction to try to synthesize compound **9**.

Other variations of the methods were also tried but none of these gave any result. It is possible that this is because adamantane is not an aromatic compound, which is required in the oxidative Heck, and regular Heck reaction.

^{1}H NMR spectrums has been taken of all the crudes even if the product did not show on TLC. All of them shows the same result as discussed above (Figure 4.10).

4.3.3 Synthesis of (*E*)-5-(2-(adamantan-1-yl)vinyl)-2-hydroxybenzoic acid **10**

One last experiment was done to see if it was possible to synthesize the new analogue, compound **10**. This reaction is the oxidative Heck reaction direct on the unprotected Wittig product, compound **6**, see Scheme 4.13. This reaction was also monitored by TLC using hexane/ethyl acetate 9:1 as eluent. The reaction run in a total of five days before it was concluded that no product was to be generated from this reaction.

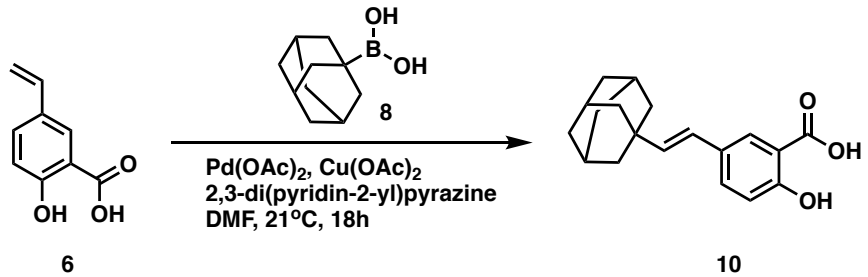

Scheme 4.13 Synthesis of (*E*)-5-(2-(adamantan-1-yl)vinyl)-2-hydroxybenzoic acid **10**.

4.4 Synthesis of three other analogues

4.4.1 Synthesis of (*E*)-6-(2-(dibenzo[*b*,*d*]furan-3-yl)vinyl)-2,2-dimethyl-4*H*-benzo[*d*][1,3]dioxin-4-one **11**

The boronic acid for the synthesis of compound **11** was commercially available, so there was no need for synthesizing it. This analogue was also made before it was discovered that the protection was not necessary.

The synthesis of compound **11** is presented in Scheme 4.14 and were carried out in the same way as the other oxidative Heck reactions. The reaction works well and gives a high yield (87%).

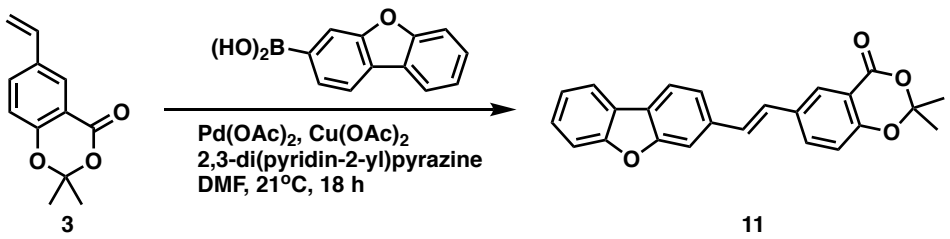

Scheme 4.14 Synthesis of (*E*)-6-(2-(dibenzo[*b*,*d*]furan-3-yl)vinyl)-2,2-dimethyl-4*H*-benzo[*d*][1,3]dioxin-4-one **11**.

The structure of compound **11** was confirmed with ^{1}H NMR spectroscopy, Figure 4.11. The protection group is present at 1.76 ppm. The rest of the signals is in the aromatic region, 8.13 ppm – 6.96 ppm, as expected. The signals at 7.19 ppm and 7.12 ppm have both a coupling constant of 16.3 Hz and this corresponds to the alkene bond. The total of 18 hydrogens in the specter is the same as number of hydrogens in the molecule. The structure was also confirmed by ^{13}C NMR spectroscopy [Appendix].

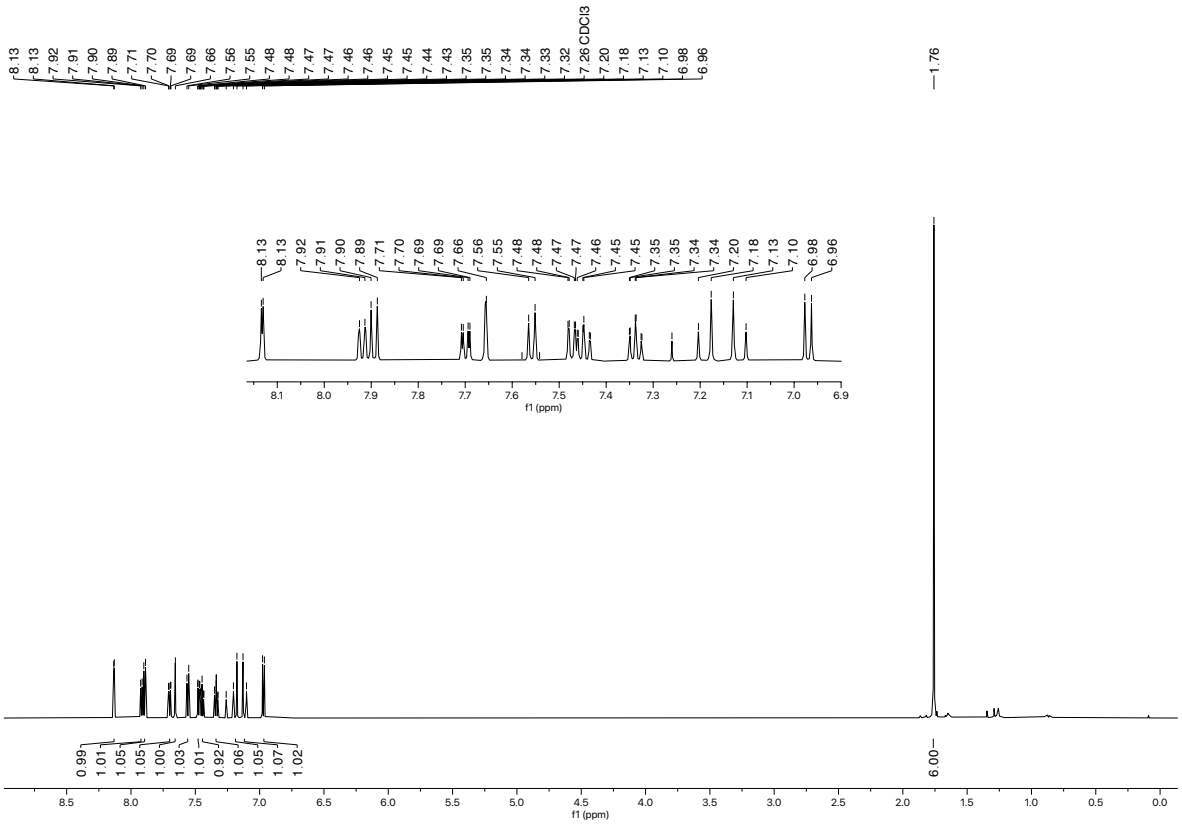

Figure 4.11 ^{1}H NMR spectrum of compound **11**.

4.4.2 Synthesis of (*E*)-5-(2-(dibenzo[*b*,*d*]furan-3-yl)vinyl)-2-hydroxybenzoic acid **12**

Compound **12** was made in two different ways. The first one (Scheme 4.15) was by deprotecting compound **11**. This was done the same way as for compound **5**, with the same problems when it comes to the yield. For the compound to be completely pure on HPLC, the yield is extremely reduced.

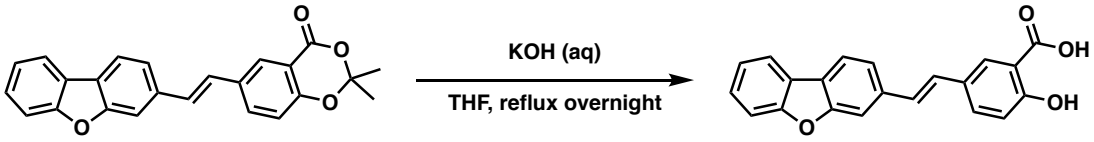

11 **12**

Scheme 4.15 Synthesis of compound **12** by deprotection of compound **11**.

A second method (Scheme 4.16) was done to better the overall yield of the synthesis towards compound **12**. The oxidative Heck reaction was done direct on the unprotected Wittig product, compound **6**, in high yield (81%).

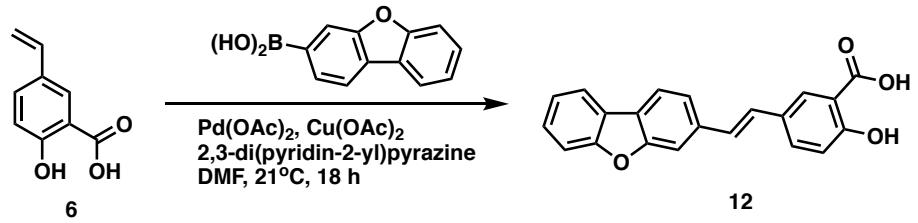

Scheme 4.16 Synthesis of (*E*)-5-(2-(dibenzo[*b*,*d*]furan-3-yl)vinyl)-2-hydroxybenzoic acid **12**.

The structure of compound **12** was confirmed by ^{1}H NMR spectroscopy for both reactions, see Figure 4.12. The specter confirms that the protection group is gone. All the signals are in the aromatic region, 8.12 ppm – 7.01 ppm, which is expected for this compound. The hydrogen signals for the hydroxy and carboxylic acid group are not visible in the specter, so the total number of hydrogens is only 12 even if the total number of hydrogens for the compound is 14. There are some traces of ethyl acetate in the specter at 4.03 ppm, 1.99 ppm and 1.17 ppm. The structure was also confirmed by ^{13}C NMR spectroscopy, the mass was confirmed with LC-MS and the purity was analyzed with HPLC [Appendix].

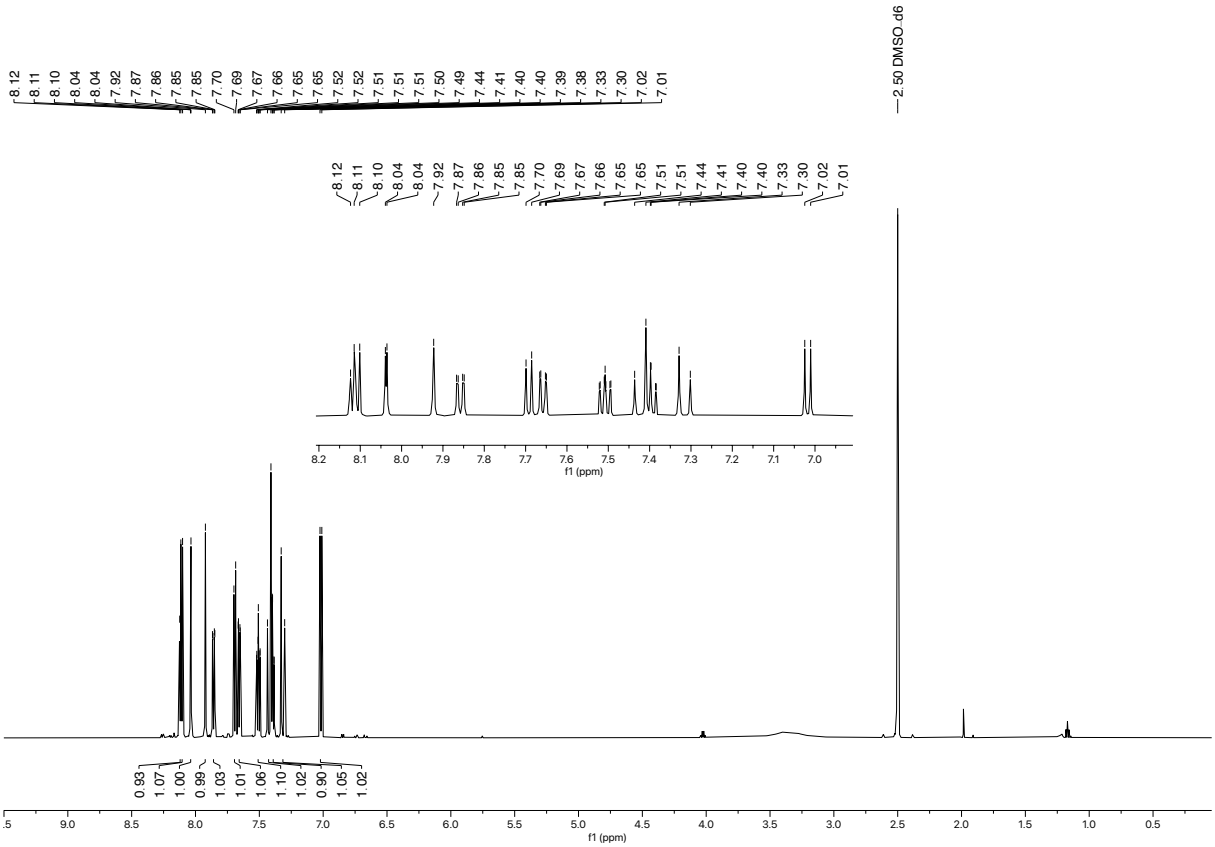

Figure 4.12 ^{1}H NMR spectrum of compound **12**.

4.4.3 Synthesis of 3-bromo-1,10-phenanthroline **13**

Compound **13** was synthesized from 1,10-phenanthroline by adding it to a round bottom flask along with nitrobenzene. This was heated to 140°C before bromine was added dropwise. The mixture was stirred for 3h and then cooled to 21°C, see Scheme 4.17. After the reaction was done, nitrobenzene was removed by a column packed with silica gel, and dichloromethane was used as eluent.

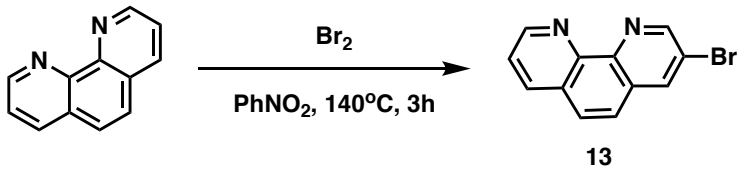

Scheme 4.17 Synthesis of 3-bromo-1,10-phenanthroline **13**.

3,8-dibromo-1,10-phenanthroline is also generated from this reaction, but this is separated from compound **13** by flash column chromatography. DCM and MeOH was used as eluent. The concentration of MeOH was increased from 0-10% from start to finish.

The yield of this reaction is only 31%. The reaction conditions were varied to see if the yield increased, but this was not successful.

The structure of compound **13** was confirmed with ^{1}H NMR spectroscopy, see Figure 4.13. All the signals are downfield in the aromatic region which is expected for this compound. There are seven hydrogens in the specter which matches the number of hydrogens in the compound. The starting material is expected to have similar signals, but it has eight hydrogens. It is therefore concluded that compound **13** is formed. The structure was also confirmed by ^{13}C NMR spectroscopy, and the mass by LC-MS spectrometry [Appendix].

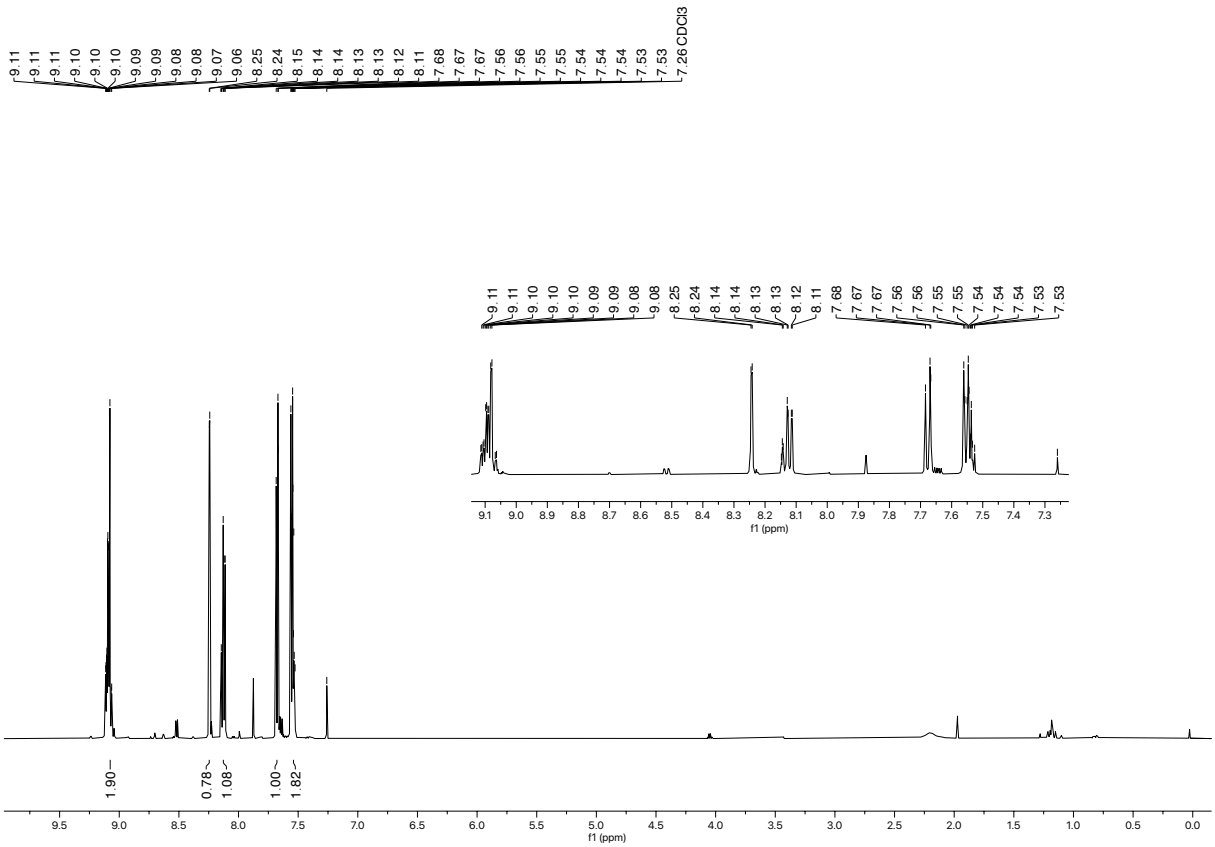

Figure 4.13 ^{1}H NMR spectrum of compound **13**.

4.4.4 Synthesis of (1,10-phenanthrolin-3-yl)boronic acid **14**

Compound **14** was tried synthesized from 3-bromo-1,10-phenanthroline **13** as shown in Scheme 4.18. As seen in the scheme, the reaction was carried out in the same way as for compound **8**. This gave no result, so it was decided to try another method as shown in Scheme 4.19.

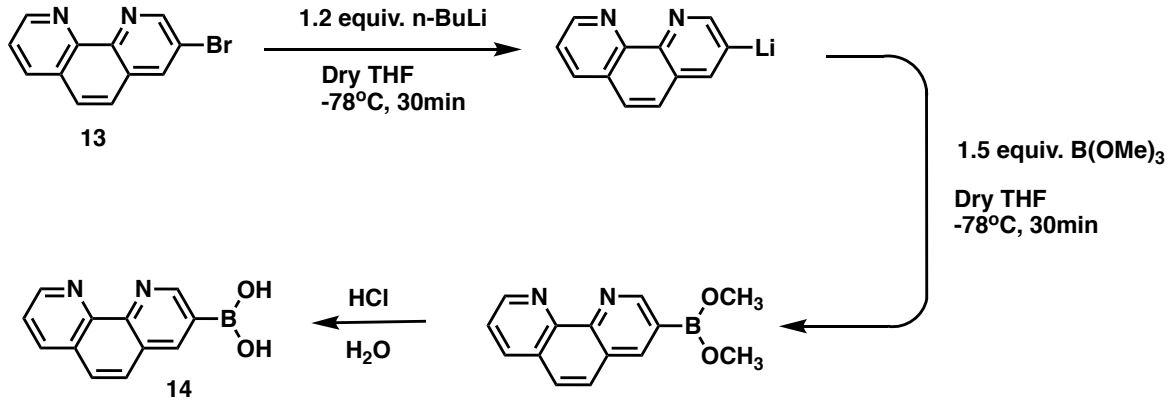

Scheme 4.18 Synthesis of (1,10-phenanthrolin-3-yl)boronic acid **14**.

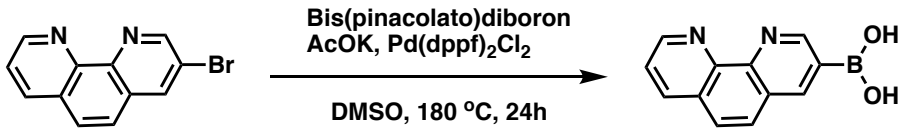

13 14

Scheme 4.19 Another method for the synthesis of (1,10-phenanthrolin-3-yl)boronic acid **14**.

This synthesis was caried out by adding 3-bromo-1,10-phenanthroline **13**, AcOK, $Pd(dppf)_2Cl_2$, bis(pinacolato)diboron and DMSO in a sealed tube reactor. This was then heated to 180°C and stirred for 24h. This reaction gave no successful result either.

4.4.5 Synthesis of (*E*)-6-(2-(1,10-phenanthrolin-3-yl)vinyl)-2,2-dimethyl-4*H*-benzo[*d*][1,3]dioxin-4-one **15**

A regular Heck reaction was tried since the synthesis of the boronic acid, compound **14**, did not work. The regular Heck reaction has not as high functional group tolerance as the oxidative Heck, so it was decided to try to do this on both the protected and the unprotected Wittig products, compound **3** and **6**.

This was done by adding compound **3**, compound **13**, $Pd(OAc)_2$, K_2CO_3 and DMF in a tube reactor. The tube reactor was then sealed and heated to 100°C for four hours. The course of the reaction was monitored by TLC where hexane/ethyl acetate 9:1 was used as eluent. The TLC showed only signals from the reagents, so the reaction was left for stirring overnight. The TLC from the next day gave the same result, so it was concluded that this reaction does not work. The reaction conditions are shown in Scheme 4.20.

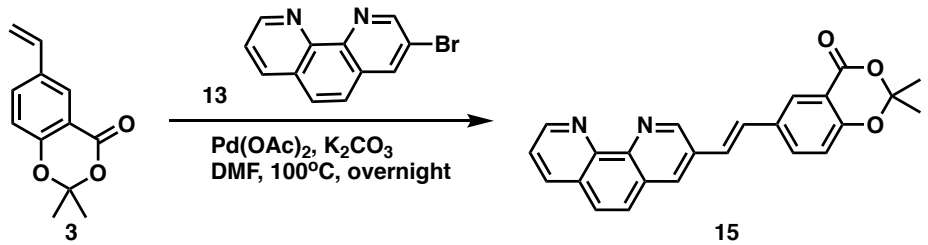

3 15

Scheme 4.20 Synthesis of (*E*)-6-(2-(1,10-phenanthrolin-3-yl)vinyl)-2,2-dimethyl-4*H*-benzo[*d*][1,3]dioxin-4-one **15**.

4.4.6 Synthesis of (*E*)-5-(2-(1,10-phenanthrolin-3-yl)vinyl)-2-hydroxybenzoic acid **16**

Compound **16** was also tried synthesized by a regular Heck reaction that was done the same way as described for compound **15**. The only difference is the starting material. In this reaction, the unprotected Wittig product, compound **6**, was used. The reaction conditions are shown in Scheme 4.21. There was no sign of compound **16** with this method either.

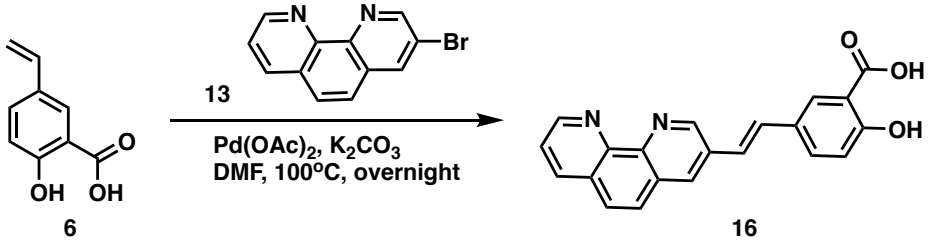

Scheme 4.21 Synthesis of (*E*)-5-(2-(1,10-phenanthrolin-3-yl)vinyl)-2-hydroxybenzoic acid **16**.

4.4.7 Synthesis of (9*H*-carbazol-2-yl)boronic acid **17**

The boronic acid, compound **17**, was synthesized from 2-bromo-9*H*-carbazole with the conditions shown in Scheme 4.22. This is the same method that were used for compound **8**. These conditions gave a yield of 45%. The reaction was carried out in the same way as for compound **8**.

In this case, the starting material is not soluble in hexane or any other solvent where the product is insoluble. Flash column chromatography is therefore required to purify the product before the next step.

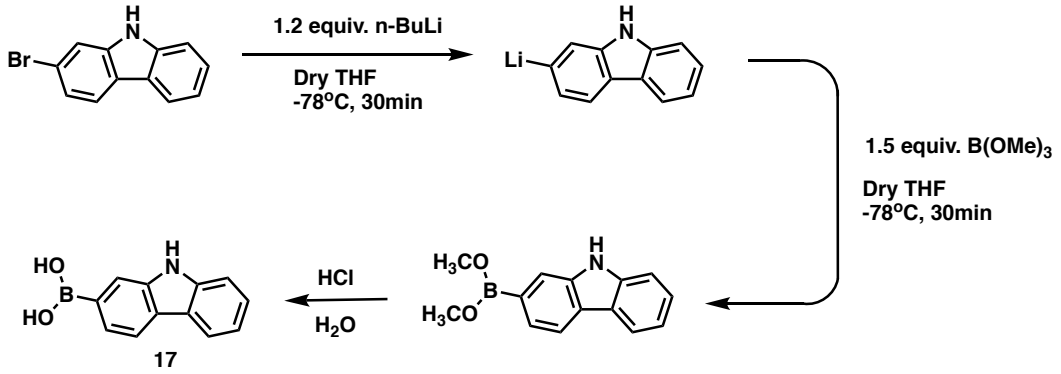

Scheme 4.22 Synthesis of (9*H*-carbazol-2-yl)boronic acid **17**.

The structure of this compound is confirmed by ^{1}H NMR spectroscopy, Figure 4.14. There is one signal in the most downfield region at 11.22 ppm for the amine. There is also a lot of signals in the aromatic region from 8.10 ppm to 7.12 ppm, which integrates to a total amount of seven hydrogens as expected for this compound. As seen in the spectrum, there is some impurities, but it was decided to use the compound without further purifications. The structure was also confirmed by ^{13}C NMR spectroscopy, and the mass was confirmed by LC-MS spectrometry [Appendix].

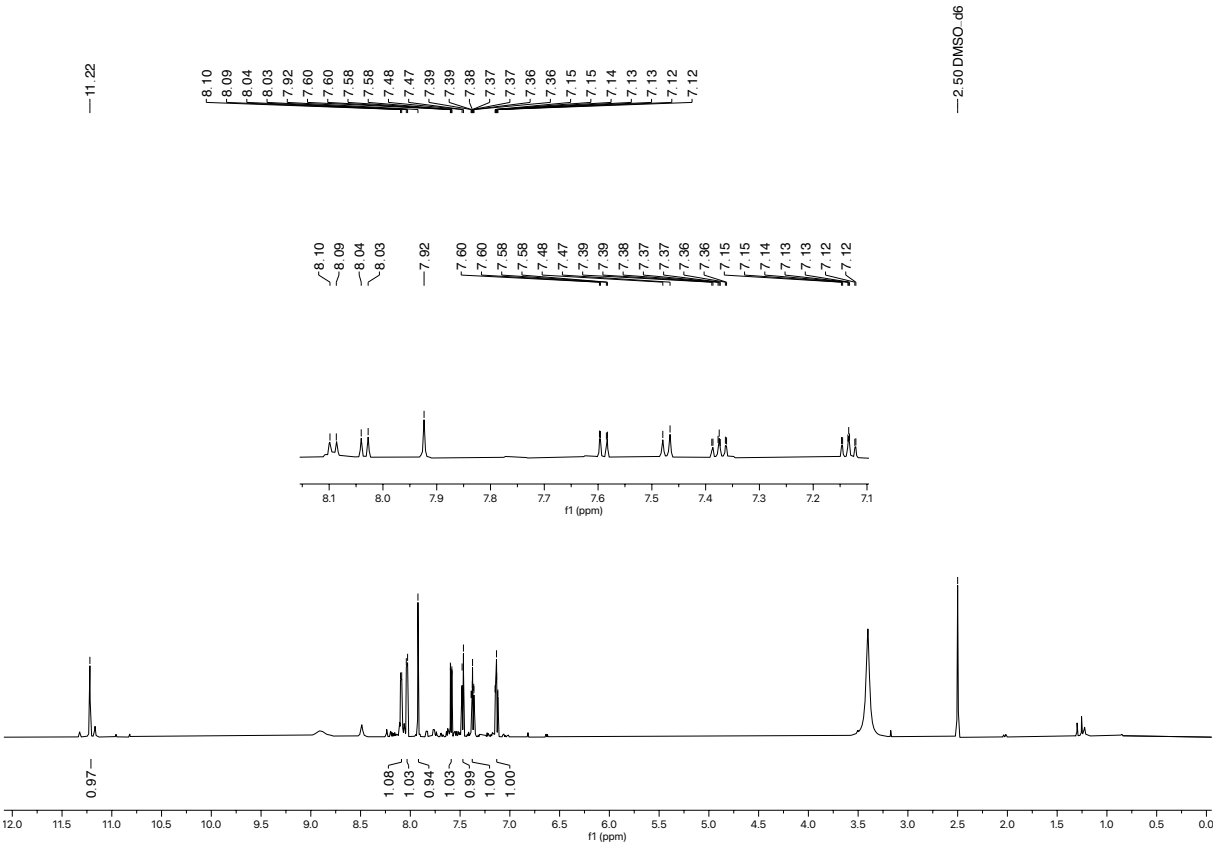

Figure 4.14 ^{1}H NMR spectrum of compound **17**.

4.4.8 Synthesis of (*E*)-5-(2-(9*H*-carbazol-2-yl)vinyl)-2-hydroxybenzoic acid **18**

The last analogue made was compound **18**. This reaction was done in the same way as all the other oxidative Heck reactions. The synthesis of compound **18** is shown in Scheme 4.23. The yield from this reaction was also high, 86%, as expected for the oxidative Heck reaction.

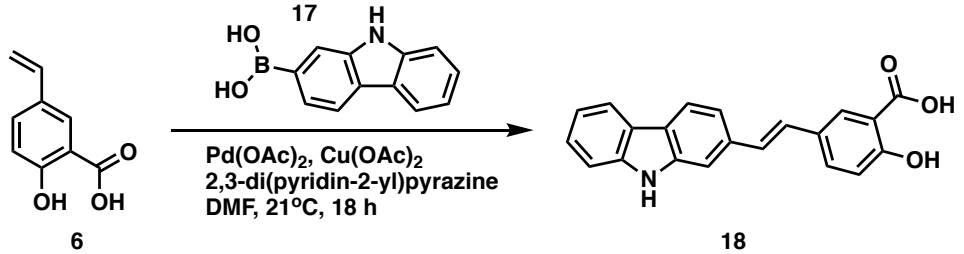

6 18

Scheme 4.23 Synthesis of (*E*)-5-(2-(9*H*-carbazol-2-yl)vinyl)-2-hydroxybenzoic acid **18**.

The structure of compound **18** was confirmed with ^{1}H NMR spectroscopy, see Figure 4.15. There is a signal at 11.27 ppm for the amine, and the other signals is in the aromatic region from 8.08 ppm to 7.00 ppm. The number of hydrogens also corresponds to the total amount of 15 hydrogens in the compound. There are only 13 visible hydrogens in the spectrum because of the hydroxy and carboxylic acid that has one hydrogen each that is not visible in the ^{1}H NMR spectrum. There are also signals from the solvent DMF in the spectrum at 7.95 ppm, 2.89 ppm and 2.73 ppm.

The purity of the compound was analyzed by HPLC as shown in Figure 4.16. There are some signals that belongs to the solvents. Since this was run as a single sample and not as a sequence, the solvent peaks were not possible to remove. The purity of the compound is therefore higher than shown in the chromatogram. The structure of compound **18** was also confirmed by ^{13}C NMR spectroscopy and the mass was confirmed by LC-MS spectrometry [Appendix].

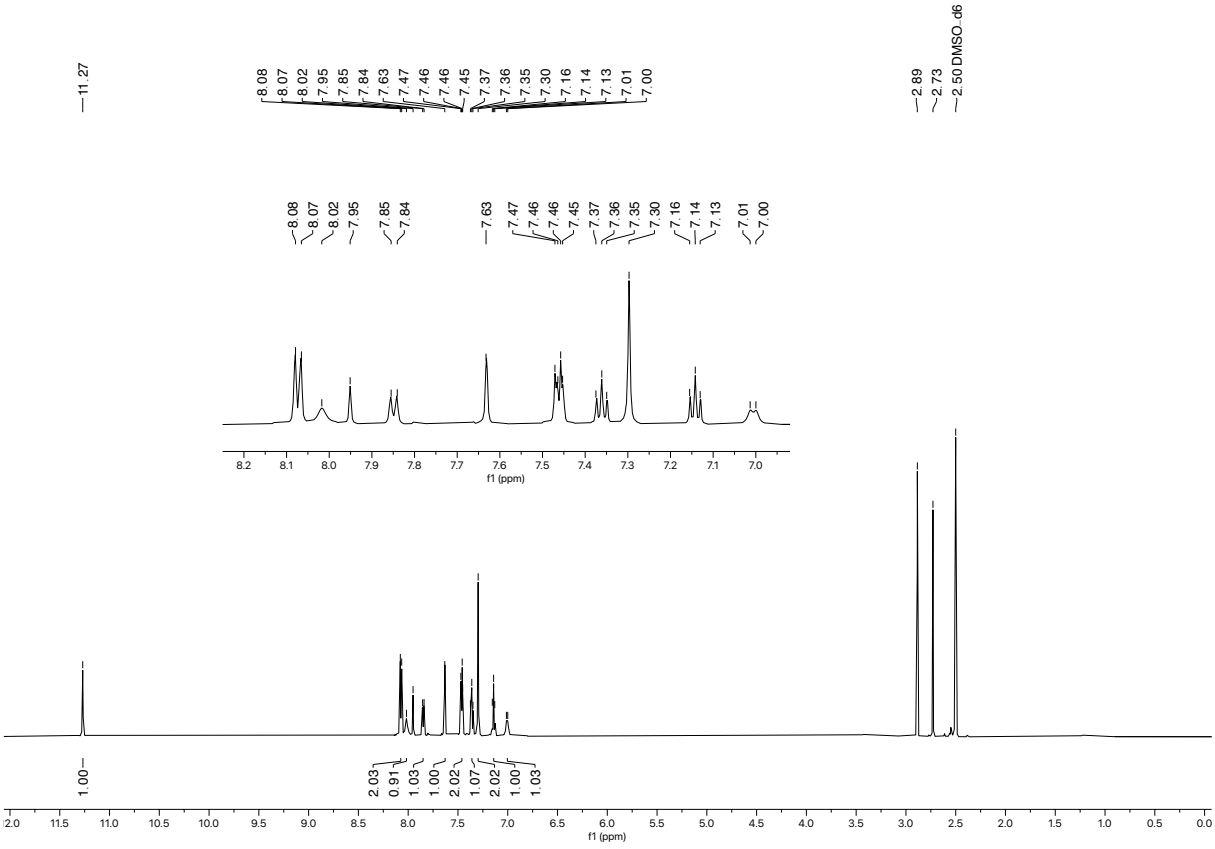

Figure 4.15 ^{1}H NMR spectrum of compound **18**.

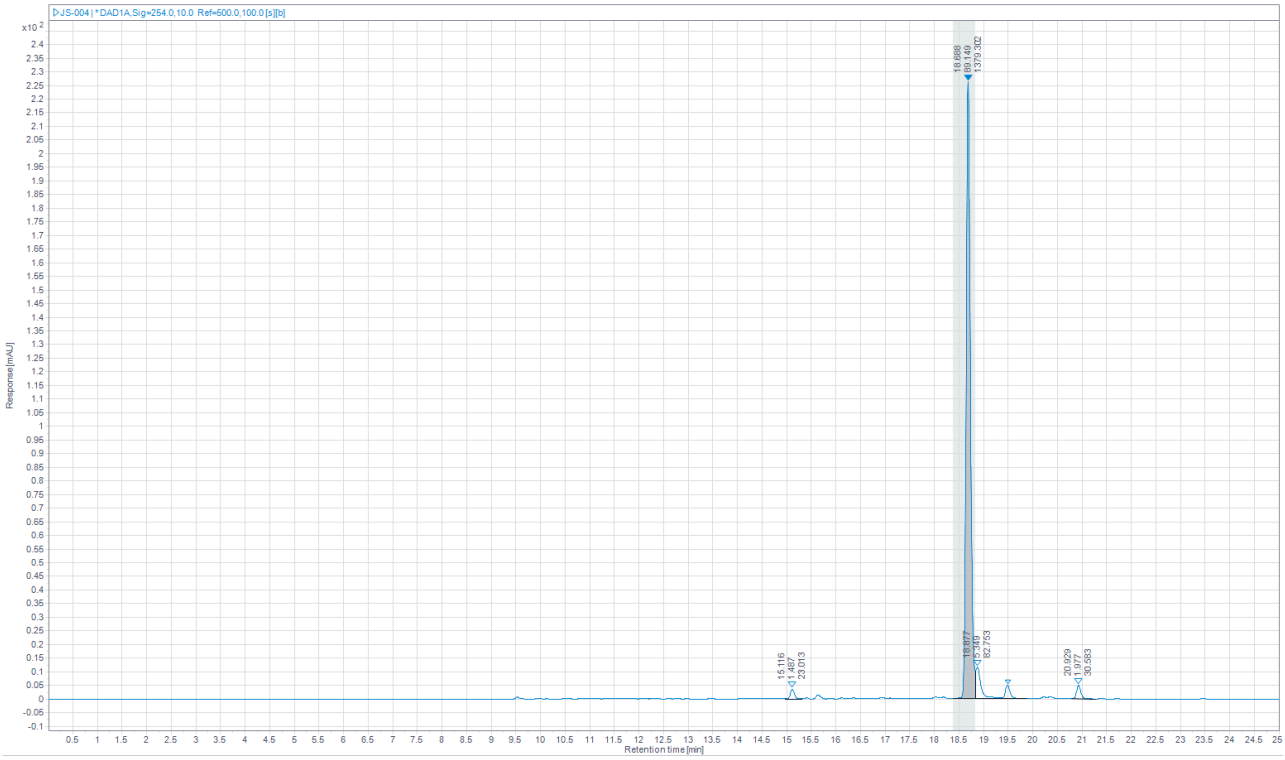

Figure 4.16 HPLC chromatogram of compound **18**.

5 SUMMARY AND FURTHER WORK

5.1 Summary

DC21 (compound **5**) was originally synthesized through a five-step synthesis, which was time consuming and required a lot of chemicals for both reaction and purification. In addition to this, the overall yield of the synthesis was only 29%.

The aim of this project was to find a new and shorter synthesis pathway for compound **5** as it is required in large scale for further testing. A new two-step synthesis was developed, and this synthesis is not as time consuming, requires far less chemicals and has an overall yield of 79%.

The new synthesis consists of a Wittig reaction followed by an oxidative Heck cross-coupling. The Wittig reaction was done on a commercially available starting material, 5-formyl-2-hydroxybenzoic acid. Potassium tert-butoxide was used as a base and methyltriphenylphosphonium bromide as the phosphonium salt to form the ylide.

After purification, the oxidative Heck reaction was done. $Pd(OAc)_2$ was used as catalyst, $Cu(OAc)_2$ as oxidant and 2,3-di-(pyridine-2-yl)pyrazine as a ligand. In addition to this, a boronic acid was required. This was also commercially available.

The aim was to do the large-scale production of compound **5** on continuous flow. There were some complications with the Wittig reaction, where there was no synthesis that gave the product at the same time as the mixture was in solution phase. The oxidative Heck on the other hand was in solution phase during the whole synthesis in batch, so this was done on continuous flow. The yield of the synthesis was only 34%, but with some optimization, the yield is expected to increase.

In addition to this, some new analogues have been synthesized. These analogues follow the same synthetic pathway as compound **5**. The difference is the boronic acids that are used. If the boronic acids required was not commercially available, it had to be synthesized. This was done with n-butyl lithium and trimethyl borate. It has been discovered that the yield of the reaction is dependent on the reaction time of n-butyl lithium.

There were two analogues that was not accomplished as desired. The synthesis of compound **9**, **10**, **14**, **15** and **16** was tried in several different ways, but none of these gave the wanted compounds.

5.2 Further work

It would be interesting to do some further work on the Wittig reaction to see if is possible to get the mixture into solution phase in a reaction where the product is formed. This would mean that the reaction can be tried on continuous flow.

The batch synthesis of compound **5** gives a yield of 90%. The flow synthesis gives only 34%. It would be interesting to see if this yield could be increased with some modifications to the flow rate of the reagents. It is also possible that a third reservoir and pump is needed.

Some further optimizations should be done to the formation of boronic acids, to get a higher yield. This would also increase the overall yield of the synthesis of any analogue, which makes the synthesis greener.

It has been found in the literature that blue light-emitting diodes (LED) irradiation can be effective in reactions involving adamantane [41]. This has not been tested in this project due to lack of equipment. The synthesis of compound **10** should be tried with LEDs to see if the compound can be synthesized.

The synthesis of compound **14** as described in this project is also expected to work. Some further optimizations of the reaction conditions should be done to get this product. The synthesis of compound **16** can then be done through an oxidative Heck reaction.

Lastly, the production of new analogues is required to find the drug with highest potential for the inhibition of the xCT antiporter.

6 EXPERIMENTAL

6.1 General methods

6.1.1 Chemicals

Most of the chemicals used in this project to synthesize compound **2-18** was purchased commercially from Sigma-Aldrich, Apollo Scientific, TCI or Synthonix, and used as received. Some chemicals like the catalyst, oxidants and ligands for the oxidative Heck cross coupling along with some inorganic compounds like bromine and potassium carbonate was already in stock. These chemicals were also used as purchased.

6.1.2 Experimental description

TLC analyses were performed on aluminum foils coated with silica gel with fluorescent indicator 254 nm, purchased from Sigma-Aldrich. The mobile phase used consisted of various mixtures of hexane and ethyl acetate or dichloromethane and methanol.

Manual flash chromatography was performed using silica gel (230-400 mesh), purchased from Sigma-Aldrich, as stationary phase. The mobile phase used consisted of various mixtures of hexane and ethyl acetate or dichloromethane and methanol.

6.1.3 Spectroscopic descriptions

NMR spectra were obtained on a Bruker Biospin AV500 (500 MHz for ^{1}H, 125 MHz for ^{13}C and 160 MHz for ^{11}B) or a Bruker Biospin AVANCE NEO 600 (600 MHz for ^{1}H and 151 MHz for ^{13}C). Chemical shifts are reported in parts per million (ppm) and are referenced to the deuterated solvent used in that experiment. The coupling constants are given in Hz and the multiplicity is reported as singlet (s), doublet (d), double doublet (dd), a doublet of doublets of doublets (ddd), triplet (t), triplet of doublets (td) and multiplet (m).

LC-MS analysis were performed on an Aglient 6420A triple quadrupole mass analyzer using electrospray ionization (ESI). This is connected to an Agilent 1200 series LC module consisting of a binary pump, column compartment/oven and autosampler. The column used was an Agilent ZORBAX SB-C18, RRHT; 2.1 x 50 mm x 1.8 μm.

HPLC analysis were performed on an Agilent 1260 Infinity II attached to a 6120 quadrupole LC/MS. The column used was a YMC-Triart Phenyl 250 x 4.6 mmI.D. S-5 μm, 12nm.

The continuous flow synthesis was performed on a Vapourtec R-series machine with an R-2 pump/injector and R-4 flow reactor using a Vapourtec R-4 Flow Reactor Heater microreactor.

6.2 Experimental procedures

6.2.1 2,2-dimethyl-4-oxo-4*H*-benzo[*d*][1,3]dioxine-6-carbaldehyde **2**

The batch synthesis:
5-formyl-2-hydroxybenzoic acid **1** (500 mg, 3.01 mmol) was dissolved in trifluoroacetic acid (TFA) (17.4 equiv., 4.00 mL, 52.4 mmol). While stirring, trifluoroacetic anhydride (TFAA) (3 equiv., 1.26 mL, 9.03 mmol) was slowly added, then acetone (3.4 equiv., 0.75 mL, 10.2 mmol). The mixture was heated to 100ºC and stirred for 22 h. Toluene (3 x 10 mL) was added to help remove TFA under reduced pressure. Saturated $NaHCO_3$ (30 mL) was added, and the reaction mixture was extracted with EtOAc (3 x 30 mL). The organic layers were combined, dried over Na_2SO_4, filtered and the solvent was removed under reduced pressure to obtain **2** as a brown solid with a yield of 98% (610 mg, 2.96 mmol). ^{1}H NMR (500 MHz, $CDCl_3$) δ 9.96 (s, 1H), 8.48 (d, *J* = 2.0 Hz, 1H), 8.12 (dd, *J* = 8.6, 2.1 Hz, 1H), 7.12 (d, *J* = 8.5 Hz, 1H), 1.78 (s, 6H).^{13}C NMR (126 MHz, $CDCl_3$) δ 189.90, 160.61, 160.11, 135.95, 133.63, 131.55, 118.61, 113.67, 107.49, 26.06

The continuous flow synthesis:
The pumps were first purged to remove any air in the system, then primed with the system solvent isopropanol with a flow rate of 2 mL/min over a period of five minutes. The reactor coil was then connected, and the solvent was then changed to acetone which was introduced with the same flow rate over a period of ten minutes. The reservoirs R1 and R2 was connected to the system, and the flow rates were manually entered. R1 contained a mixture of 5-formyl-2-hydroxybenzoic acid (10.0 g, 60.2 mmol), TFA (145 mL, 1.90 mol) and TFAA (25.0 mL, 181 mmol). R2 contained acetone (30.0 mL). The flow rates were set to 0.283 mL/min for P1 and 0.06 mL/min for P2. The product was collected in R3. After all the reagents had gone through the reactor coil, the reservoirs were exchanged with acetone. The flow rate was increased to 2 mL/min for ten minutes. Then acetone was replaced by isopropanol at the same flow rate for another ten minutes.

Toluene (3 x 100 mL) was added to the crude to help remove TFA under reduced pressure. Saturated $NaHCO_3$ (100 mL) was added, and the reaction mixture was extracted with EtOAc (3 x 100 mL). The organic layers were combined, dried over Na_2SO_4, filtered and the solvent was removed under reduced pressure to obtain **2** as a brown solid with a yield of 65% (8.10 g, 39.3 mmol). ^{1}H NMR (500 MHz, $CDCl_3$) δ 9.96 (s, 1H), 8.48 (d, *J* = 2.0 Hz, 1H), 8.12 (dd, *J* = 8.6, 2.1 Hz, 1H), 7.12 (d, *J* = 8.5 Hz, 1H), 1.78 (s, 6H).^{13}C NMR (126 MHz, $CDCl_3$) δ 189.90, 160.61, 160.11, 135.95, 133.63, 131.55, 118.61, 113.67, 107.49, 26.06

6.2.2 2,2-dimethyl-6-vinyl-4*H*-benzo[*d*][1,3]dioxin-4-one **3**

At 0ºC, methyltriphenylphosphonium bromide (1.2 equiv., 1.04 g, 2.91 mmol) was slowly added to a suspension of NaH 60% (3 equiv., 290 mg, 7.27 mmol) in anhydrous DCM (5 mL). The mixture was then left for stirring for 30 min., whereupon compound **2** (500 mg, 2.42 mmol) was added to the mixture. The mixture was then stirred for 18 h at 21ºC. The reaction mixture was quenched with a saturated solution of $NaHCO_3$ in water. The quenched post-reaction mixture was extracted with DCM (3 x 50 mL). The combined organic layers were dried over Na_2SO_4, filtered and the solvent was removed under reduced pressure. The crude was purified through silica gel column chromatography (hexane/ethyl acetate 9:1) to afford compound **3** as a yellow oil with a yield of 48% (239 mg, 1.17 mmol). ^{1}H NMR (600 MHz, $CDCl_3$) δ 7.98 (d, *J* = 2.3 Hz, 1H), 7.60 (dd, *J* = 8.5, 2.3 Hz, 1H), 6.93 (d, *J* = 8.5 Hz, 1H), 6.67 (dd, *J* = 17.6, 10.9 Hz, 1H), 5.72 (d, *J* = 17.6 Hz, 1H), 5.27 (d, *J* = 10.9 Hz, 1H), 1.73 (s, 6H). ^{13}C NMR (151 MHz, $CDCl_3$) δ 155.59, 135.03, 134.08, 132.70, 117.50, 114.43, 113.63, 106.64, 25.95.

A second method for synthesizing compound **3**.

Acetic anhydride (1 equiv., 0.50 mL, 609 μmol) and acetone (1.00 mL) was added to a microwave vial containing compound **6** (100 mg, 609 μmol) at 21ºC. The mixture was cooled to -78ºC in a dry ice/acetone bath before one drop of concentrated H_2SO_4 was added to the reaction mixture. The mixture was then left to warm to 21ºC and stirred overnight. The solvents were then removed under reduced pressure. Hexane (3 x 10 mL) was added to help removing the residual solvents. The crude was purified through silica gel column chromatography (hexane/ethyl acetate 9:1) to afford **3** as a yellow oil with a yield of 24% (30.0 mg, 146 μmol). ^{1}H NMR (600 MHz, $CDCl_3$) δ 7.98 (d, *J* = 2.3 Hz, 1H), 7.60 (dd, *J* = 8.5, 2.3 Hz, 1H), 6.93 (d, *J* = 8.5 Hz, 1H), 6.67 (dd, *J* = 17.6, 10.9 Hz, 1H), 5.72 (d, *J* = 17.6 Hz, 1H), 5.27 (d, *J* = 10.9 Hz, 1H), 1.73 (s, 6H). ^{13}C NMR (151 MHz, $CDCl_3$) δ 155.59, 135.03, 134.08, 132.70, 117.50, 114.43, 113.63, 106.64, 25.95.

6.2.3 (*E*)-6-(2-(9,9-dimethyl-9*H*-fluoren-2-yl)vinyl)-2,2-dimethyl-4*H*-benzo[*d*][1,3]dioxin-4-one **4**

Compound **3** (500 mg, 2.45 mmol), 2,3-di(pyridin-2-yl)pyrazine (5%, 28.0 mg, 122 μmol), $Pd(OAc)_2$ (5%, 27.0 mg, 122 μmol) and (9,9-dimethyl-9*H*-fluorene- 2-yl)boronic acid (1.1 equiv., 641 mg, 2.69 mmol) were transferred to a round bottom flask and dissolved in DMF (8 mL). $Cu(OAc)_2$ monohydrate (1.5 equiv., 733 mg, 3.67 mmol) were then added and the mixture were stirred for 18 h at 21ºC. The progress of the reaction was monitored by means of TLC using hexane/ethyl acetate 9:1 as eluent. The mixture was extracted with DCM (3 x 50 mL) from a solution EDTA in water (0.2 M, 50 mL). The organic phases were combined, dried over anhydrous Na_2SO_4, filtered, and concentrated under reduced pressure. The mixture was purified using a chromatography column packed with silica gel with hexane/ethyl acetate 99.5:0.5 as eluent to obtain title compound **4** as a white solid with a yield of 81% (789 mg, 1.99 mmol). ^{1}H

NMR (600 MHz, $CDCl_3$) δ 8.15 (d, *J* = 2.4 Hz, 1H), 7.74 – 7.70 (m, 3H), 7.59 (s, 1H), 7.47 (ddd, *J* = 16.0, 7.3, 1.9 Hz, 2H), 7.37 – 7.31 (m, 2H), 7.19 (d, *J* = 16.3 Hz, 1H), 7.12 (d, *J* = 16.3 Hz, 1H), 6.98 (d, *J* = 8.5 Hz, 1H), 1.77 (s, 6H), 1.54 (s, 6H). ^{13}C NMR (151 MHz, $CDCl_3$) δ 161.03, 155.04, 154.07, 153.80, 139.15, 138.66, 135.91, 134.09, 132.49, 129.50, 127.26, 126.95, 126.89, 125.87, 125.75, 122.51, 120.31, 120.18, 119.95, 117.44, 113.61, 106.43, 46.68, 27.08, 25.75.

6.2.4 (*E*)-5-(2-(9,9-dimethyl-9*H*-fluoren-2-yl)vinyl)-2-hydroxybenzoic acid **5**

Compound **4** (500 mg, 1.26 mmol) was dissolved in THF (2.6 mL) at 21°C. KOH (4.7 equiv. 332 mg, 5.93 mmol) dissolved in water (2.6 mL) was slowly added and the reaction mixture was refluxed overnight. The mixture was then cooled to 21°C, acidified to pH 1, and extracted with EtOAc (3 x 50 mL). The organic layers were combined, washed with brine, dried over Na_2SO_4, and concentrated in vacuo. The crude product, a yellow oil, was dissolved in $CHCl_3$ and the product precipitated. The solution was vacuum filtered to obtain the title compound **5** as a white solid with a yield of 31% (141 mg, 395 µmol). ^{1}H NMR (600 MHz, DMSO) δ 8.03 (d, *J* = 2.4 Hz, 1H), 7.85 – 7.82 (m, 2H), 7.80 – 7.77 (m, 2H), 7.55 – 7.51 (m, 2H), 7.37 – 7.28 (m, 3H), 7.21 (d, *J* = 16.3 Hz, 1H), 7.01 (d, *J* = 8.5 Hz, 1H), 1.46 (s, 6H). ^{13}C NMR (151 MHz, DMSO) δ 171.85, 160.63, 153.82, 153.54, 138.37, 137.98, 136.54, 133.00, 128.74, 128.46, 127.25, 127.07, 126.86, 125.97, 122.75, 120.29, 120.07, 117.72, 113.17, 46.36, 26.90. $[M-H]^-$: Calculated for $C_{24}H_{19}O_3$ 355.1, found 355.1

A second method was used to synthesize compound **5** for both batch and flow synthesis.

The batch synthesis:
Compound **6** (100 mg, 609 µmol), 2,3-di(pyridin-2-yl)pyrazine (5%, 7.14 mg, 30.5 µmol), $Pd(OAc)_2$ (5%, 6.84 mg, 30.5 µmol) and (9,9-dimethyl-9*H*-fluorene- 2-yl)boronic acid (1.1 equiv., 160 mg, 670 µmol) were transferred to a round bottom flask and dissolved in DMF (8 mL). $Cu(OAc)_2$ monohydrate (1.5 equiv., 182 mg, 914 µmol) were then added and the mixture were stirred for 18 h at 21°C. The progress of the reaction was monitored by means of TLC using hexane/ethyl acetate 9:1 as eluent. The mixture was extracted with DCM (3 x 30 mL) from a solution EDTA in water (0.2 M, 30 mL). The organic phases were combined, dried over anhydrous Na_2SO_4, filtered, and concentrated under reduced pressure. The mixture was purified using a chromatography column packed with silica gel with hexane/ethyl acetate 6:4 as eluent to obtain title compound **5** as a white solid with a yield of 90% (196 mg, 550 µmol). ^{1}H NMR (600 MHz, DMSO) δ 8.03 (d, *J* = 2.4 Hz, 1H), 7.85 – 7.82 (m, 2H), 7.80 – 7.77 (m, 2H), 7.55 – 7.51 (m, 2H), 7.37 – 7.28 (m, 3H), 7.21 (d, *J* = 16.3 Hz, 1H), 7.01 (d, *J* = 8.5 Hz, 1H), 1.46 (s, 6H). ^{13}C NMR (151 MHz, DMSO) δ 171.85, 160.63, 153.82, 153.54, 138.37, 137.98, 136.54, 133.00, 128.74, 128.46, 127.25, 127.07, 126.86, 125.97, 122.75, 120.29, 120.07, 117.72, 113.17, 46.36, 26.90. $[M-H]^-$: Calculated for $C_{24}H_{19}O_3$ 355.1, found 355.1

The continuous flow synthesis:
The pumps were first purged to remove any air in the system, then primed with the system solvent isopropanol with a flow rate of 2 mL/min over a period of five minutes. The reactor coil was then connected, and the solvent was then changed to DMF which was introduced with the same flow rate over a period of ten minutes. The reservoirs R1 and R2 was connected to the system, and the flow rates were manually entered. R1 contained a mixture of compound **6** (500 mg, 3.05 mmol), 2,3-di(pyridin-2-yl)pyrazine (5%, 36.0 mg, 152 μmol), $Pd(OAc)_2$ (5%, 34.0 mg, 152 μmol) and (9,9-dimethyl-9*H*-fluorene- 2-yl)boronic acid (1.1 equiv., 798 mg, 3.35 mmol) in DMF (10 mL). R2 contained $Cu(OAc)_2$ monohydrate (1.5 equiv., 912 mg, 4.57 mmol) in DMF (15 mL). The flow rates were set to 0.167 mL/min for P1 and 0.250 mL/min for P2. The product was collected in R3. After all the reagents had gone through the reactor coil, the reservoirs were exchanged with DMF. The flow rate was increased to 2 mL/min for ten minutes. Then DMF was replaced by isopropanol at the same flow rate for another ten minutes.

The crude was extracted with DCM (3 x 50 mL) from a solution EDTA in water (0.2 M, 50 mL). The organic phases were combined, dried over anhydrous Na_2SO_4, filtered, and concentrated under reduced pressure. The mixture was purified using a chromatography column packed with silica gel with hexane/ethyl acetate 6:4 as eluent to obtain title compound **5** as a white solid with a yield of 34% (371 mg, 1.04 mmol). ^{1}H NMR (600 MHz, DMSO) δ 8.03 (d, *J* = 2.4 Hz, 1H), 7.85 – 7.82 (m, 2H), 7.80 – 7.77 (m, 2H), 7.55 – 7.51 (m, 2H), 7.37 – 7.28 (m, 3H), 7.21 (d, *J* = 16.3 Hz, 1H), 7.01 (d, *J* = 8.5 Hz, 1H), 1.46 (s, 6H). ^{13}C NMR (151 MHz, DMSO) δ 171.85, 160.63, 153.82, 153.54, 138.37, 137.98, 136.54, 133.00, 128.74, 128.46, 127.25, 127.07, 126.86, 125.97, 122.75, 120.29, 120.07, 117.72, 113.17, 46.36, 26.90. $[M-H]^-$: Calculated for $C_{24}H_{19}O_3$ 355.1, found 355.1

6.2.5 2-hydroxy-5-vinylbenzoic acid **6**

Methyltriphenylphosphonium bromide (1.2 equiv., 1.29 g, 3.61 mmol) was charged to a round bottle before slowly adding potassium tert-butoxide (1M, 3 equiv., 9.36 mL, 9.03 mmol) in THF at 0ºC. The mixture was then left for stirring for 30 min., whereupon 5-formyl-2-hydroxybenzoic acid **1** (500 mg, 3.01 mmol) was added to the mixture. The mixture was warmed to 21ºC and stirred for 24 h. The progress of the reaction was monitored by means of TLC using hexane/ethyl acetate + 1% formic acid 4:6 as eluent. The mixture was extracted from acidic water with DCM (3 × 50 ml), dried over Na_2SO_4 and purified through silica gel column chromatography (hexane/ethyl acetate + 1% formic acid 4:6). The desired product **6** was obtained as a white solid with a yield of 88% (434 mg, 2.65 mmol). ^{1}H NMR (500 MHz, DMSO) δ 7.82 (d, *J* = 2.4 Hz, 1H), 7.69 (dd, *J* = 8.5, 2.4 Hz, 1H), 6.95 (d, *J* = 8.5 Hz, 1H), 6.70 (dd, *J* = 17.7, 10.9 Hz, 1H), 5.70 (dd, *J* = 17.7, 0.9 Hz, 1H), 5.16 (dd, *J* = 11.0, 1.0 Hz, 1H). ^{13}C NMR (126 MHz, DMSO) δ 171.73, 160.81, 135.41, 132.73, 128.59, 128.21, 117.51, 112.89, 112.64. $[M-H]^-$: Calculated for $C_9H_7O_3$ 163.1, found 163.1.

6.2.6 Methyltriphenylphosphonium iodide **7**

To a solution of triphenylphosphine (5.00 g, 19.1 mmol) in THF (7 mL), iodomethane (1.1 equiv., 2.98 g, 1.31 mL, 21.0 mmol) was slowly added. The reaction was flushed with N_2, heated at reflux and continuously stirred for 18 h. Compound **7** formed a white precipitate that was filtrated off and isolated as a white solid in a yield of 95% (7.34 g, 18.2 mmol). ^{1}H NMR (500 MHz, $CDCl_3$) δ 7.79 – 7.64 (m, 15H), 3.13 (d, *J* = 13.2 Hz, 3H).

6.2.7 Adamantan-1-ylboronic acid **8**

A dried round bottom flask was charged with 1-bromoadamantane (1.00 g, 4.65 mmol) and anhydrous THF (20 mL) under argon. It was cooled to −78°C in a dry ice/acetone bath for 5 min before adding 2.0 M n-BuLi in pentane (2 equiv., 4.65 mL, 9.30 mmol) dropwise over a period of 10 min. After addition, it was left for stirring for 30 min before adding trimethyl borate (3 equiv., 1.55 mL, 13.9 mmol) as a neat liquid. The reaction mixture was then stirred for another 30 min. The mixture was allowed to warm to 21°C before being acidified with 3 M HCl and extracted with dichloromethane (3 x 50 mL). The combined organic phases were washed with saturated NaCl solution (1 x 25 mL) and dried over anhydrous Na_2SO_4. The solution was filtered, and the solvent removed under reduced pressure, giving a white semisolid contaminated with a yellow oil. The crude product was stirred with hexane (mixture of isomers) (3 x 15 mL). The solvent was removed with vacuum filtration to provide compound **8** as a white solid in a yield of 41% (340 mg, 1.89 mmol). ^{1}H NMR (500 MHz, DMSO) δ 7.32 (s, 2H), 1.34 – 1.18 (m, 7H), 0.84 (t, *J* = 7.2 Hz, 5H), 0.57 (dd, *J* = 8.2, 7.2 Hz, 3H). ^{11}B NMR (160 MHz, DMSO) δ 32.34.

6.2.8 (*E*)-6-(2-(adamantan-1-yl)vinyl)-2,2-dimethyl-4*H*-benzo[*d*][1,3]dioxin-4-one **9**

Several different syntheses were tried to synthesize compound **9**.

Compound **3** (100 mg, 489 µmol), 2,3-di(pyridin-2-yl)pyrazine (5%, 5.74 mg, 24.5 µmol), $Pd(OAc)_2$ (5%, 5.50 mg, 24.5 µmol) and adamantan-1-ylboronic acid **8** (1.1 equiv., 97.0 mg, 539 µmol) were transferred to a round bottom flask and dissolved in DMF (2 mL). $Cu(OAc)_2$ monohydrate (1.5 equiv., 147 mg, 734 µmol) were then added and the mixture were stirred for 18 h at 21°C. The progress of the reaction was monitored by means of TLC using hexane/ethyl acetate 9:1 as eluent. The mixture was extracted with DCM (3 x 30 mL) from a solution EDTA in water (0.2 M, 30 mL). The organic phases were combined, dried over anhydrous Na_2SO_4, filtered, and concentrated under reduced pressure. The desired product **9** was not obtained from this synthesis.

Compound **3** (100 mg, 489 µmol), bathocuproine (5%, 8.83 mg, 24.5 µmol), $Pd(OAc)_2$ (5%, 5.50 mg, 24.5 µmol) and adamantan-1-ylboronic acid **8** (1.1 equiv., 97.0 mg, 539 µmol) were transferred to a pressure-resistant reaction tube (10 mL) and dissolved in acetonitrile (2 mL). MnO_2 (1.5 equiv., 63.9 mg, 734 µmol) were then added and the mixture were heated to 100°C and stirred for 4h. After cooling, the solvent was evaporated under reduced pressure. The desired product **9** was not obtained from this synthesis.

Compound **3** (100 mg, 489 µmol), $Pd(OAc)_2$ (10%, 11.0 mg, 49.0 µmol) and 1-bromoadamantane (1.2 equiv., 126 mg, 588 µmol) were transferred to a pressure-resistant reaction tube (10 mL) and dissolved in DMF (2 mL). K_2CO_3 (2 equiv., 135 mg, 979 µmol) were then added and the mixture were heated to 60°C and stirred for 16h. After cooling, the solvent was evaporated under reduced pressure. The desired product **9** was not obtained from this synthesis.

6.2.9 (*E*)-5-(2-(adamantan-1-yl)vinyl)-2-hydroxybenzoic acid **10**

Compound **6** (100 mg, 609 µmol), 2,3-di(pyridin-2-yl)pyrazine (5%, 7.14 mg, 30.5 µmol), $Pd(OAc)_2$ (5%, 6.84 mg, 30.5 µmol) and adamantan-1-ylboronic acid **8** (1.1 equiv., 121 mg, 670 µmol) were transferred to a round bottom flask and dissolved in DMF (2 mL). $Cu(OAc)_2$ monohydrate (1.5 equiv., 182 mg, 914 µmol) were then added and the mixture were stirred for 18 h at 21°C. The progress of the reaction was monitored by means of TLC using hexane/ethyl acetate 9:1 as eluent. The mixture was extracted with DCM (3 x 30 mL) from a solution EDTA in water (0.2 M, 30 mL). The organic phases were combined, dried over anhydrous Na_2SO_4, filtered, and concentrated under reduced pressure. The desired product **10** was not obtained from this synthesis.

6.2.10 (*E*)-6-(2-(dibenzo[*b*,*d*]furan-3-yl)vinyl)-2,2-dimethyl-4*H*-benzo[*d*][1,3]dioxin-4-one **11**

Compound **3** (300 mg, 1.47 mmol), 2,3-di(pyridin-2-yl)pyrazine (5%, 17.2 mg, 73.5 µmol), $Pd(OAc)_2$ (5%, 16.5 mg, 73.5 µmol) and dibenzo[*b*,*d*]furan-3-ylboronic acid (1.1 equiv., 343 mg, 1.62 mmol) were transferred to a reactor tube and dissolved in DMF (5 mL). $Cu(OAc)_2$ monohydrate (1.5 equiv., 440 mg, 2.20 mmol) were then added and the mixture were stirred for 18 h at 21°C. The progress of the reaction was monitored by means of TLC using hexane/ethyl acetate 9:1 as eluent. The mixture was extracted with $CHCl_2$ (3 x 50 mL) from a solution EDTA in water (0.2 M, 50 mL). The organic phases were combined, dried over anhydrous Na_2SO_4, filtered, and concentrated under reduced pressure. The mixture was purified using a chromatography column packed with silica gel with hexane/ethyl acetate 99.5:0.5 as eluent to obtain title compound **11** as a white solid with a yield of 87% (472 mg, 1.27 mmol). ^{1}H NMR (600 MHz, $CDCl_3$) δ 8.13 (d, J = 2.3 Hz, 1H), 7.92 (d, J = 6.9 Hz, 1H), 7.89 (d, J = 8.0 Hz, 1H), 7.70 (dd, J = 8.5, 2.4 Hz, 1H), 7.66 (s, 1H), 7.56 (d, J = 8.2 Hz, 1H), 7.47 (dd, J = 8.1, 1.5 Hz, 1H), 7.46 – 7.43 (m, 1H), 7.34 (td, J = 7.4, 1.0 Hz, 1H), 7.19 (d, J = 16.3 Hz, 1H),

7.12 (d, *J* = 16.2 Hz, 1H), 6.97 (d, *J* = 8.5 Hz, 1H), 1.76 (s, 6H). ^{13}C NMR (151 MHz, $CDCl_3$) δ 161.01, 156.63, 155.22, 136.32, 134.22, 132.15, 129.02, 127.12, 127.05, 126.79, 123.96, 123.90, 122.76, 121.63, 120.63, 120.51, 117.49, 113.62, 111.56, 109.06, 106.49, 25.76.

6.2.11 (*E*)-5-(2-(dibenzo[*b*,*d*]furan-3-yl)vinyl)-2-hydroxybenzoic acid **12**

Compound **6** (330 mg, 891 µmol) was dissolved in THF (2.6 mL) at 21°C. KOH (4.7 equiv., 235 mg, 4.19 mmol) dissolved in water (2.6 mL) was slowly added and the reaction mixture was refluxed overnight. The mixture was then cooled to 21ºC, acidified to pH 1, and extracted with EtOAc (3 x 50 mL). The organic layers were combined, washed with brine, dried over Na_2SO_4, and concentrated in vacuo. The crude product, a yellow oil, was dissolved in $CHCl_3$ and the product precipitated. The solution was vacuum filtered to obtain the title compound **12** as a white solid with a yield of 39% (116 mg, 351 µmol). ^{1}H NMR (600 MHz, DMSO) δ 8.12 (d, *J* = 5.3 Hz, 1H), 8.10 (s, 1H), 8.04 (d, *J* = 2.3 Hz, 1H), 7.92 (s, 1H), 7.86 (dd, *J* = 8.8, 2.3 Hz, 1H), 7.69 (d, *J* = 8.2 Hz, 1H), 7.66 (dd, *J* = 8.2, 1.5 Hz, 1H), 7.51 (ddd, *J* = 8.4, 7.2, 1.3 Hz, 1H), 7.42 (d, *J* = 16.3 Hz, 1H), 7.39 (dd, *J* = 7.4, 1.0 Hz, 1H), 7.32 (d, *J* = 16.3 Hz, 1H), 7.02 (d, *J* = 8.5 Hz, 1H). ^{13}C NMR (151 MHz, DMSO) δ 171.77, 160.77, 156.14, 155.89, 137.29, 133.19, 128.63, 128.47, 128.09, 127.44, 126.80, 123.56, 123.18, 121.91, 121.17, 121.02, 117.73, 113.20, 111.61, 108.84. $[M-H]^-$: Calculated for $C_{21}H_{13}O_4$ 329.3, found 329.0

A second method was used to synthesize compound **12**.

Compound **6** (200 mg, 1.22 mmol), 2,3-di(pyridin-2-yl) pyrazine (5%, 14.3 mg, 61.0 µmol), $Pd(OAc)_2$ (5%, 14.7 mg, 61.0 µmol) and dibenzo[*b*,*d*]furan-3-ylboronic acid (1.1 equiv., 284 mg, 1.34 mmol) were transferred to a reactor tube and dissolved in DMF (5 mL). $Cu(OAc)_2$ monohydrate (1.5 equiv., 365 mg, 1.83 mmol) were then added and the mixture were stirred for 18 h at 21ºC. The progress of the reaction was monitored by means of TLC using hexane/ethyl acetate 9:1 as eluent. The mixture was extracted with $CHCl_2$ (3 x 50 mL) from a solution EDTA in water (0.2 M, 50 mL). The organic phases were combined, dried over anhydrous Na_2SO_4, filtered, and concentrated under reduced pressure. The crude was purified using a chromatography column packed with silica gel with hexane/ethyl acetate 99.5:0.5 as eluent to obtain title compound **12** as a white solid with a yield of 81% (324 mg, 981 µmol). ^{1}H NMR (600 MHz, DMSO) δ 8.12 (d, *J* = 5.3 Hz, 1H), 8.10 (s, 1H), 8.04 (d, *J* = 2.3 Hz, 1H), 7.92 (s, 1H), 7.86 (dd, *J* = 8.8, 2.3 Hz, 1H), 7.69 (d, *J* = 8.2 Hz, 1H), 7.66 (dd, *J* = 8.2, 1.5 Hz, 1H), 7.51 (ddd, *J* = 8.4, 7.2, 1.3 Hz, 1H), 7.42 (d, *J* = 16.3 Hz, 1H), 7.39 (dd, *J* = 7.4, 1.0 Hz, 1H), 7.32 (d, *J* = 16.3 Hz, 1H), 7.02 (d, *J* = 8.5 Hz, 1H). ^{13}C NMR (151 MHz, DMSO) δ 171.77, 160.77, 156.14, 155.89, 137.29, 133.19, 128.63, 128.47, 128.09, 127.44, 126.80, 123.56, 123.18, 121.91, 121.17, 121.02, 117.73, 113.20, 111.61, 108.84. $[M-H]^-$: Calculated for $C_{21}H_{13}O_4$ 329.3, found 329.0

6.2.12 3-bromo-1,10-phenanthroline **13**

1,10-phenanthroline monohydrochloride monohydrate (1.00 g, 4.26 mmol) and $PhNO_2$ (2 mL) was added to a round bottom flask and heated to 140ºC. Br_2 (1.5 equiv. 0.330 mL, 6.39 mmol) in $PhNO_2$ (1 mL) was then added dropwise over a period of 10 min. and the mixture was stirred at 140°C for 3h. The mixture was allowed to cool to 21ºC before ammonium hydroxide (50 mL) was added and the solution was extracted with $CHCl_2$ (3 x 50 mL). The combined organic phases were washed with water, dried over $MgSO_4$ and concentrated in vacuo. Silica gel was used to remove $PhNO_2$ with $CHCl_2$ as eluent. After $PhNO_2$ eluted out, the product was recovered by gradually increasing the polarity to 10% MeOH in $CHCl_2$. Flash column chromatography afforded the desired product **13** as a white powder with a yield of 31% (343 mg, 1.32 mmol). ^{1}H NMR (600 MHz, $CDCl_3$) δ 9.15 – 9.00 (m, 2H), 8.24 (d, *J* = 2.3 Hz, 1H), 8.16 – 8.10 (m, 1H), 7.70 – 7.66 (m, 1H), 7.60 – 7.48 (m, 2H). ^{13}C NMR (151 MHz, $CDCl_3$) δ 151.02, 150.61, 145.84, 144.29, 137.32, 136.04, 129.55, 128.50, 127.87, 125.34, 123.29, 119.81.

6.2.13 (1,10-phenanthrolin-3-yl)boronic acid **14**

A dried round bottom flask was charged with compound **13** (500 mg, 1.93 mmol) and anhydrous THF (10 mL) under argon. It was cooled to −78 °C in a dry ice/acetone bath for 5 min before adding 2.5 M n-BuLi in hexane (1.2 equiv., 930 mmL, 2.32 mmol) dropwise over a period of 10 min. After addition, it was left for stirring for 30 min before adding trimethyl borate (1.5 equiv., 323 mmL, 2.89 mmol) as a neat liquid. The reaction mixture was then stirred for another 30 min. The mixture was allowed to warm to 21ºC before being acidified with 3 M HCl and extracted with dichloromethane (3 x 50 mL). The combined organic phases were washed with saturated NaCl solution (1 x 25 mL) and dried over anhydrous Na_2SO_4. The solution was filtered, and the solvent removed under reduced pressure. The desired product **14** was not obtained from this synthesis.

Another method for the synthesis of compound **14** was tried.

Compound **13** (100 mg, 386 µmol), AcOK (3 equiv., 114 mg, 1.16 mmol), $Pd(dppf)_2Cl_2$ (5%, 14.1 mg, 19.3 µmol) and bis(pinacolato)diboron (1 equiv. 98.0 mg, 386 µmol) was transferred to a tube reactor and solved in DMSO (5 mL). The reaction mixture was then heated to 180ºC and stirred for 24h. The mixture was then extracted with diethyl ether (3 x 30 mL) from acidic water (30 mL). The organic phases were combined, dried over anhydrous Na_2SO_4, filtered, and concentrated under reduced pressure. The desired product **14** was not obtained from this synthesis.

6.2.14 (*E*)-6-(2-(1,10-phenanthrolin-3-yl)vinyl)-2,2-dimethyl-4*H*-benzo[*d*][1,3]dioxin-4-one **15**

Compound **3** (100 mg, 490 μmol), $Pd(OAc)_2$ (8%, 8.79 mg, 39.2 μmol), K_2CO_3 (2 equiv., 135 mg, 979 μmol), compound **13** (1 equiv., 127 mg, 490 μmol) and DMF (5 mL) were transferred tube reactor. The tube reactor was then sealed and heated to 100°C. The reaction was left for stirring at 100°C overnight. The course of the reaction was monitored by TLC where hexane/ethyl acetate 9:1 was used as eluent. The mixture was extracted with $CHCl_2$ (3 x 30 mL). The organic phases were combined, dried over anhydrous Na_2SO_4, filtered, and concentrated under reduced pressure. The desired product **15** was not obtained from this synthesis.

6.2.15 (*E*)-5-(2-(1,10-phenanthrolin-3-yl)vinyl)-2-hydroxybenzoic acid **16**

Compound **6** (100 mg, 609 μmol), $Pd(OAc)_2$ (8%, 10.9 mg, 48.7 μmol), K_2CO_3 (2 equiv., 168 mg, 1.22 mmol), compound **13** (1 equiv., 158 mg, 609 μmol) and DMF (5 mL) were transferred tube reactor. The tube reactor was then sealed and heated to 100°C. The reaction was left for stirring at 100°C overnight. The course of the reaction was monitored by TLC where hexane/ethyl acetate 9:1 was used as eluent. The mixture was extracted with $CHCl_2$ (3 x 30 mL) from acidic water (30 mL). The organic phases were combined, dried over anhydrous Na_2SO_4, filtered, and concentrated under reduced pressure. The desired product **16** was not obtained from this synthesis.

6.2.16 (9*H*-carbazol-2-yl)boronic acid **17**

A dried round bottom flask was charged with 2-bromo-9*H*-carbazole (1.00 g, 4.06 mmol) and anhydrous THF (20 mL) under argon. It was cooled to −78°C in a dry ice/acetone bath for 5 min before adding 2.5 M n-BuLi in hexane (1.2 equiv., 1.95 mL, 4.88 mmol) dropwise over a period of 10 min. After addition, it was left for stirring for 30 min before adding trimethyl borate (1.5 equiv., 680 mmL, 6.09 mmol) as a neat liquid. The reaction mixture was then stirred for another 30 min. The mixture was allowed to warm to 21°C before being acidified with 3 M HCl and extracted with dichloromethane (3 x 50 mL). The combined organic phases were washed with saturated NaCl solution (1 x 50 mL) and dried over anhydrous Na_2SO_4. The solution was filtered, and the solvent removed under reduced pressure. The crude product was purified using a chromatography column packed with silica gel with hexane/ethyl acetate 7:3 as eluent to obtain title compound **17** as a white solid in a yield of 45% (390 mg, 1.85 mmol). ^{1}H NMR (600 MHz, DMSO) δ 11.22 (s, 1H), 8.70 (d, J = 249.0 Hz, 2H), 8.09 (d, J = 7.1 Hz, 1H), 8.03 (d, J = 7.7 Hz, 1H), 7.92 (s, 1H), 7.59 (dd, J = 7.8, 1.1 Hz, 1H), 7.47 (d, J = 8.1 Hz, 1H), 7.37 (ddd, J = 8.2, 7.0, 1.3 Hz, 1H), 7.13 (ddd, J = 8.0, 7.1, 1.2 Hz, 1H). ^{13}C NMR (151 MHz, DMSO) δ 140.09, 139.43, 125.66, 124.32, 123.72, 122.35, 120.32, 118.84, 118.28, 116.93, 110.94. $[M-H]^-$: Calculated for $C_{12}H_9BNO_2$ 210.0, found 210.1.

6.2.17 (*E*)-5-(2-(9*H*-carbazol-2-yl)vinyl)-2-hydroxybenzoic acid **18**

Compound **6** (200 mg, 1.22 mmol), 2,3-di(pyridin-2-yl) pyrazine (5%, 14.3 mg, 61.0 µmol), $Pd(OAc)_2$ (5%, 14.7 mg, 61.0 µmol) and (9*H*-carbazol-2-yl)boronic acid **16** (1.1 equiv., 283 mg, 1.34 mmol) were transferred to a reactor tube and dissolved in DMF (5 mL). $Cu(OAc)_2$ monohydrate (1.5 equiv., 365 mg, 1.83 mmol) were then added and the mixture were stirred for 18 h at 21ºC. The progress of the reaction was monitored by means of TLC using hexane/ethyl acetate 9:1 as eluent. The mixture was extracted with $CHCl_2$ (3 x 50 mL) from a solution EDTA in water (0.2 M, 50 mL). The organic phases were combined, dried over anhydrous Na_2SO_4, filtered, and concentrated under reduced pressure. The crude was purified using a chromatography column packed with silica gel with hexane/ethyl acetate 6:4 as eluent to obtain title compound **18** as a white solid with a yield of 86% (346 mg, 1.05 mmol). ^{1}H NMR (600 MHz, DMSO) δ 11.27 (s, 1H), 8.07 (d, *J* = 8.3 Hz, 2H), 8.02 (s, 1H), 7.85 (d, *J* = 8.6 Hz, 1H), 7.63 (s, 1H), 7.46 (dd, *J* = 7.4, 3.4 Hz, 2H), 7.36 (t, *J* = 7.6 Hz, 1H), 7.30 (s, 2H), 7.14 (t, *J* = 7.4 Hz, 1H), 7.01 (d, *J* = 8.1 Hz, 1H). ^{13}C NMR (151 MHz, DMSO) δ 162.30, 140.31, 140.17, 134.84, 132.89, 128.71, 127.95, 126.44, 125.46, 122.39, 121.91, 120.29, 120.06, 118.63, 117.17, 110.89, 108.96, 35.77, 30.76. $[M-H]^-$: Calculated for $C_{21}H_{14}NO_3$ 328.3, found 328.1.

7 REFERENCES

[1] J. P. Thakkar, T. A. Dolecek, C. Horbinski, Q. T. Ostrom, D. D. Lightner, J. S. Barnholtz-Sloan, J. L. Villano, *Cancer Epidemiol Biomarkers Prev.,* **2014**, 23(10), 1985-1996.
[2] D. N. Louis, H. Ohgaki, O. D. Wiestler, W. K. Cavenee, P. C. Burger, A. Jouvet, B. W. Scheithauer, P. Kleihues, *Acta Neuropathol,* **2007**, 114, 97-109.
[3] G. Iacob, E. B. Dinca, *J Med Life,* **2009**, 2, 386-393.
[4] https://moffitt.org/cancers/glioblastoma/diagnosis/causes/, *Glioblastoma Causes*, retrieved 02.08.22
[5] Q. T. Ostrom, H. Gittleman, P. Farah, A. Ondracek, T. Chen, Y. Wolinsky, N. E. Stroup, C. Kruchko, J. S. Barnholtz-Sloan, *Neuro Oncol.,* **2013**, 15, 1-56.
[6] https://www.mayoclinic.org/diseases-conditions/glioblastoma/cdc-20350148, *Glioblastoma,* retrieved 12.07.22.
[7] S. Oberndorfer, E. Lindeck-Pozza, H. Lahrmann, W. Struhal, P. Hitzenberger, W. Grisold, *J Palliat Med,* **2008**, 11(1), 26-30.
[8] C. Alifieris, D. T. Trafalis, *Pharmacology & Therapeutics,* **2015**, 152, 63-82.
[9] M. E. Davis, *Clin. J Oncol Nurs*, **2016**, 20 (5), 2-8.
[10] R. Stupp, W. P. Mason, M. J. Ven den Bent, M. Weller, B. Fisher, M. J. B. Taphoorn, K. Belanger, A. A. Brandes, C. Marosi, U. Bogdahn, J. Curschmann, R. C. Janzer, S. K. Ludwin, T. Gorlia, A. Allgeier, D. Lacombe, J. G. Cairncross, E. Eisenhauer, R. O. Mirimanoff, *N. Engl. J. Med.,* **2005**, 352, 987-996.
[11] F. Hanif, K. Muzaffar, K. Perveen, S. M. Malhi, S. U. Simjee, *Asian Pac. J. Cancer Prev.,* **2017**, 18(1), 3-9.
[12] J. Lewerenz, S. J. Hewett, Y. Huang, M. Lambros, P. W. Gout, P. W. Kalivas, A. Massie, I. Smolders, A. Methner, M. Pergande, S. B. Smith, V. Ganapathy, P. Maher, *Antioxid Redox Signal,* **2013**, 18 (5), 522-555.
[13] J. K. M. Lim, A. Delaidelli, S. W. Minaker, H.-F. Zhang, M. Colovic, H. Yang, G. L. Negri, S. von Karstedt, W. W. Lockwood, P. Schaffer, G. Leprivier, P. H. Sorensen, *PNAS,* **2019**, 116 (19), 9433-9442.
[14] D. Cirillo, S. Sarowar, P. Ø. Enger, H.-R. Bjørsvik, *ChemMedChem,* **2021**, 16, 2650 – 2668.
[15] P. W. Gout, A. R. Buckley, C. R. Simms, N. Bruchovsky, *Leukemia*, **2001**,15,1633–1640.
[16] V. C. Neumann, K. A. Grindulis, *Sulphasalazine in Rheumatoid Arthritis: An old drug revived*; SAGE Publications **1984**.
[17] L. Sleire, B. Skeie, I. A. Netland, H. E. Førde, E. Dodoo, F. Selheim, L. Leiss, J. I. Heggdal, P.-H. Pedersen, J. Wang, P. Ø. Enger, *Oncogene,* **2015**, 34, 5951–5959.
[18] H. Schröder, D. E. Campbell, *Clin. Pharmacol.Ther*., **1972**, 13, 539–551.
[19] K. M. Das, M. A. Eastwood, J. P. McManus, W. Sircus, *N. Engl. J. Med*., **1973**, 289, 491–495.
[20] D. L. Pavia, G. M. Lampman, G. S. Kriz, J. R. Vyvyan, "Introduction to Spectroscopy", *Cengage Learning,* 5th edition, **2015**.
[21] J. R. Mohrig, D. G. Alberg, G. E. Hofmeister, P. F. Schatz, C. N. Hammond, "Laboratory Techniques in Organic Chemistry", *W. H. Freeman and Company*, 4th edition, **2014**.
[22] C. S. Ho, C. W. K. Lam, M. H. M. Chan, R. C. K. Cheung, L. K. Law, L. C. W. Lit, K. F. Ng, M. W. M. Suen, H. L. Tai, *Clin. Biochem. Rev.*, **2003**, 24, 3-12.
[23] J. T. Watson, O. D. Sparkman, "Introduction to Mass Spectrometry", *Wiley,* 4th edition, **2009**.
[24] J. Leonard, B. Lygo, G. Procter, "Advanced Practical Organic Chemistry", *CRC Press*, 3rd edition, **2012**.
[25] F. Darvas, T. A. Hamlin, V. Hessel, G. Dorman, K. F. Jensen, R. Becker, M. M. E. Delville, M. Fekete, F. Fülöp, T. Glasnov., "Flow Chemistry – Fundamentals: Fundamentals", *De Gruyter, Inc.*, **2014**.
[26] D. Sleveland, H-R. Bjørsvik, *Org. Process Res. Dev.,* **2012**, 16, 1121 – 1130.
[27] F. M. Akwi, P. Watts, *Chem. Commun.,* **2018**, 54, 13894-13928.
[28] M. Guidi, P. H. Seeberger, K. Gilmore, *Chem. Soc. Rev.,* **2020**, 49, 8910 – 8932.
[29] https://www.nobelprize.org/prizes/chemistry/1979/wittig/facts/, *Georg Wittig Facts*, retrieved 05.07.22
[30] C. Willis, M. Wills, "Organic Synthesis", *Oxford*, **1995**.
[31] S. Warren, P. Wyatt, "Organic Synthesis: The Disconnection Approach", *Wiley*, 2nd edition, **2008**.
[32] G. Wittig, U. Schoellkopf, *Chem. Ber*., **1954**, 87, 1318-1330.
[33] A-L. Lee, *Org. Biomol. Chem.,* **2016**, 14, 5357-5366.
[34] S. Zhang, L. Shi, Y. Ding, *J. Am. Chem. Soc.,* **2011**, 133, 20218-20229.
[35] F. M. Moghaddam, R. Pourkaveh, A. Karimi, *J. Org. Chem.* **2017**, 82 (19), 10635–10640.
[36] G. L. Patrick, "an introduction to Medicinal Chemistry", *Oxford University Press,* 6th edition, **2017**.
[37] M. P. Paudyal, L. Wu, Z.-Y. Zhang, C. D. Spilling, C. F. Wong, *Bioord. Med. Chem.,* **2014**, 22, 6781-6788.
[38] https://chem.libretexts.org/Bookshelves/Organic_Chemistry/Map%3A_Organic_Chemistry_(Bruice)/14%3A_NMR_Spectroscopy/14.12%3A_Coupling_Constants_Identify_Coupled_Protons, *Coupling Constants Identify Coupled Protons,* retrieved 08.08.22
[39] https://www.sigmaaldrich.com/NO/en/sds/aldrich/156671, *Safety Data Sheet Potassium tert-Butoxide*, retrieved 06.08.22.
[40] R. E. Gawley, "Encyclopedia of Reagents for Organic Synthesis", *Wiley,* **2001**.
[41] G.-Z. Wang, R. Shang, W.-M. Cheng, Y. Fu, *J. Am. Chem. Soc.*, **2017**, 139, 18307-18312.

APPENDIXES

1 List of compounds

Compound number	Structure	Compound number	Structure
1	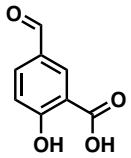	10	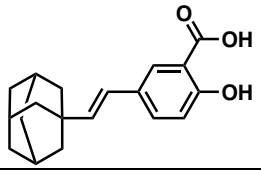
2	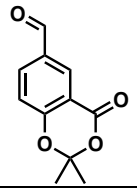	11	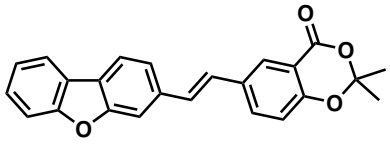
3	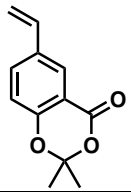	12	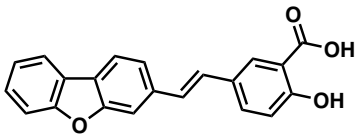
4	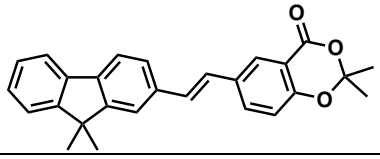	13	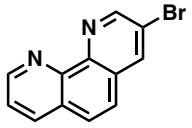
5	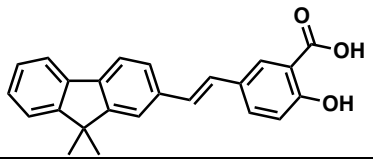	14	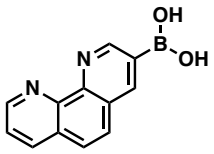
6	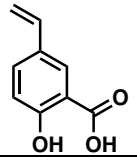	15	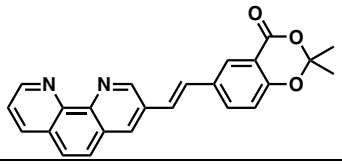
7	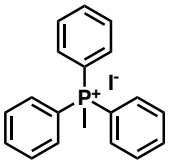	16	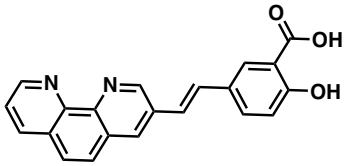
8	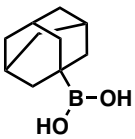	17	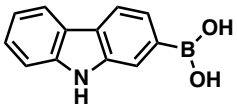
9	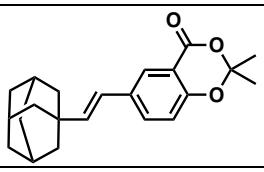	18	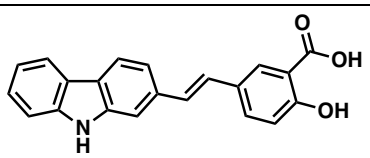

2 NMR spectrums of compound **2**

^{1}H NMR spectrum of compound **2**

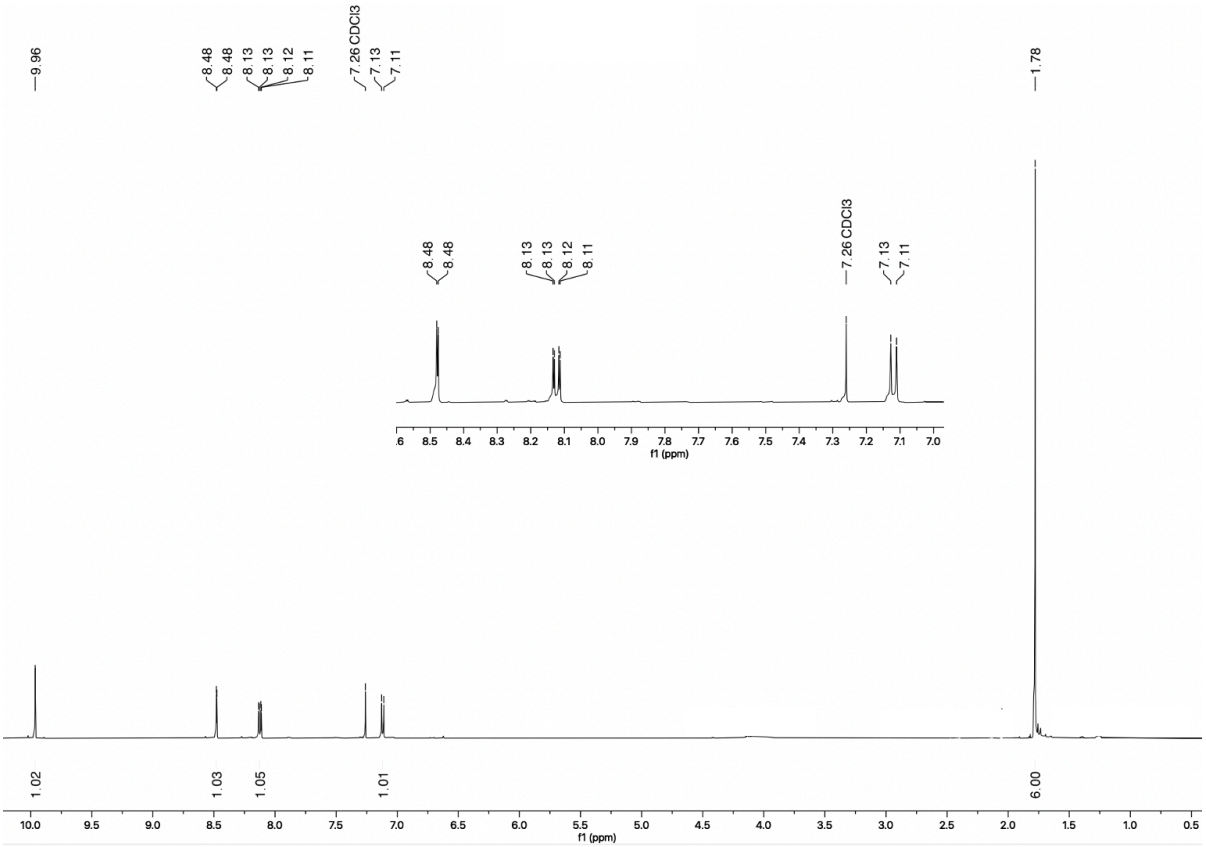

^{13}C NMR spectrum of compound **2**

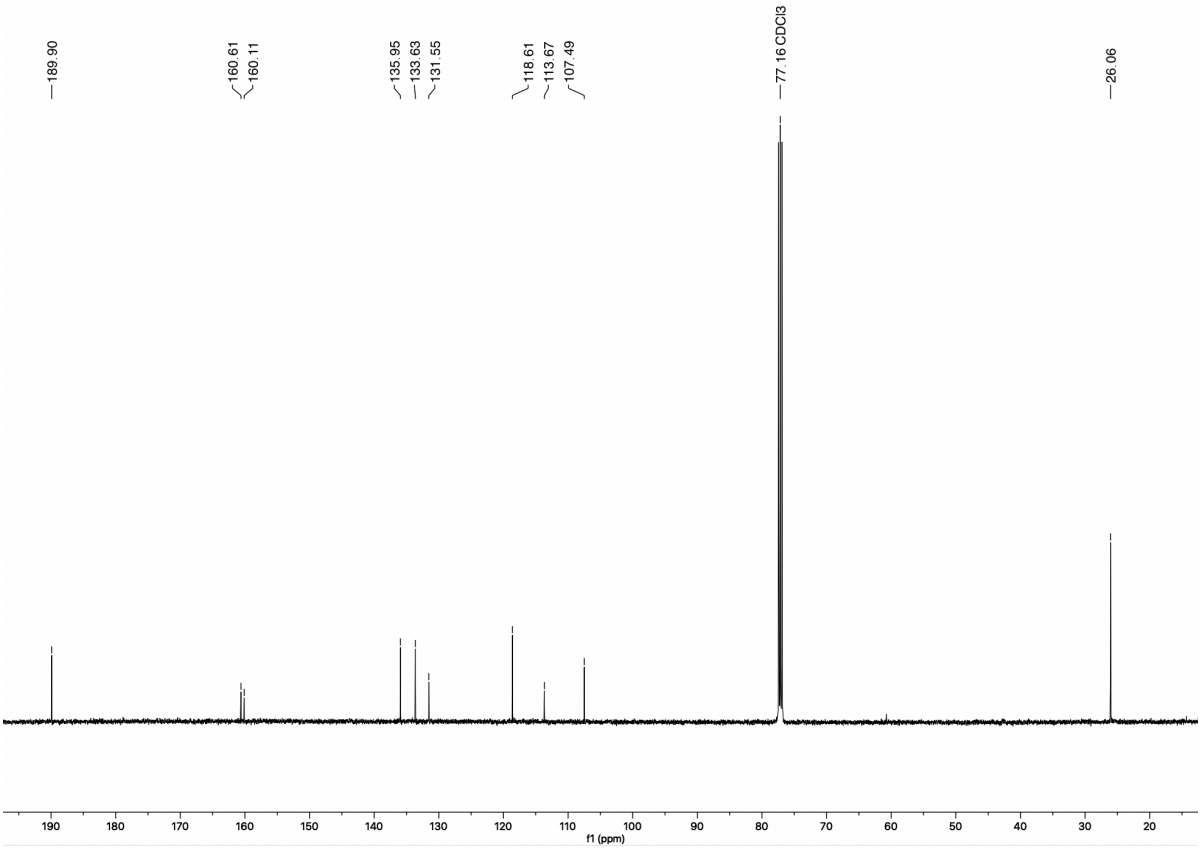

3 NMR spectrums of compound **3**

^{1}H NMR spectrum of compound **3**

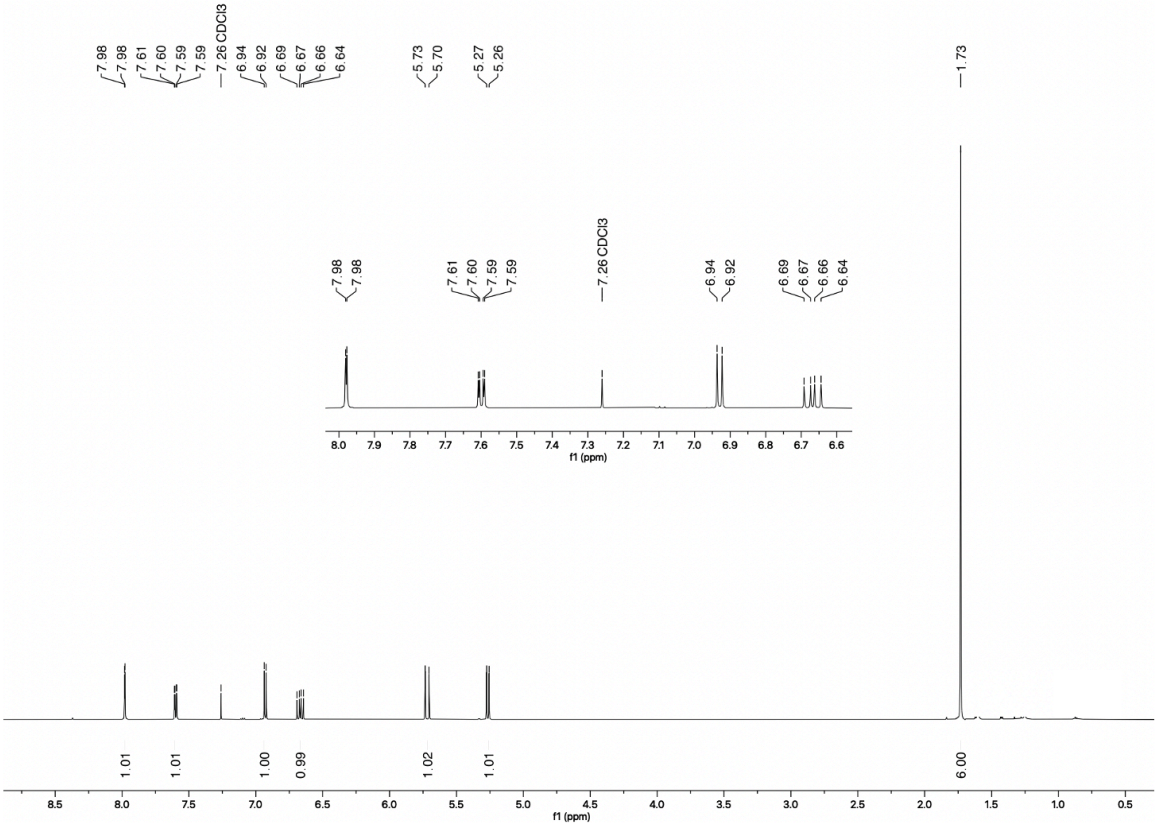

^{13}C NMR spectrum of compound **3**

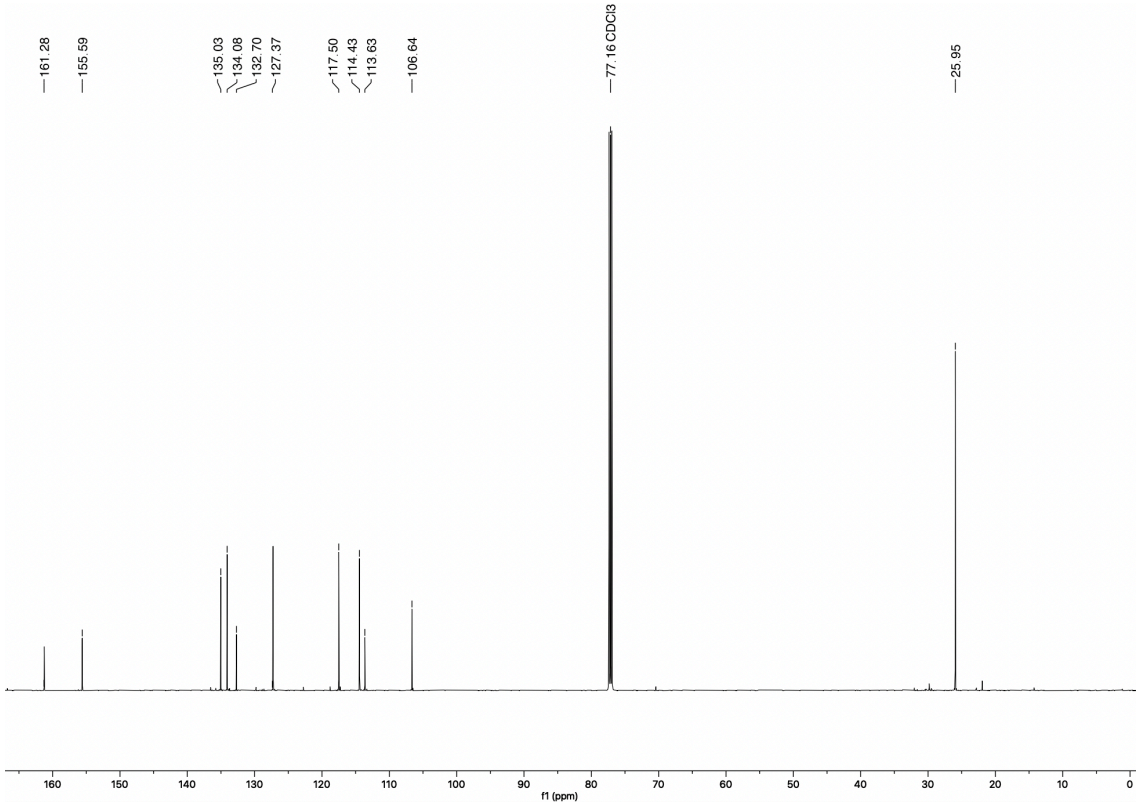

4 NMR spectrums of compound **4**

^{1}H NMR spectrum of compound **4**

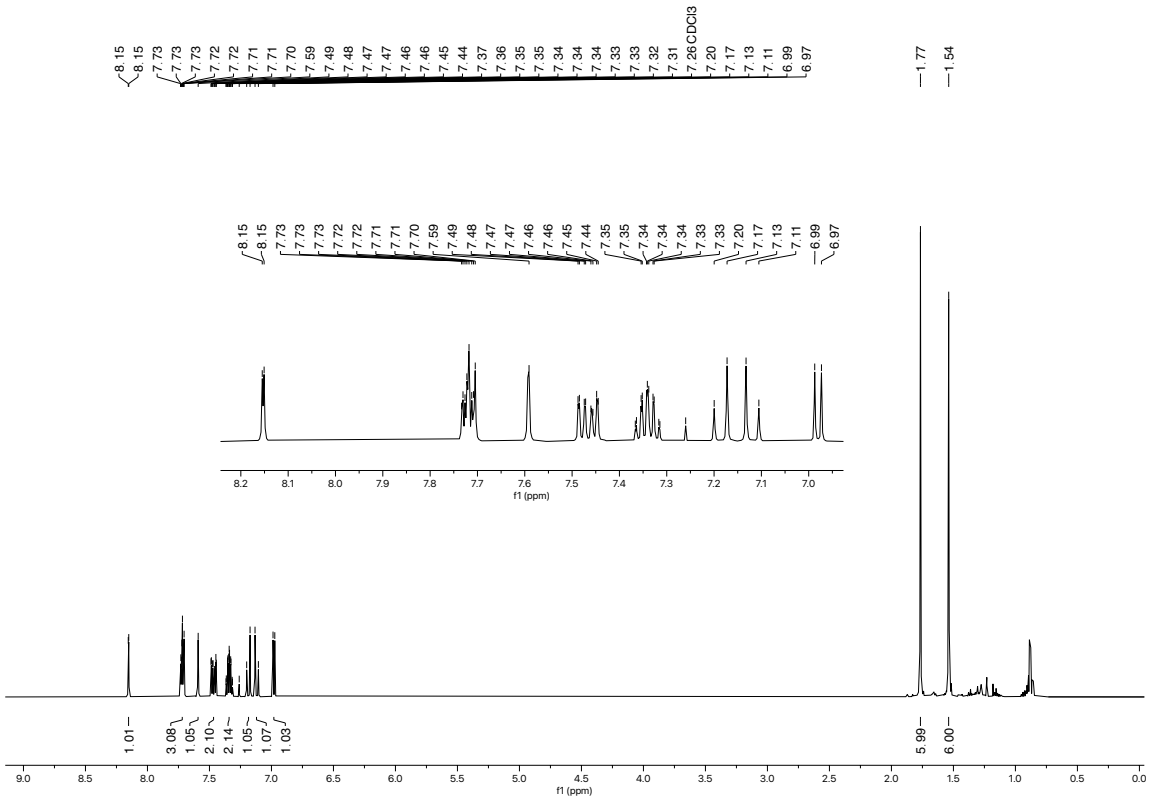

^{13}C NMR spectrum of compound **4**

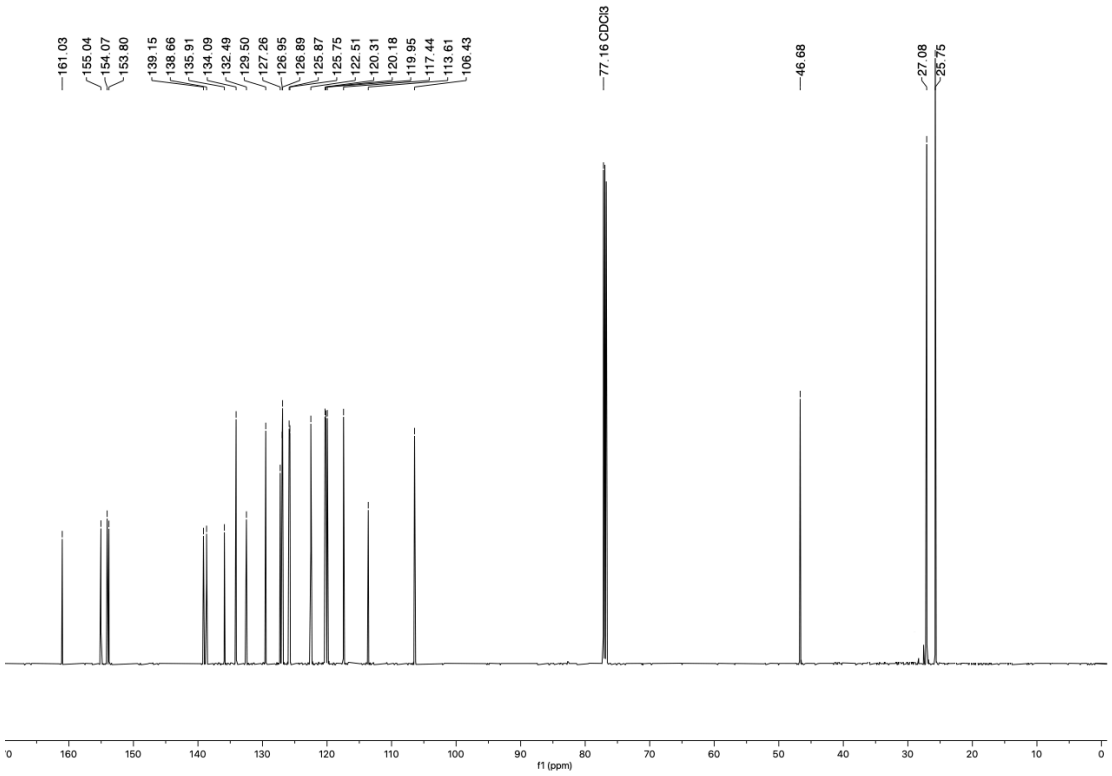

5 NMR, HPLC and LC-MS spectrums of compound **5**

^{1}H NMR spectrum of compound **5**

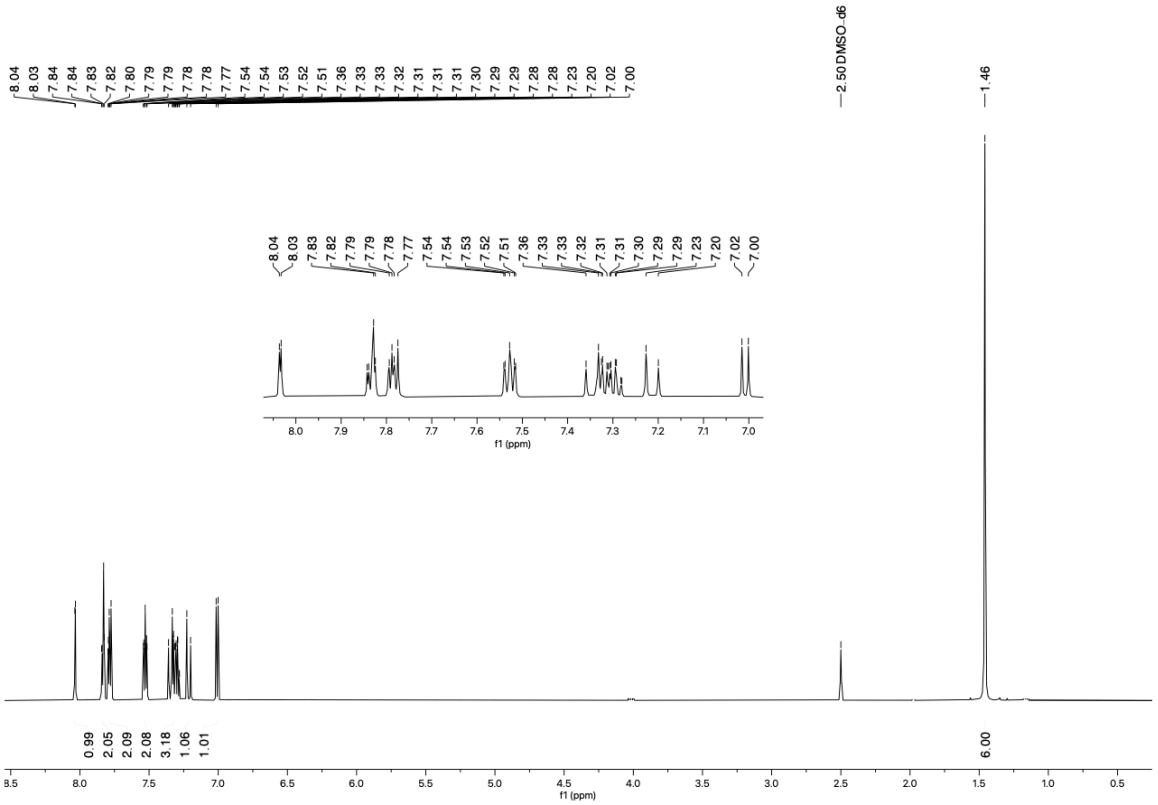

^{13}C NMR spectrum of compound **5**

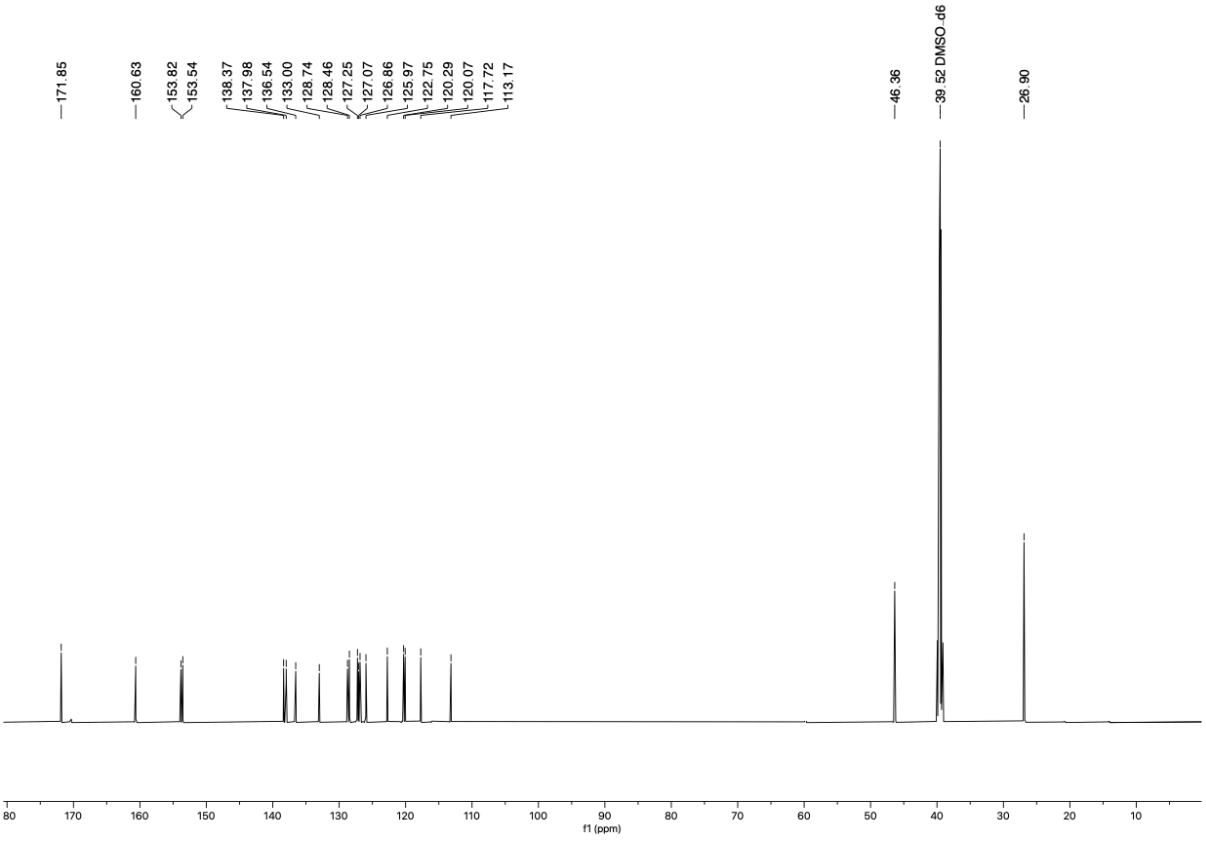

LC-MS spectrum of compound **5**

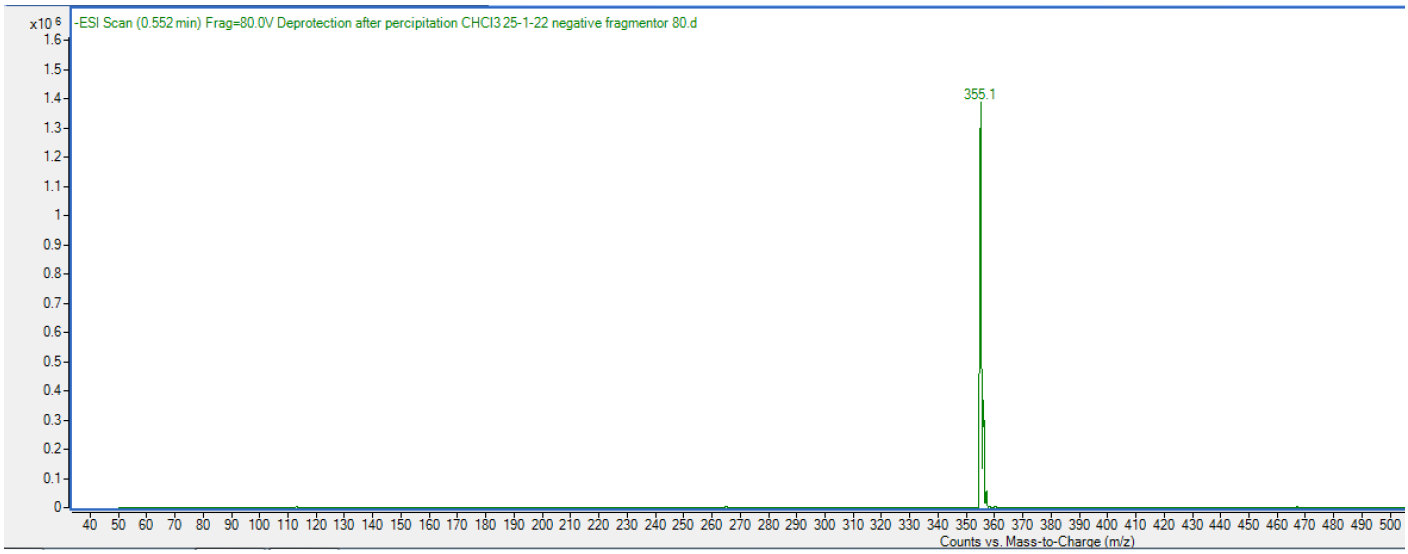

HPLC chromatogram of compound **5**

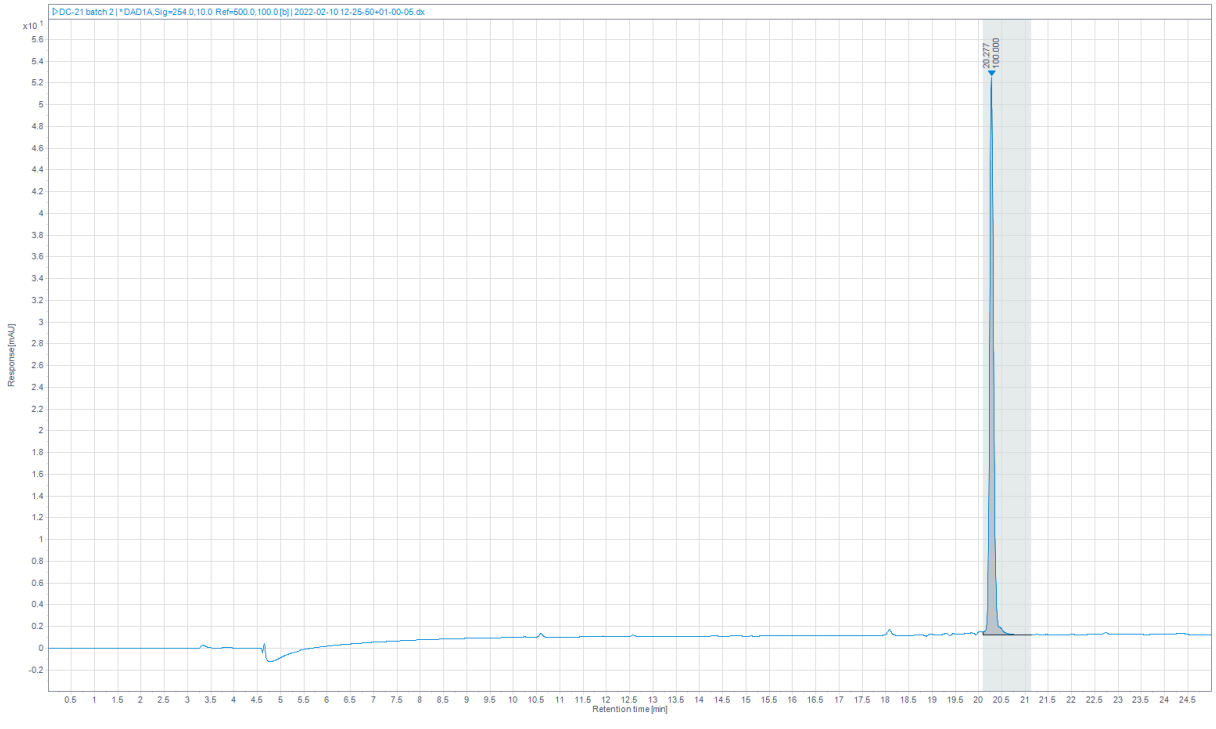

6 NMR and LC-MS spectrums of compound **6**

^{1}H NMR spectrum of compound **6**

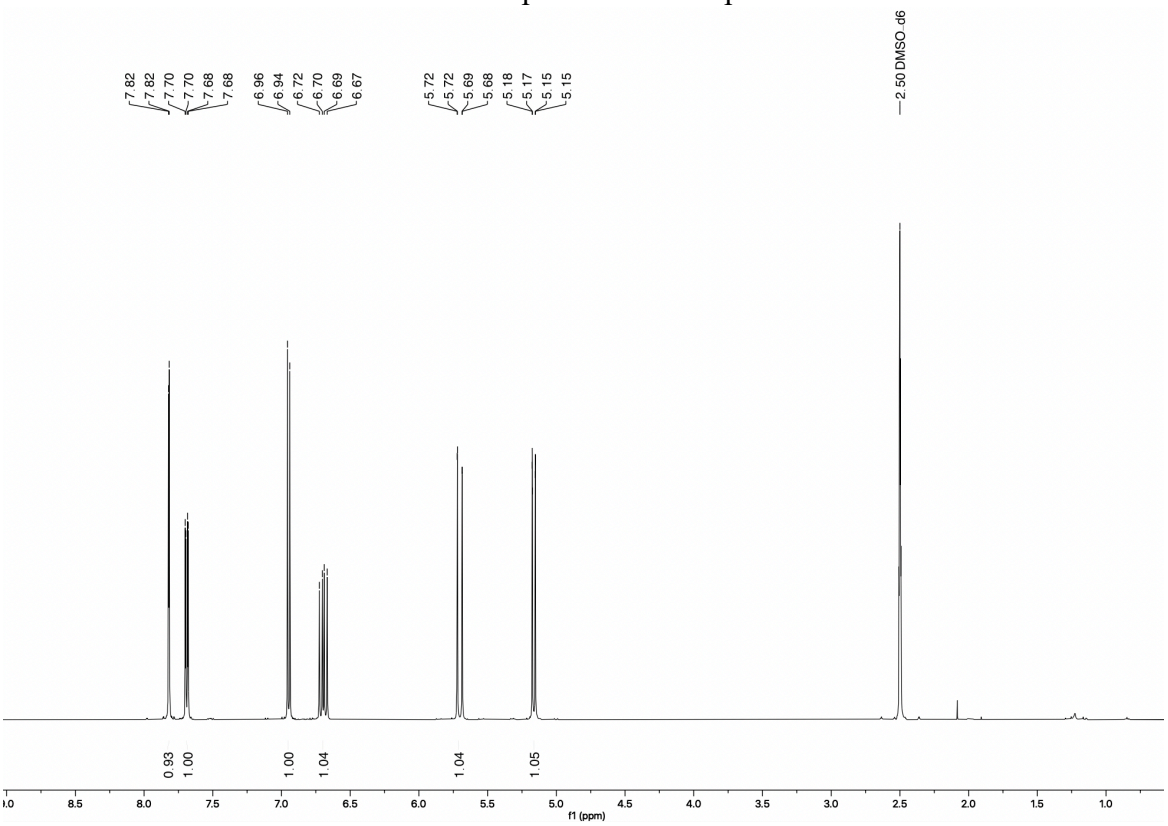

^{13}C NMR spectrum of compound **6**

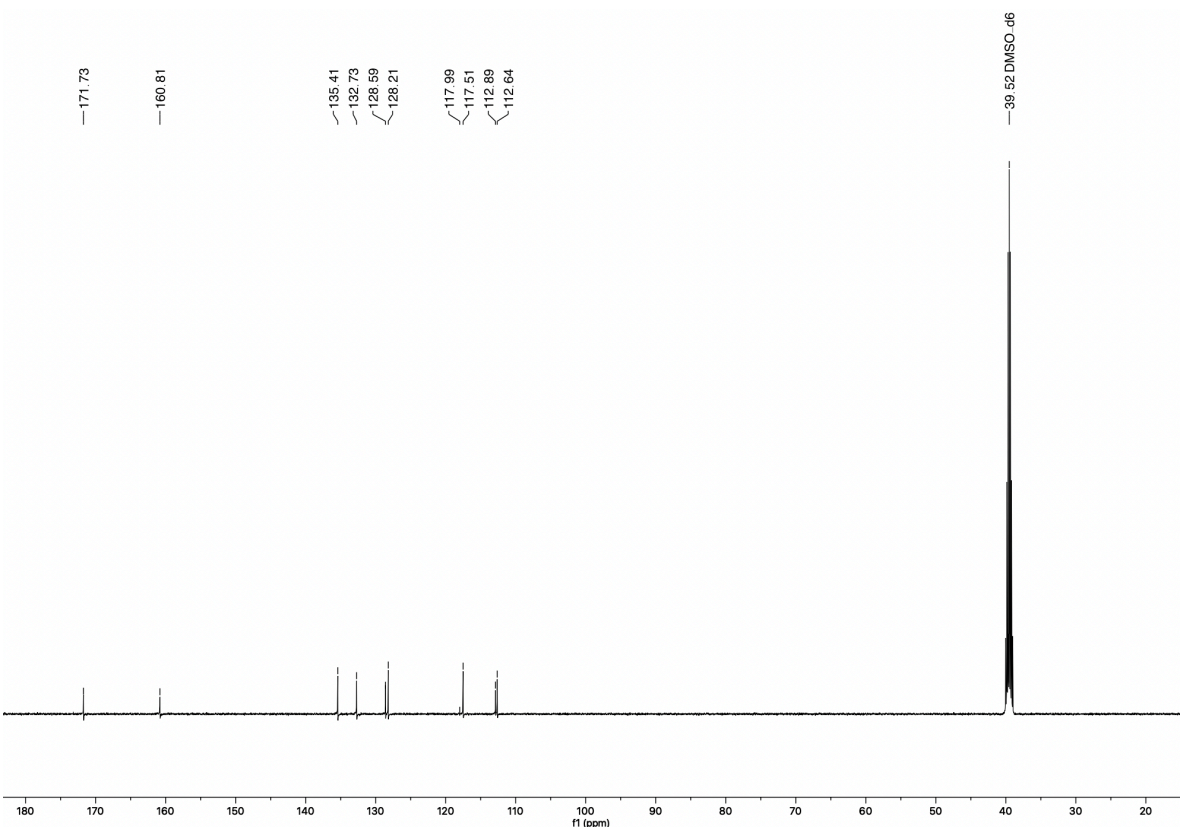

LC-MS spectrum of compound **6**

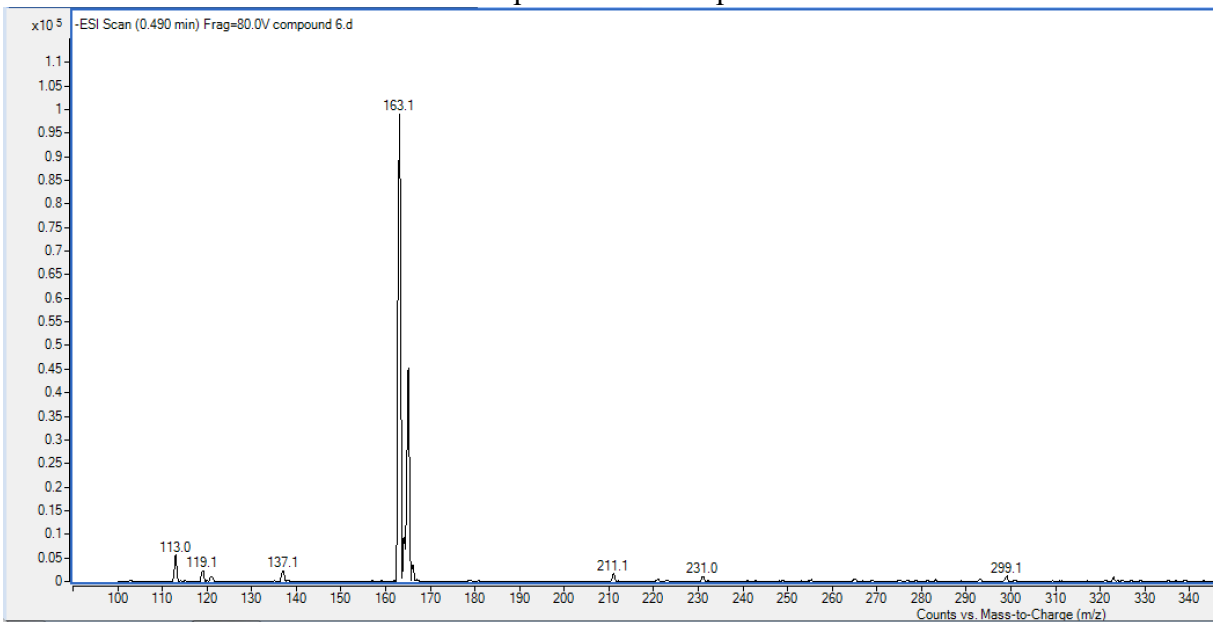

7 ^{1}H-NMR spectrum of compound **7**

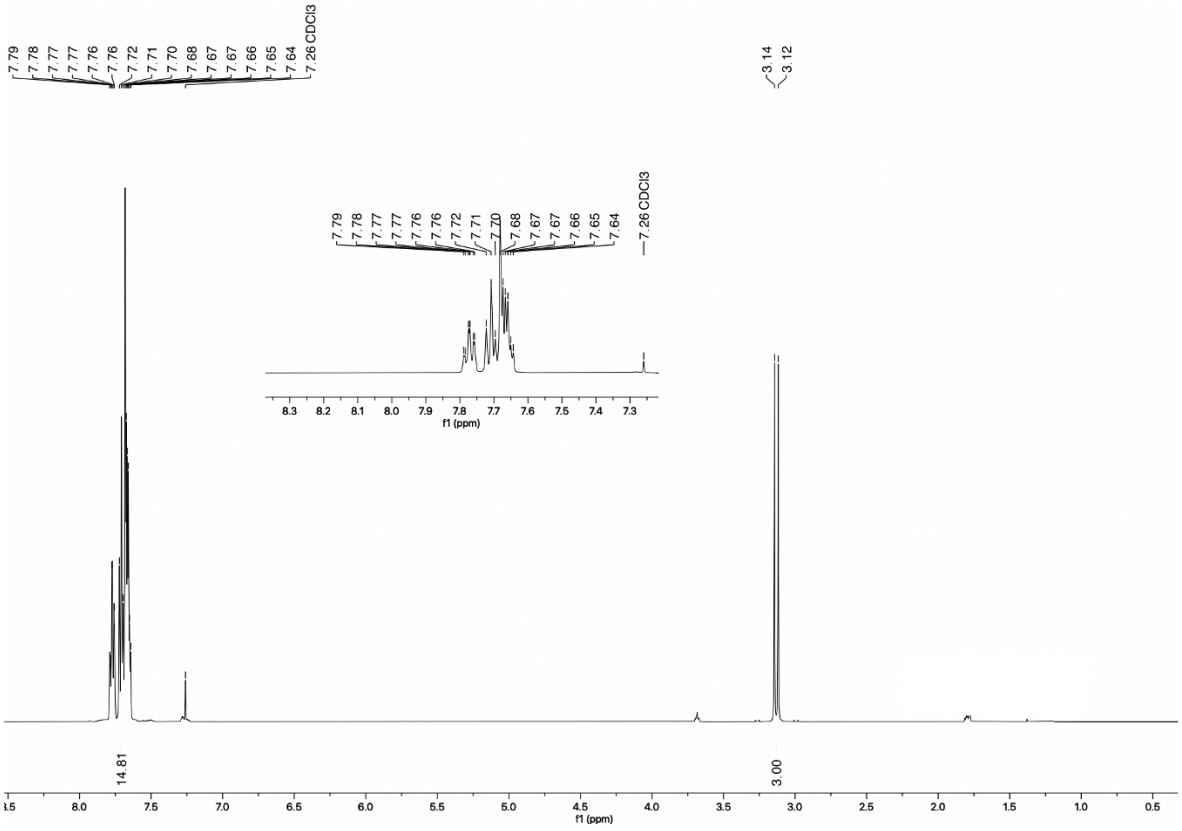

8 NMR spectrums of compound **8**

^{1}H NMR spectrum of compound **8**

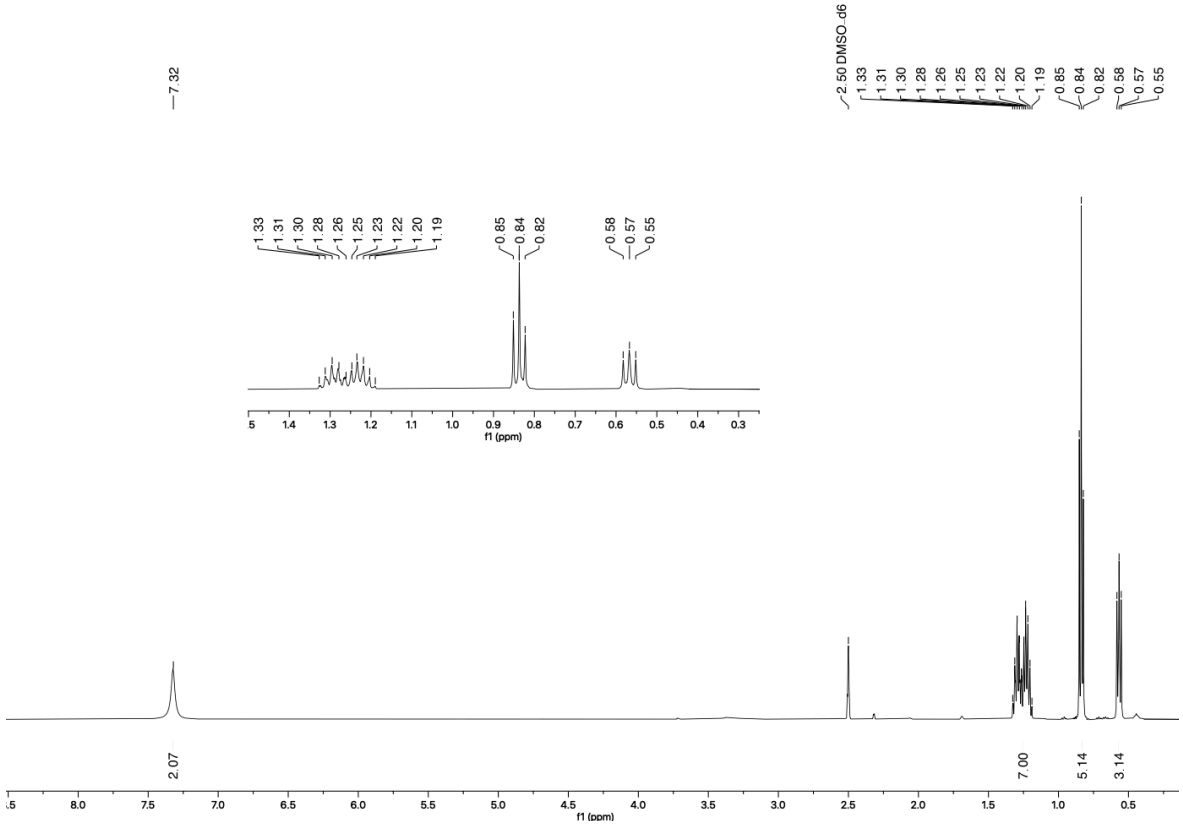

^{11}B NMR spectrum of compound **8**

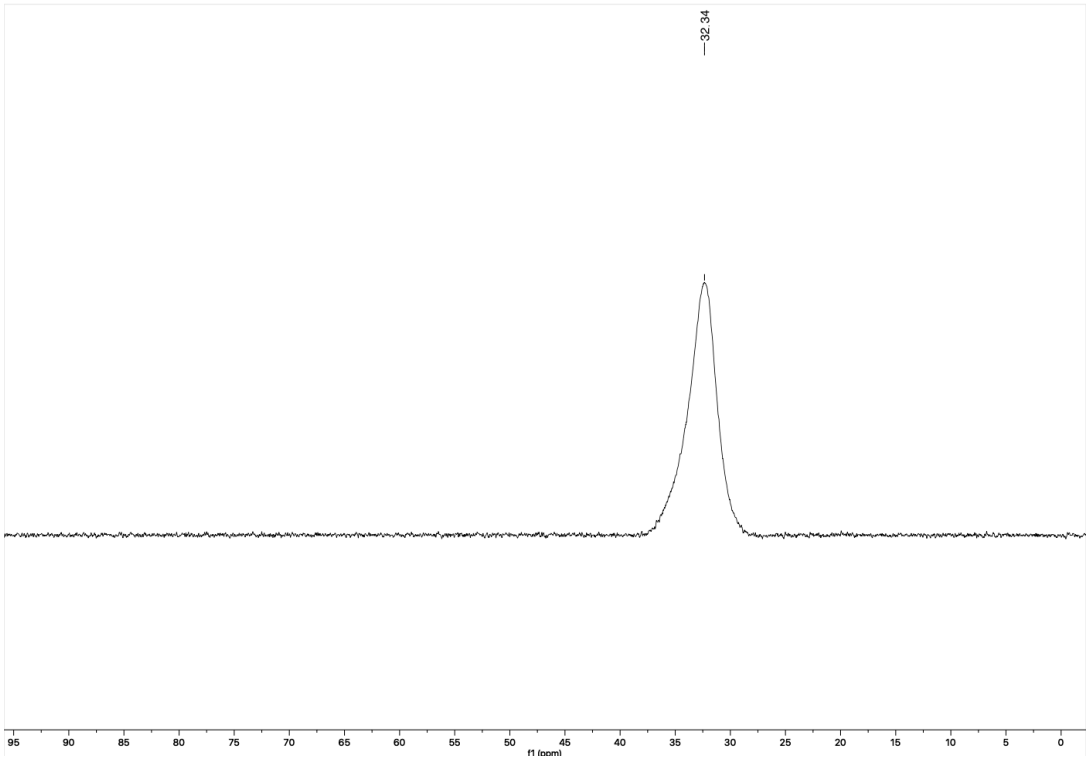

9 NMR spectrums of compound **11**

^{1}H NMR spectrum of compound **11**

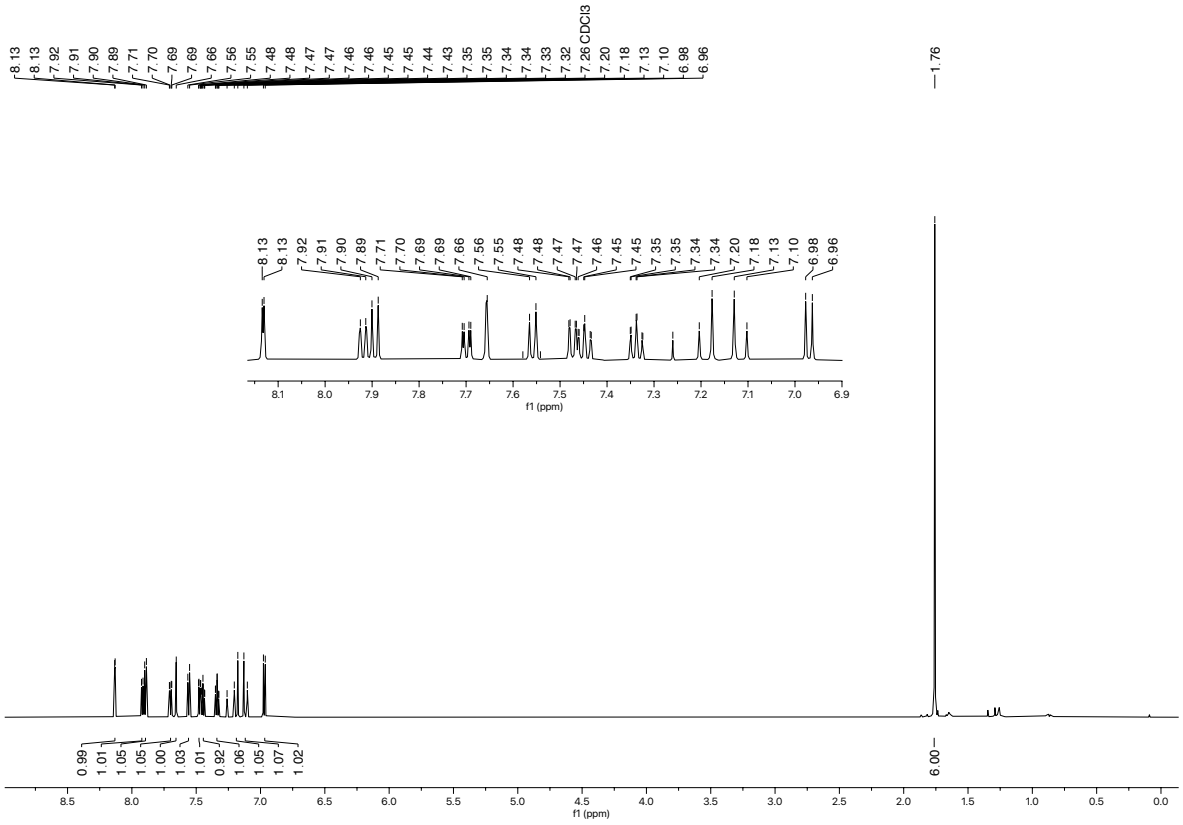

^{13}C NMR spectrum of compound **11**

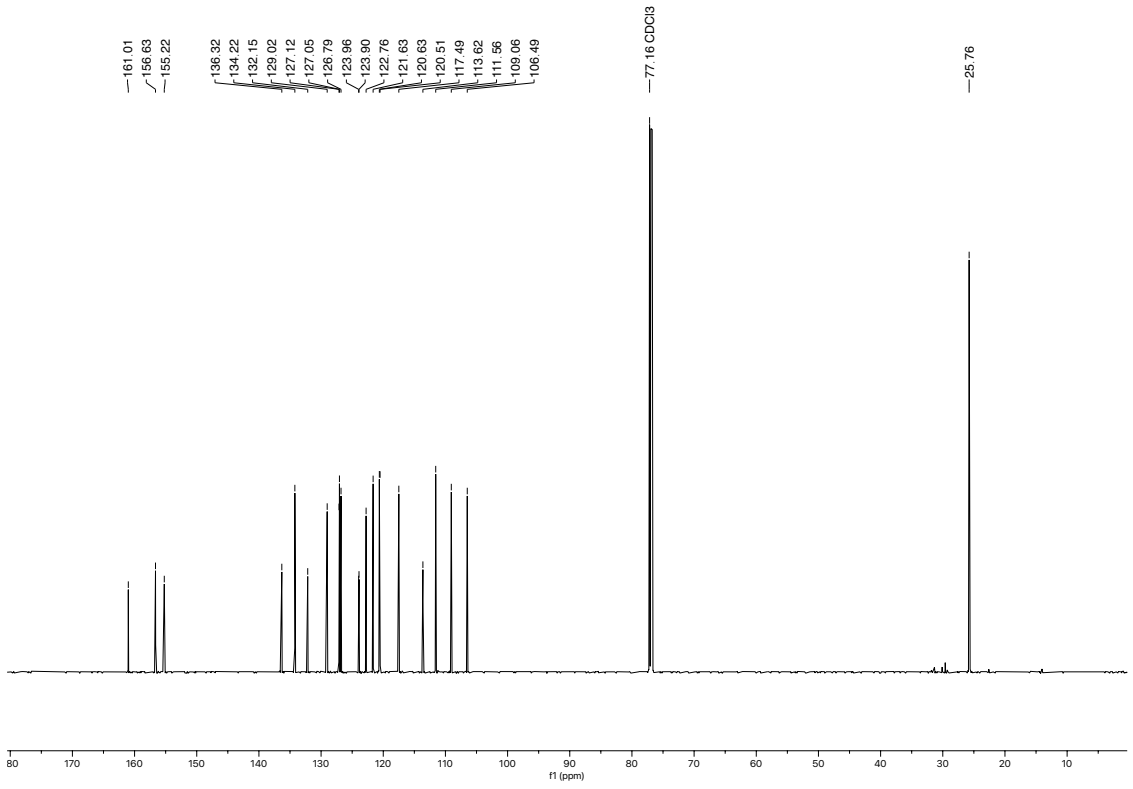

10 NMR, HPLC and LC-MS spectrums of compound **12**

^{1}H NMR spectrum of compound **12**

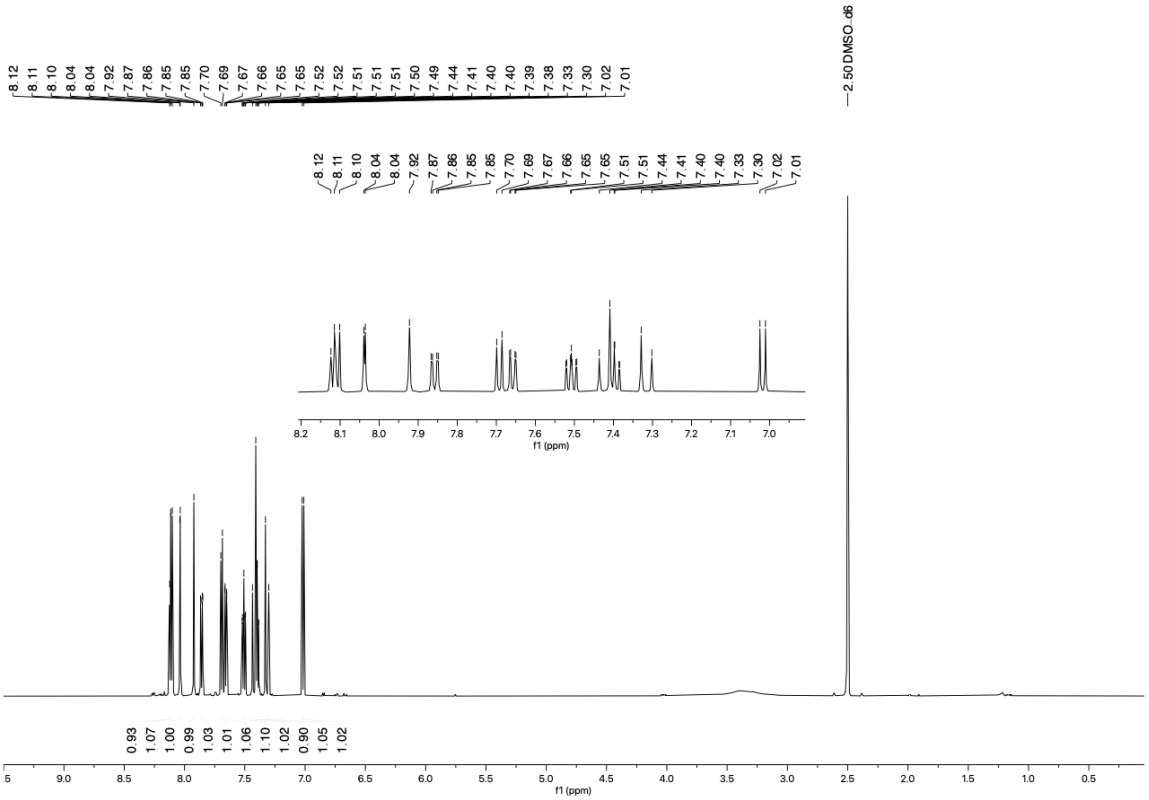

^{13}C NMR spectrum of compound **12**

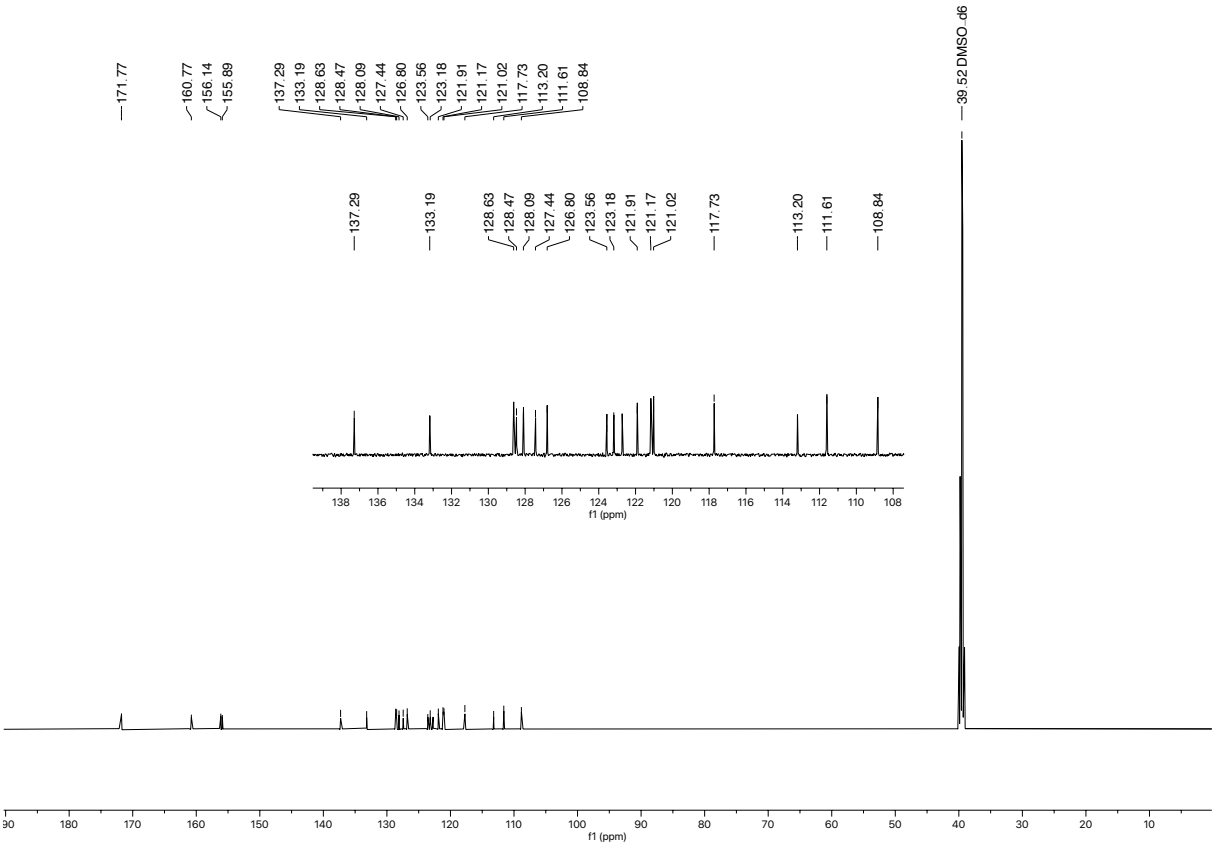

LC-MS spectrum of compound **12**

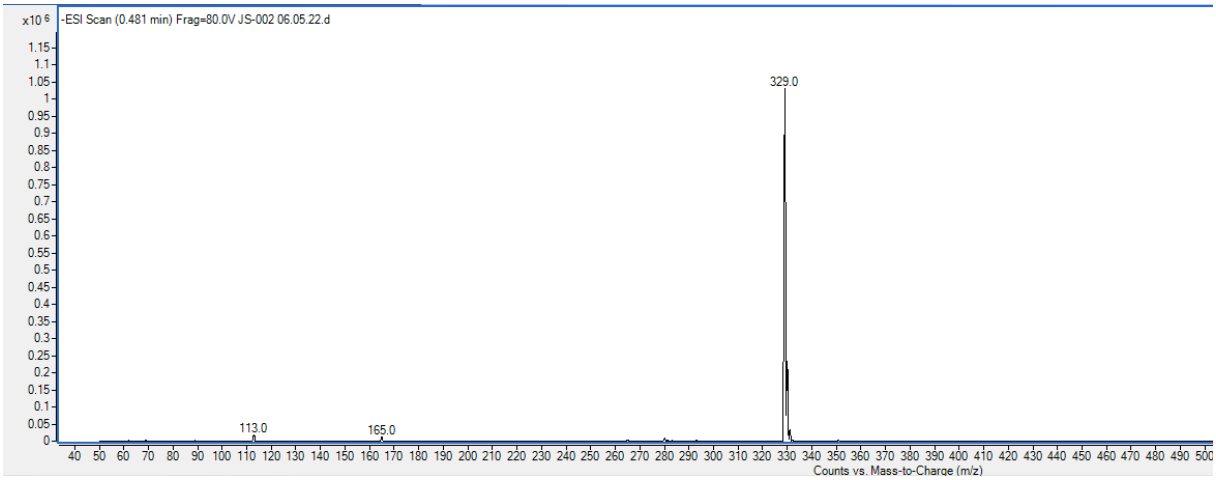

HPLC chromatogram of compound **12**

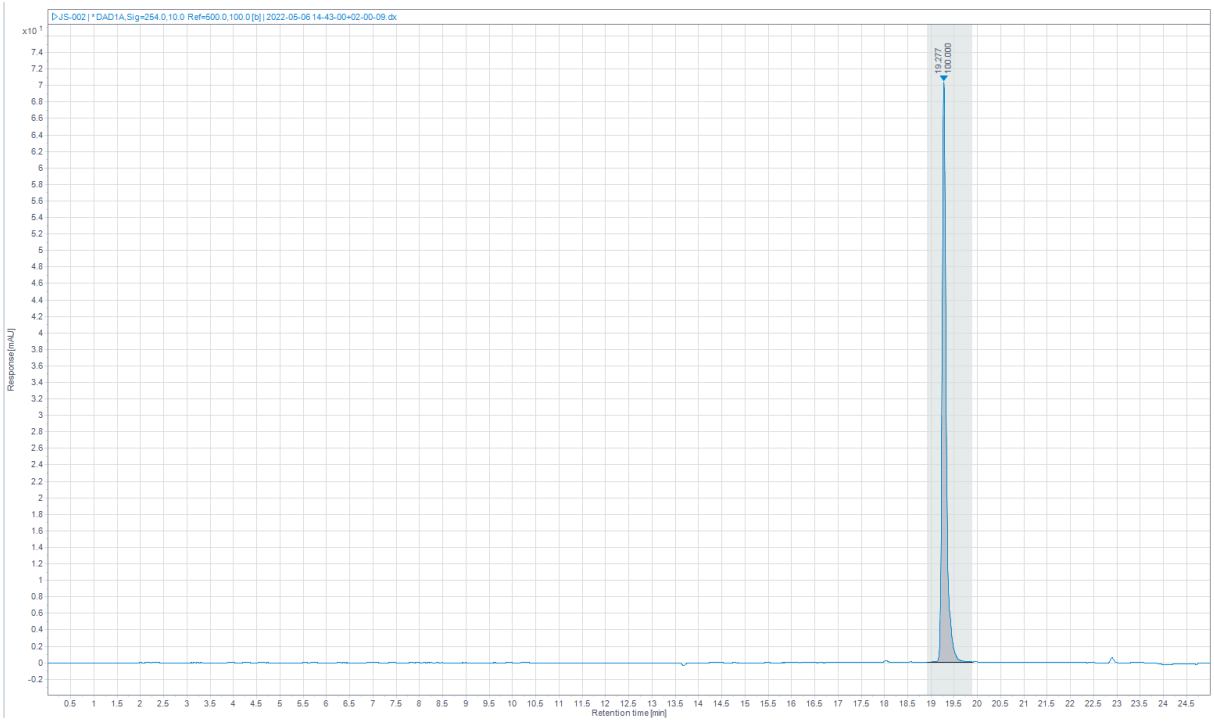

11 NMR and LC-MS spectrums of compound **13**

^{1}H NMR spectrum of compound **13**

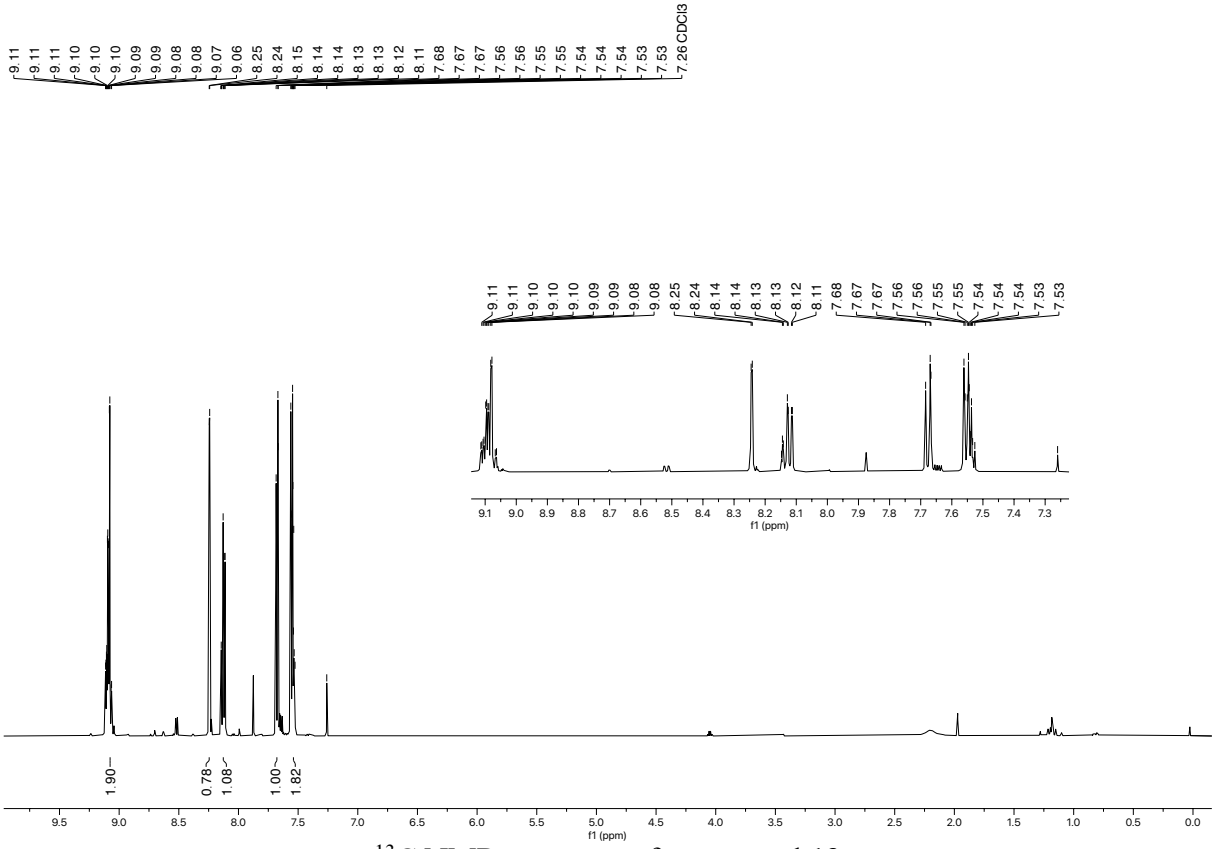

^{13}C NMR spectrum of compound **13**

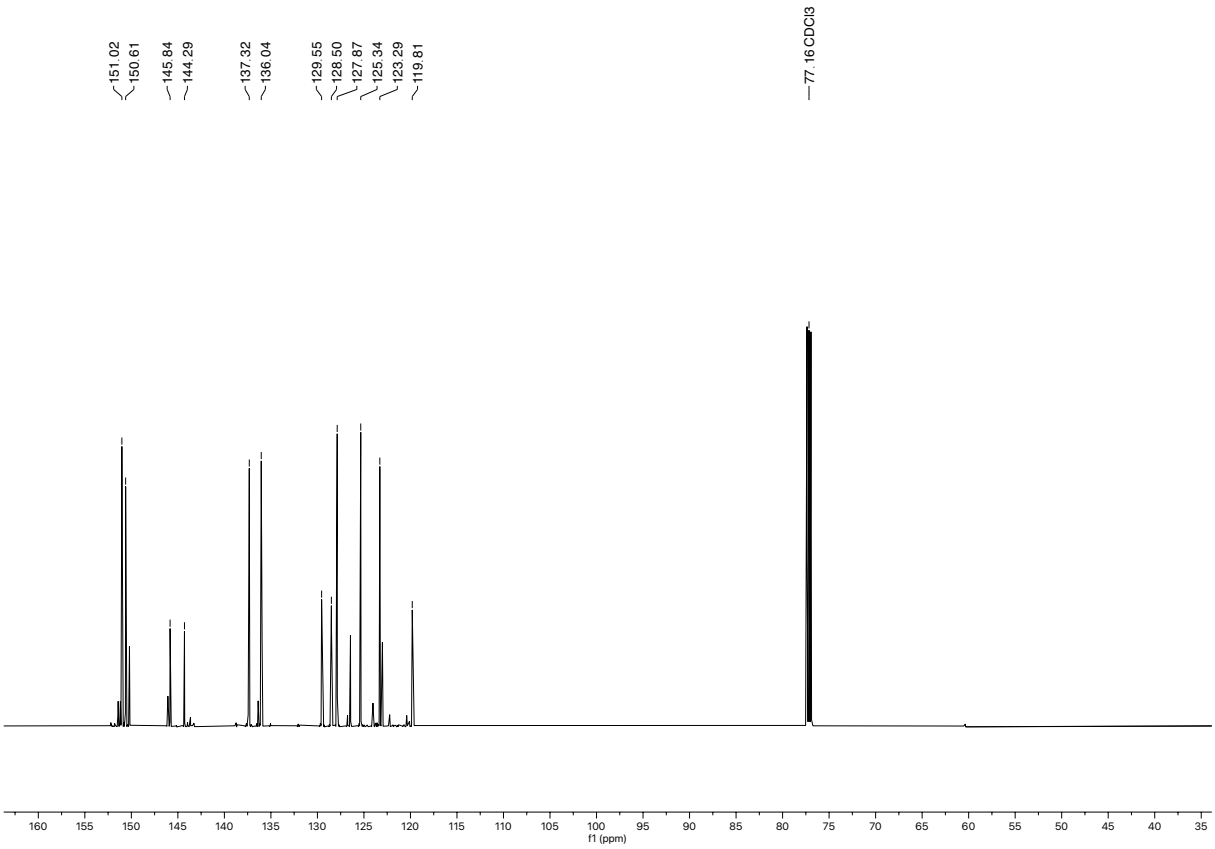

LC-MS spectrum of compound **13**

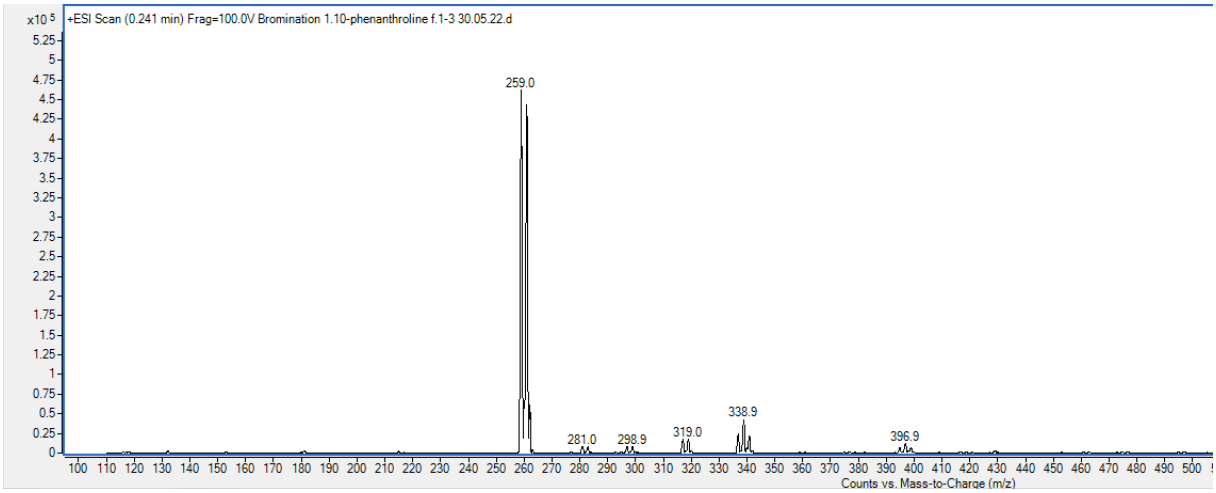

12 NMR spectrums of compound **17**

^{1}H NMR spectrum of compound **17**

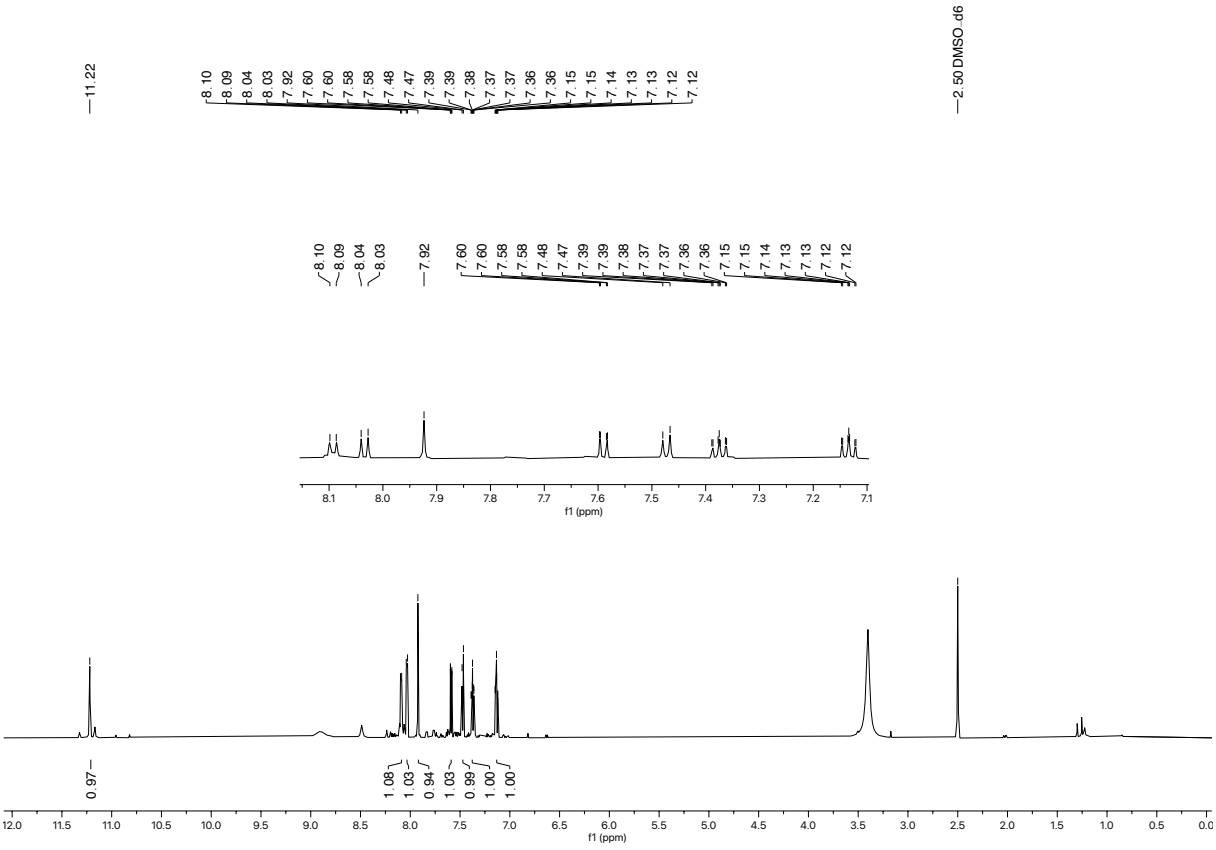

^{13}C NMR spectrum of compound **17**

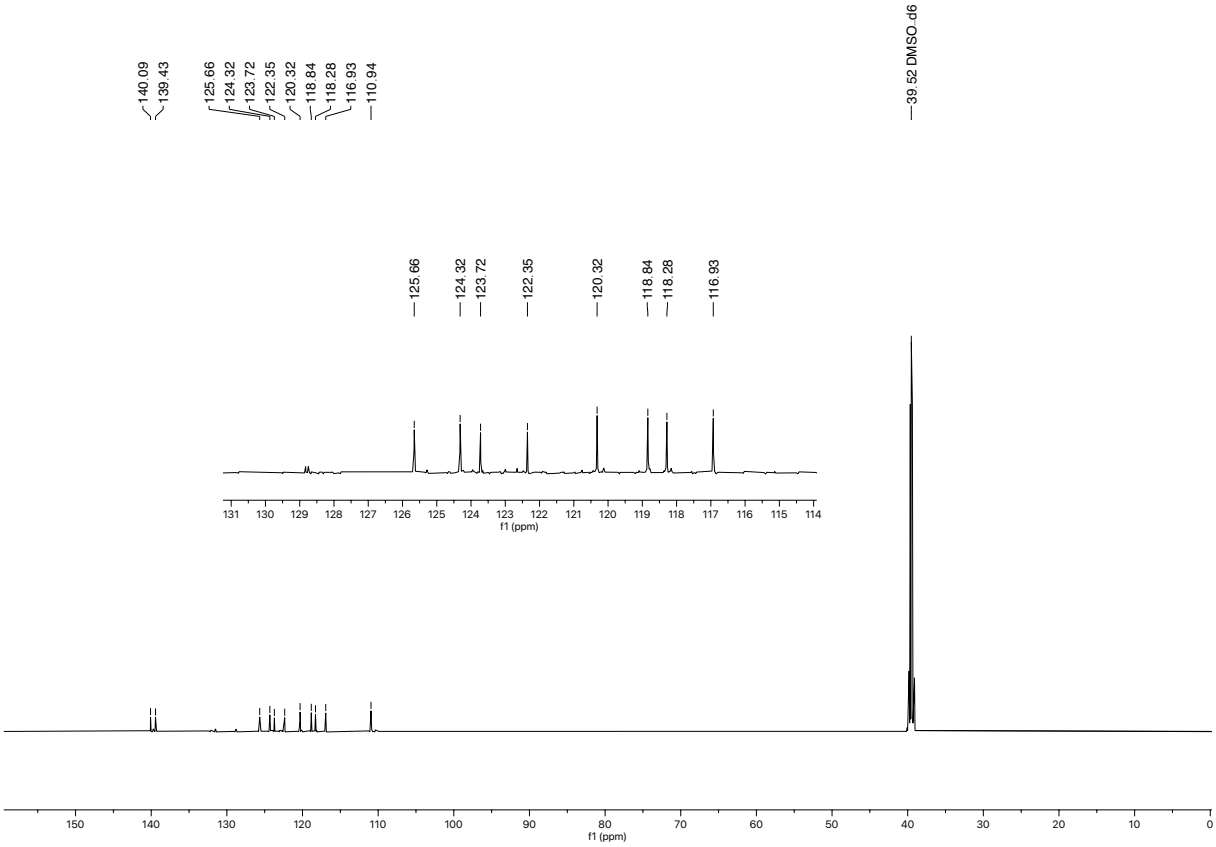

LC-MS spectrum of compound **17**

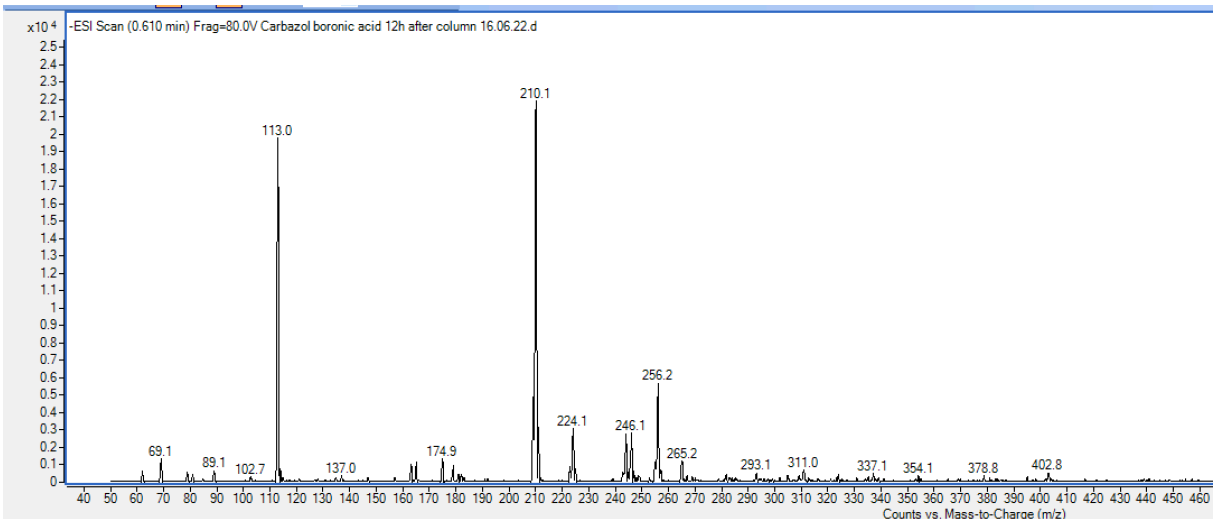

13 NMR, HPLC and LC-MS spectrums of compound **18**

^{1}H NMR spectrum of compound **18**

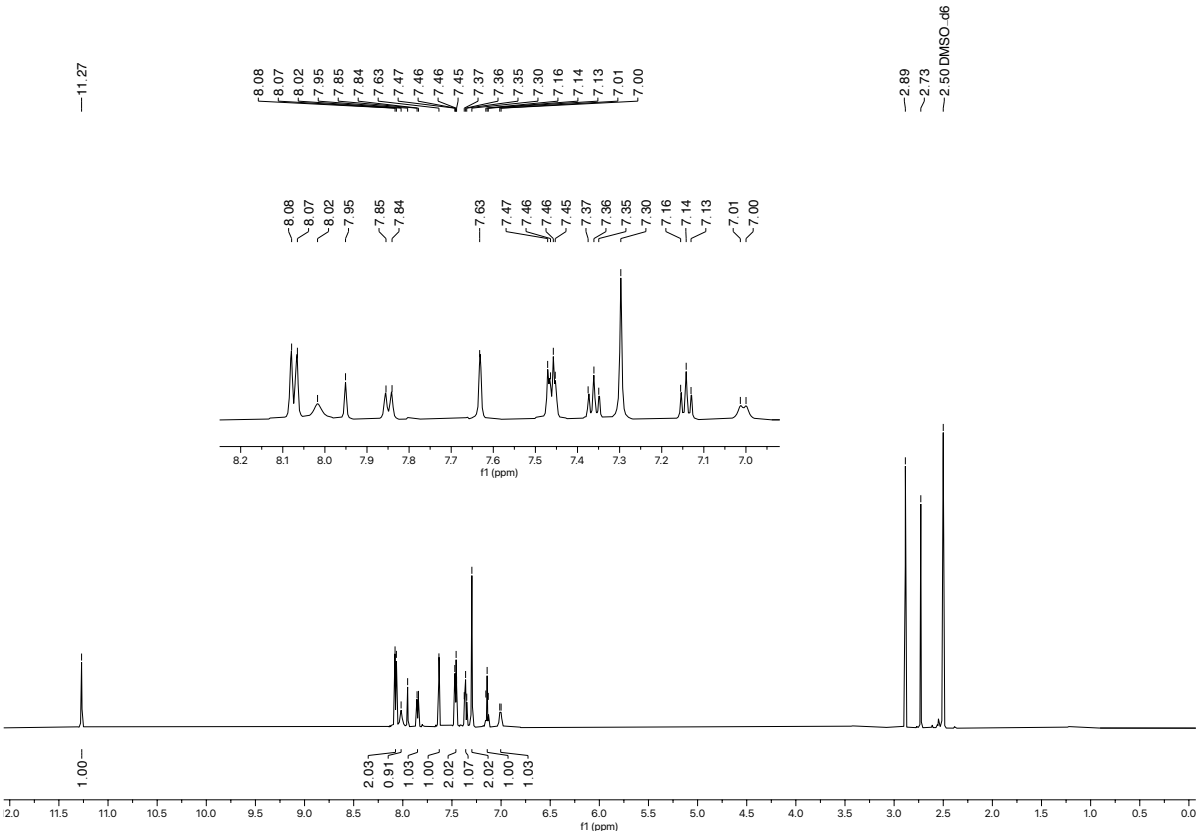

^{13}C NMR spectrum of compound **18**

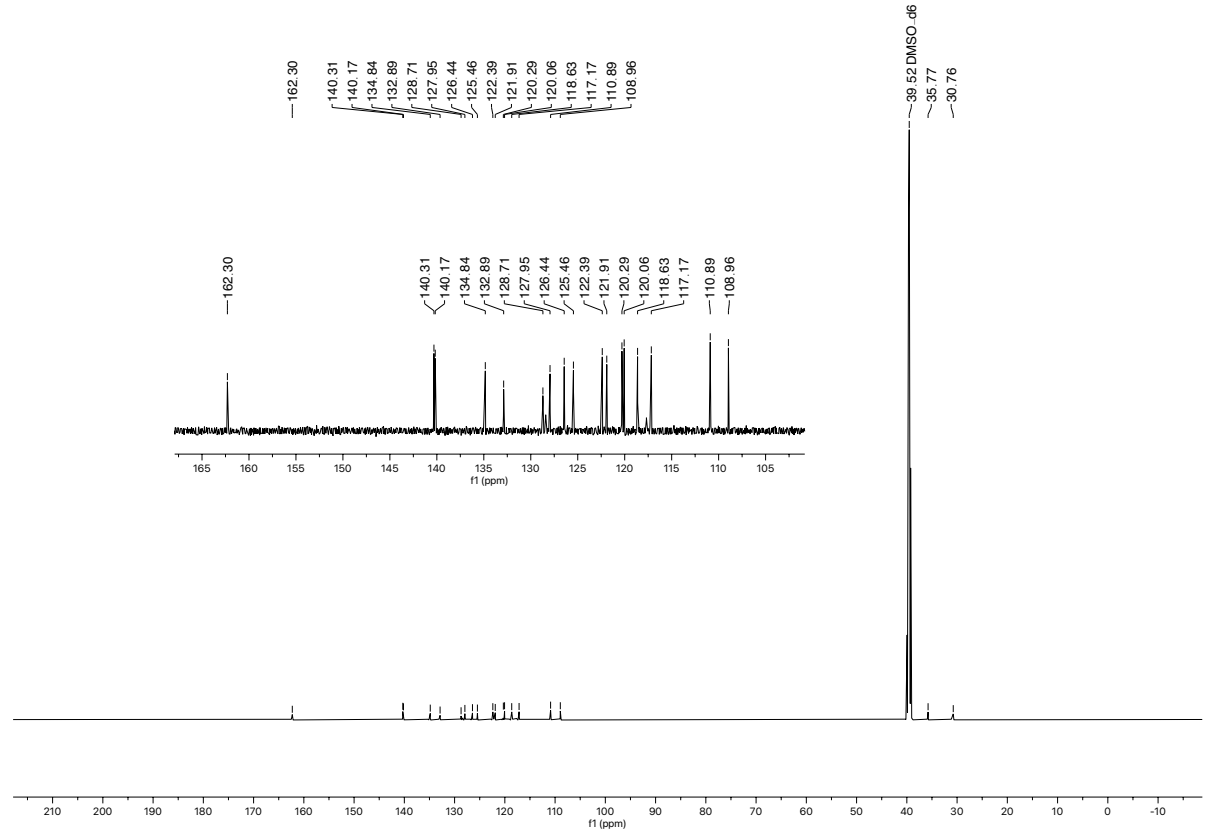

LC-MS spectrum of compound **18**

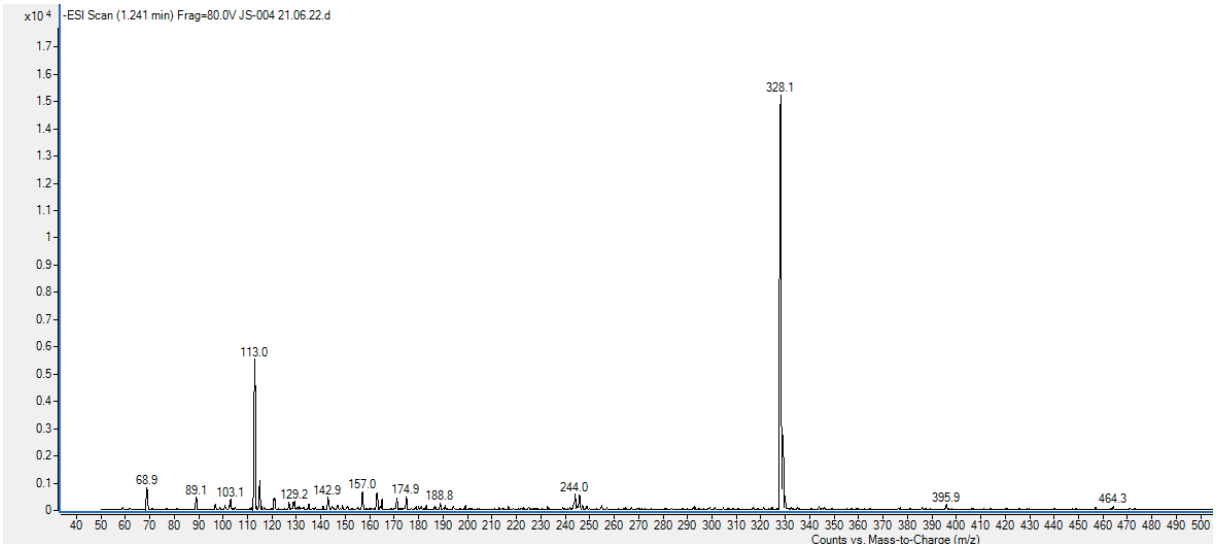

HPLC chromatogram of compound **18**